A Metabolically Efficient Leg Brace

by

Andrew Williams Carvey
B.S. Mechanical Engineering
Massachusetts Institute of Technology, 2003

Submitted to the Department of Mechanical Engineering
In Partial Fulfillment of the Requirements for the Degree of
Masters of Science in Mechanical Engineering

at the

MASSACHUSETTS INSTITUTE OF TECHNOLOGY

September 2006

Signature of Author .....
Andrew W. Carvey
Department of Mechanical Engineering
August 26th, 2006

Certified by .....
David R. Wallace
Associate Professor of Mechanical Engineering
Thesis Supervisor

Accepted by .....
Lallit Anand
Chairman, Department Committee on Graduate Students

A Metabolically Efficient Leg Brace

by

Andrew Williams Carvey
B.S. Mechanical Engineering
Massachusetts Institute of Technology, 2003

Submitted to the Department of Mechanical Engineering on
August 26th, 2006, in partial fulfillment of the requirements for the degree of
Masters of Science in Mechanical Engineering

Abstract

Locomotion assistive devices can be broadly classified as either being passive or powered. Both have been created to aid in the leg's generation of a ground reaction force which supports the torso during locomotion, yet their inherent design has limited their functional growth to date. While many differing gait simulations have demonstrated stable solutions for lossless gait cycles, passive orthoses only diminish the user's impediment, and though powered gait exoskeletons can augment strength and endurance, they are limited by their energy demanding actuators.

In response to these two extremes, an energy efficient locomotion assist device was developed from the basis of lossless gait models that did not require external power, and augmented locomotion by harvesting the inherent energy associated with the gait cycle. The simplest anthropomorphic leg can be modeled with a peg-leg shank, a knee, a thigh and a point mass for the head, arms and torso. Using a tuned non-linear hardening torsion spring at the knee joint, the torso support that is required between the ground and pelvis for lossless gait simulations can be generated; allowing the close physical realization of the theoretical.

It was found that a single torsion spring can generate the leg thrusts necessary for a realistic range of walking and running gait velocities without the addition of any external power. While frictional losses do inhibit the locomotion assist device's efficiency, since the device functions in parallel with the user's leg, any losses can be supplemented with minimal muscular activity. These results give strong indication that a new avenue of gait assistive and gait augmenting devices that require minimal actuation energy is feasible.

Thesis Supervisor: David R. Wallace
Title: Associate Professor Mechanical Engineering

Acknowledgments

·David R. Wallace
·Mark Belanger
·Ken Overgard, TJ Purtell, Dan Yeo, Adrian McLymont, James Moore, Greg Haynes
·Bill Fienup, Malima Wolf, Lael Odhner
·Steve Bathurst, Andre Devitt, Eric Scarborough
·My Family
·Matthew Robb Carvey - my Chemical Brother
·CAD Lab Members: Bill, Barry, James, … EVERYBODY!!!
·John Rokosz
·Chandler Hatton, Becky Kusko, Amelia Verostko, Shelly Tien, and all the other Ladies who helped me through my research … cause it's ALL about the Ladies.

·All who has spoken kind words throughout this journey.

"Human subtlety will never devise an invention more beautiful, more simple or more direct than does nature because in her inventions nothing is lacking, and nothing is superfluous."

-Leonardo da Vinci

Table of Contents

List of Figures

1 Introduction

1.1 Background

Human locomotion assist devices are of great interest to the medical industry and military for rehabilitation and gait enhancement. While walking assists such as leg braces and canes have been in use for years, the next desired step is in the development of a performance augmentation device for human locomotion. Research in this field has been ongoing for many years; however the high energy demands of the motors, pistons and actuators of most present designs have been a persistent, difficult obstacle for practical implementation.

Contrary to our current powered efforts, nature shows that legged locomotion in animals can be very efficient; a horse is a prime example [1]. The tuned muscle-tendon bundles in their legs elastically store and return the energy associated with the gait cycle about their leg joints. Instead of loosing a majority of the energy associate with ground impact, their springy legs can efficiently compress and catapult themselves along their desired trajectory with minimal muscular work.

Using recent research on how humans minimize energy consumption during locomotion in conjunction with the architecture found in nature's efficient gait and present day exoskeletons, it is believed that an energy efficient performance augmentation device is feasible.

1.2 Method

The human gait cycle and associated anatomy was analyzed. Accounting for the human factors associated with locomotion, extraneous components were simplified and clustered. A relationship was made between the core principles of human locomotion and the architecture used in nature's efficient gait. Applying the concept of elastic leg joints to the simplified human gait cycle, a model of a passive locomotion assist device for humans was created, and simulations were conducted. Working from human gait data, the elastic component of the model were tuned to best match the human gait cycle. These results were used to create a passive mobility assist exoskeleton that functions in parallel with the leg. Performance tests were conducted to evaluate the brace's performance, human compliance and its ability to reduce the metabolic effort of associate gait tasks.

1.3 Results

A theoretical model for a KAFO with a bi-modal state controlled torsion spring at the knee joint was developed to reduce the metabolic energy required for torso support during locomotion. Simulations for this device were conducted and showed two things. First, closed loop lossless gait cycles were fully attainable over a range of locomotion velocities using a single design architecture. Second, altering the engineering parameters of the LAD's torsion spring could better tune the KAFO's dynamic response to better suite different use's gait cycle and different initial conditions. From these simulation results, a prototype LAD was constructed for a healthy bodied middle aged male. The physical performance of the torsion springs for the LAD's knee joint had a measured torsional response with an average error of +0.33%. This corresponded to an average ground reaction force thrust error of -15.7%. The evaluation of the exoskeleton's ability to assist with torso support on humans was conducted by comparing the quadriceps muscular EMG data during squat thrusts for one healthy human subject. The results showed that the LAD reduced the quadriceps required metabolic effort during torso support by 43%. The initial exoskeleton prototype was bulky and heavy, decreasing the leg's controllable response. This made it unfeasible to conduct useful dynamic gait data. Though the presented KAFO brace has dynamic roadblocks, the initial results strongly imply that further development of a lighter and more streamlined KAFO of this architecture could greatly assist individuals with lower leg dysfunction, or healthy people wishing augment their locomotion performance.

1.4 Conclusion

An exoskeleton which successfully augmented components of human locomotion was created and tested. The difficulties associated with the high energy demands of previous powered locomotion assist devices was avoided by following the efficient locomotion architecture found in nature, using the leg muscles for the necessary force actuators. Optimizing the passive elastic exoskeleton design resulted in both a reduction in muscle forces and a simulated metabolic savings during locomotion. Though the passive assistive exoskeleton acting in parallel with the leg does slightly alter the gait cycle, the efficiency benefits outweigh the additional cost. This design shows many promising qualities for both locomotion endurance and medical rehabilitation purposes.

2 Background and Prior Art

In order to successfully develop an exoskeleton capable of aiding human locomotion, the core fundamentals of the problem must be determined, the overall objective of the project must be defined, and the method by which further advances are to be accomplished must be solidly understood. A brief explanation human locomotion is given; followed by the mechanical requirements which allow a stable gait cycle. Background research on prior locomotion assist devices reveal the designs and components which worked successfully, and the limitations and pitfalls of failed designs. Weighing the pros and cons of the potentially successful designs, a steadfast direction can be determined and explored.

2.1 Fundamentals of Locomotion - Overview

The general term locomotion is defined as "the self-powered, patterned motion of limbs or other anatomical parts by which an individual customarily moves itself from place to place" [2]. Human locomotion is further clarified as "[the] process in which the erect, moving body is supported by first one leg and then the other." [3] This process is the cyclic pattern of body motions that is repeated again and again, step by step and usually in a manner that minimizes metabolic energy at a given speed.

In human locomotion, the function of the legs is to support the body's torso at a consistent steady state height above the ground while moving in a periodic manner such that the person progresses over terrain. This torso supporting force is known as the Ground Reaction Force (GRF) [3]. The

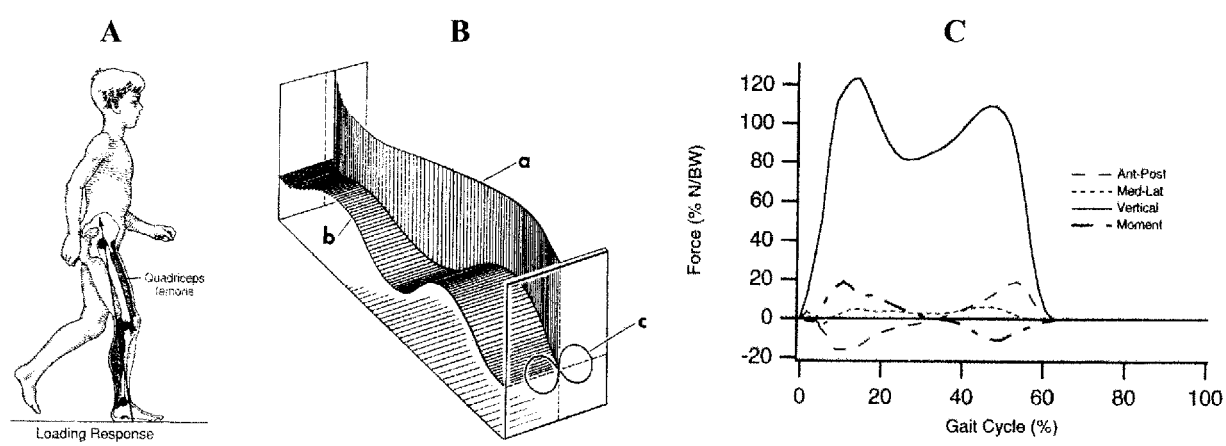

Figure 2.1: Three fundamental qualities of locomotion. (A) The leg generates a GRF on the pelvis which supports the torso [3]. (B) The undulating displacement of the pelvis throughout a gait cycle [3]. (C) The vertical component of a GRF normalized to body weight for one gait cycle [3].

GRF is the varying vector force that the leg generates between the foot's Center of Pressure (COP) in contact with the ground and the pelvis. The torso is comprised of the pelvis, thorax, neck, head, arms and all corresponding skeletal and tissue elements. The GRF is formally defined as the vector sum of the vertical, horizontal and transverse force components. A snapshot of the leg's torso supporting GRF and its vector trajectory during a gait cycle is shown in Figure 2.1A. Since the torso is periodically supported by opposing legs that swing forwards and back, the body's velocity speeds up and slows down as it rises and falls a few centimeters while it weaves from side to side (Figure 2.1B) [3]. As a result, the GRF vector forces also vary throughout the gait cycle. Figure 2.1C show the vertical component of the GRF normalized to the person's body weight over a complete walking gait cycle.

2.2 Torso Support

The primary functional requirement for locomotion is the generation of the appropriate forces necessary to support the body above the ground such that it can move from one location to the next. This torso supporting GRF generated by the leg is created by skeletal bones and muscular tissue functioning in parallel with each other. Bones function as structural elements that transfer forces between the ground and the pelvis (Figure 2.2A). Since the leg is a multi-jointed structure that supports a mass against a gravitational field, the system is inherently unstable (Figure 2.2B). For this reason, support torques generated by muscles and tendons are required at each joint to control the position and motion of the bones in order to keep the system at equilibrium above the ground. Working together, the legs generate the required GRF which supports the torso and allows locomotion.

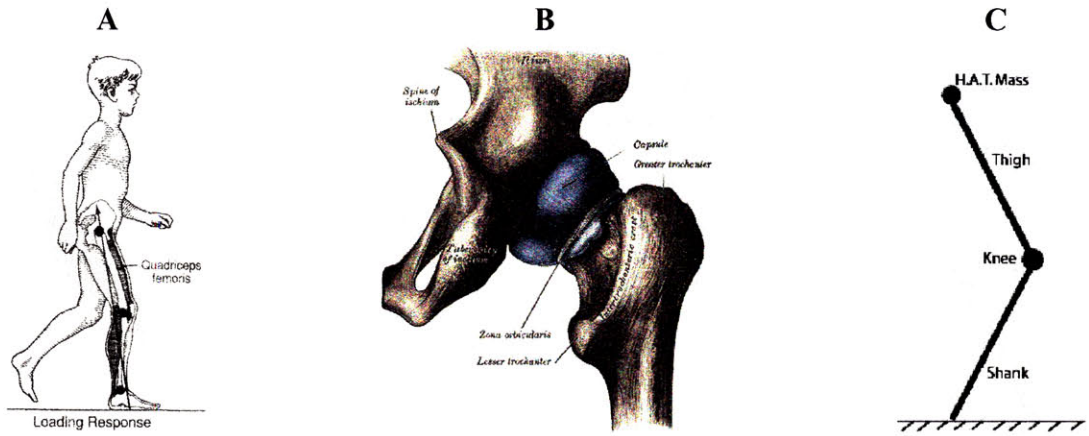

Figure 2.2: The hip socket is the interface for the leg to transfer the GRFs to the pelvis. Image (A) from [3] and image (B) from [4].

In order to support the torso during locomotion, both the primary torque generating muscles and secondary stabilizing and balancing muscles must be taken into consideration. If the primary torque generating muscle is not strong enough, then another means of generating an augmenting

GRF is necessary, such as indirect LADs. However, if secondary stabilizing muscles and tissue are not strong enough to balance the torso or provide swing clearance, then a stabilizing LAD called a gait orthosis must be used. Muscular or tissue deficiencies in certain areas can inhibit other critical muscles from appropriately generating the GRF correctly.

2.3 Existing Locomotion Assist Devices (LADs)

Unfortunately, accidents, age and disease can have detrimental effects on legs, inhibiting their ability to generate the joint torques required for 'normal' locomotion. Due to tissue damage and/or muscular deficiencies, the GRF generated by the leg is sometimes no longer sufficient to support the torso in all situations, causing the leg to buckle under the load, and the person will fall. In efforts to improve support and prevent tragic falls, man has developed multiple different Locomotion Assist Devices (LADs) which aid in generating the required supporting force between the ground and body. These LADs (e.g. canes, wheelchairs and leg braces), each aid in the generation of the GRF in different means and to varying degrees, and can be categorized by their method of aiding support: either indirectly, directly, in parallel, or in series with the leg.

2.3.1 LADs - Indirect Support

If the legs are not strong enough to generate a sufficient GRF to support the torso, a supplementary means of generating the remaining required GRF is necessary. Indirect LADs (e.g. canes, crutches and walkers) (Figure 2.3A), augment the GRF by allowing the user to generate a portion of the support force via their arms sockets (Figure 2.3B). Since the loads and work required by the legs for locomotion is partially supported by the arms, the user can locomote without worrying about their leg giving out, which could result in a dangerous fall.

Figure 2.3: (A) Canes, crutches and walkers [5] [6] [7] allow users to generate a portion of the GRF via their arm sockets, (B) diminishing the forces required by the leg, allowing a more natural gait cycle [8].

2.3.2 LADs – Direct Support

Thus far, legs have generated part of all of the GRF. Since people without use of their legs still need to be able to navigate their environment. For this reason wheelchairs were developed to supports the torso via its seat by directly exerting a GRF to the pelvis; bypassing the need of legs for transportation. A differentiating locomotion characteristic of directly supporting LADs is that they roll over the ground. By keeping the torso at a steady height above the ground with no vertical displacement, the GRF the wheelchair exerts on the user is steady 1x body weight. A lack of any noticeable torso bobbing allows for highly efficient locomotion that can be either driven by the user or powered from a battery (Figure 2.4). Although their efficiency makes them desirable LADs, they are not without flaw. Their wheeled design inherently limits their mobility to relatively smooth, unobstructed terrain and can cause possible social difficulties.

Figure 2.4: Wheelchairs allow non-legged locomotion - which can be highly energy efficient. Images from [9] and [10].

2.3.3 LADs – Parallel Support

The function of the leg during locomotion is to appropriately support the torso without throughout the gait cycle. Assuming that the structural bones in a leg are sufficiently strong such that they will not fracture, torso support is governed by appropriate leg joint torques that are generated by muscles. Unfortunately, muscular deficiencies in secondary stabilizing muscles can inhibit critical primary muscles from generating the correct joint torques necessary for support and balance, or can prevent the joints from getting to the correct positions prior to support. For this reason stabilizing LADs called gait orthosis were developed to function in parallel with the leg, allowing muscles to more accurately generate muscular support forces which allow anthropomorphic motion. Figure 2.5 shows examples for ankle, knee and hip orthosis. It should be noted that gait orthosis are also used if other tissue such as tendons, ligaments or cartilage is damaged, as is often the case in people who wear knee braces.

Figure 2.5: Gait Orthosis – Ankle [11], Knee [12], Leg and Hip [13].

Gait orthoses are bracing devices worn on the leg to modify the structural and functional characteristics of the neuromuscular and skeletal systems [14]. They are simple exoskeletons that function in parallel with the leg and aid in stabilizing joints. Since orthoses naturally constrains leg joints, the primary support muscles can create joint torques closer to that of uninhibited legs despite localized weaknesses. They can correct for deformity, restrict movement or reduce the weight-bearing forces of a leg. Much like canes or walkers, gait orthosis do not augment the generation of a GRF beyond that of an uninjured person; instead, these braces aid locomotion for the disability or injured by decreasing their impediment. Knee braces that affect the GRF support of the leg will be discussed in a later Section 2.4.

2.3.4 LADs – Series 'Support' & Other

So far, the three LAD flavors have targeted at people with locomotion deficiencies. LADs that function in series with the leg are quite different because they target healthy individuals whom wish to alter or enhance their locomotion. Unlike parallel supporting orthosis, series supporting LADs do not directly assist muscles, but rather alter the leg's movements and thrust demands, allowing more favorable thrust requirements. This is usually done with a pogo-stick-like device or other energy storing mechanism situated between the ground and the bottom of the user's foot (Figure 2.6A - C), or some other thrust altering method such as explosives (Figure 2.6D).

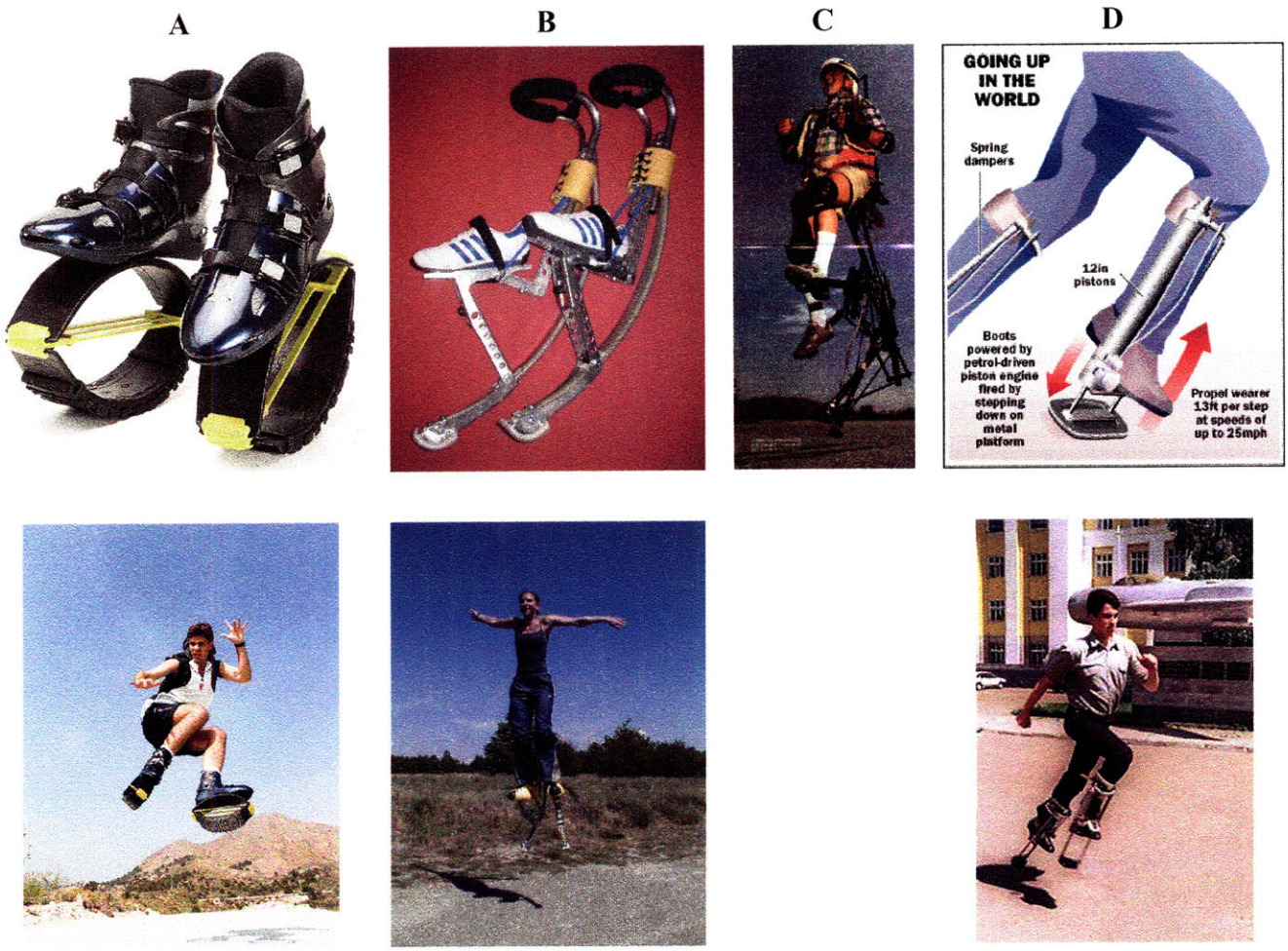

Figure 2.6: LADs that function in series with the leg alter the user's natural gait cycle. Images (left to right) from [15], [16], [17] and [18].

Though series elastic LADs may initially appear to reduce the energy of locomotion, they do not. By altering the thrust demands, slightly lower thrust are required but for longer durations. This allows the user to have enhanced locomotion since more energy is associated with the system. Since the elastic mechanism transfers forces between the ground and the bottom of the foot, series supporting LADs can not directly support the torso; but rather only decrease the knee torque requirements.

2.4 LADs – Parallel Support: A Closer Look

LADs which function in parallel with the leg have the ability to act as a structurally supporting exoskeleton and can direct some of the GRF past the knee, resulting in a lower required supporting knee torque. Assuming that the leg bone is of adequate strength, rotational control of leg joints is required for appropriate GRF generation. Different leg joint torsional control methodologies allow parallel acting LADs to be subdivided into four categories:

1. An immobilized or rotationally constrained leg joint
2. A gait-controlled bimodal leg joint that is free to rotate or frozen in place
3. A flexural elastic leg joint
4. An externally powered leg joint
5. Some combination of the above

2.4.1 Immobilizing or Rotationally Constraining LADs

In normal locomotion, the rotational control of leg joints is governed by muscular tissue. If the muscular tissue at a leg joint is weakened or injured, gait orthosis are often used for stabilization and for preventing further injury. Immobilizing LADs do not allow for flexion or extension of the joint, and since they generate a support torque, decrease the torque requirements of the joint. Although an immobilizing knee LAD does decrease the knee torque requirements, they are primarily used on non-load bearing legs, in conjunction with crutches.

Rotationally constraining LADs allow a constrained range of motion, and are often used to prevent further injury. These orthosis usually have a variable range of rotation which can be set using stop pins and adjusted by the user in order to best fit their rehabilitation needs, or to prevent their leg joint from rotating past a point which it can no longer support the body. This design allows for energy absorption flowing heel strike, but also aides in torso support at the extremes of the stop pins, preventing any further rotation. They are commonly used after knee reconstructive surgery, when too much knee flexion could have detrimental affects to the success of the surgery. This design offers the same support at its extremes of rotation as an immobilizing orthosis while still allowing rotation flexion for shock absorption and extension for thrust generation. Support for the leg develops at the extremes of the 'stop pins', preventing any further rotation. When locked in the extended position, it effectively becomes a knee immobilizer. Figure 2.7 gives examples of immobilizing and rotationally constraining leg orthosis.

Figure 2.7: Gait orthosis which immobilize or constrain the rotation of leg joint support the torso naturally via the leg through the pelvis. Images (left to right) from [19], [20], [11], [21] and [22].

2.4.2 Gait Controlled Bimodal LADs

In a normal walking gait, the knee will flex approximately 20° after heel strike in order to decelerate the vertical component of the torso's velocity. In preparation for the next step during the swing phase, the knee flexes approximately 60° in order to decrease the distance between hip and foot, preventing the foot from colliding with the ground during its swing phase [3]. An immobilizing and a rotationally constraining knee orthosis often inhibit this from occurring. An immobilized knee can not flex at foot strike, resulting in high impact loads. In order to obtain adequate ground clearance during the swing phase, the wearer is required to rotate their pelvis in the coronal plane and swing the leg out sidewise, drastically altering their gait cycle. Though a rotationally constrained knee orthosis does allow some flexion which could account for the impact absorbing rotation, knee flexion during the swing phase is still a problem. Since the leg naturally rotates approximately 60° in preparation for the next step, and most rotationally constraining knee orthosis are set less than this, they too interfere with the normal gait cycle. For this reason a knee orthosis was developed which appropriately constrained knee flexion for the leg according to the gait phase.

A gait controlled bimodal orthosis has a weight sensitive locking mechanism at the knee which has two states: a one way clutch state, and a free swing state. At heel strike, the start of the stance phase, the orthosis activates the one way knee clutch, inhibiting any further knee flexion while still allowing leg extension. This alleviates the muscular requirement of generating the support torque for the knee, while still allowing the leg to extend and thrust if desired and possible. At toe off, the start of the swing phase, the orthosis switches states allowing free rotation about the knee joint (Figure 2.8) (A) Total Knee, (B) Stance Control Orthotic Knee, (C) Rheo Knee and with Flex Foot addition.

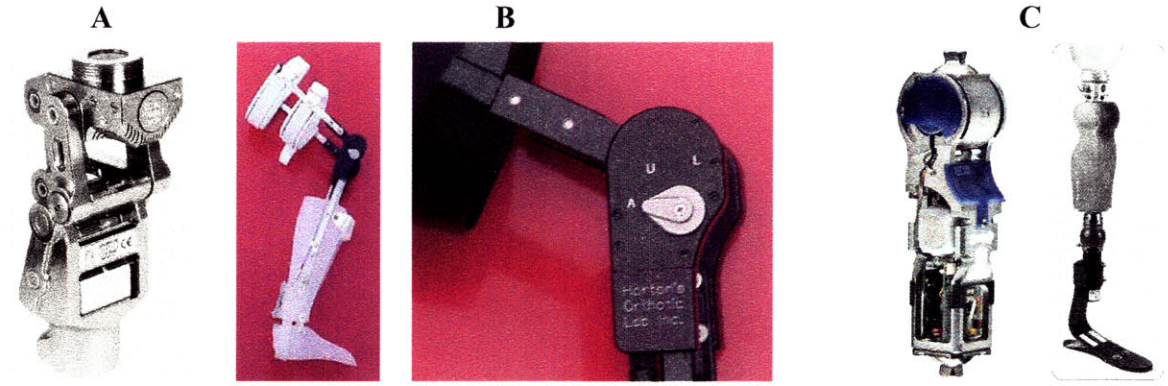

Figure 2.8: Knee orthosis which are functionally dependent upon the gait phase. The knee inhibits flexion and allows extension during the support phase, yet the knee is free to rotate during the swing phase. Image (A) from [23], images in (B) from [24], images in (C) from [25] and [26].

So, this orthosis creates torso support by inhibiting further leg flexion during the stance phase while still allowing knee extension for thrust generation, and full knee flexion during the swing phase.

2.4.3 Elastic Joint Restoring LADs

Though leg orthosis with a constrained rotational range of motion do generate support at the extremes of the range, there is no support over the intermediate rotational range. Neither a rotationally constraining orthosis nor a bimodal orthosis assist in leg extension. Since people using gait orthosis often have weaker muscles, generating these required restoring leg torques can be difficult and tiring. Gait orthosis with elastically restoring joints have been developed to help solve this problem.

The support potential of orthosis with elastically restoring joints is an extremely exciting field. Elastic joint orthosis support the body by creating a restoring force at leg joints upon flexion; akin to muscular actions. As the joint segment rotates, an elastic material flexes, stores energy and supplements the support torque. As the leg joint rotates more and more, the restoration joint torque increases. Since this restoring torque created by the flexural orthosis is dependent upon both the spring constant of the material and the magnitude of its rotation from steady state, these orthosis are designed with a certain dynamic response in mind. Though this response was designed to follow the characteristics of the user's gait cycle, variations in gait conditions can have a noticeable impact on their effective functionality.

Though there are many patents on conceptual LADs with elastic joints, relatively few designs have been implemented. Figure 2.9 shows four embodiments of elastically restoring joint mechanisms. Figure 2.9A is an elastic ankle orthosis developed by Ossur to assist in ankle position restoration. Figure 2.9B is a tunable elastic ankle prosthesis developed by Ossur which

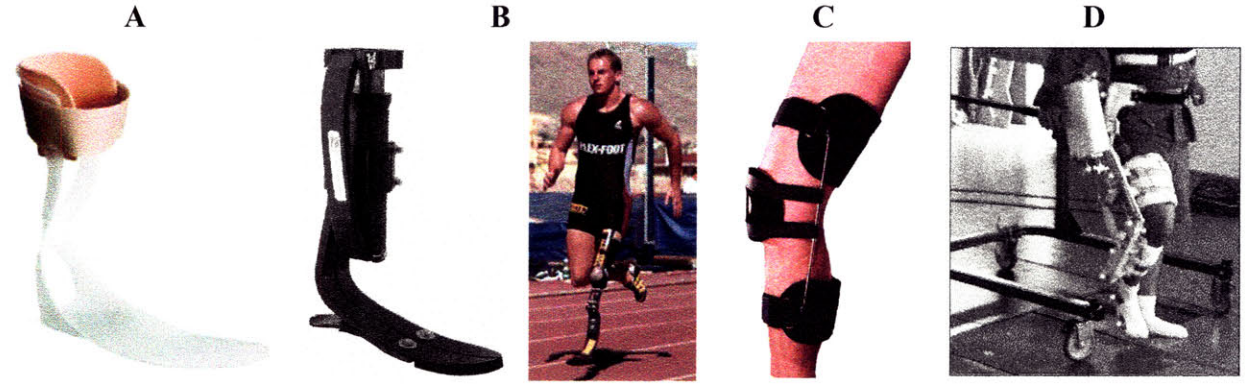

Figure 2.9: Leg orthosis support leg joints via a restoration flexional torque. Image (A) from [26], images in (B) from [26] and [27], image (C) from [28], and image (D) from [29].

allowed an amputee sprinter to run the 100 meter race in 11 seconds [27]. Though this prosthesis replaces the function of the ankle and foot, it clearly demonstrates the success that elastically restoring LADs can assist individuals in need. Figure 2.9C is not technically an orthosis or prosthesis but rather a rehabilitation training aid used for strengthening the knee muscles used during flexion by creating a resistive force as the knee is flexed. This idea of an elastically restoring knee joint was expanded upon by researchers at University of Delaware (Figure 2.9D) [29]. Springs were attached to their exoskeleton in order to generate a gravity balancing thrust for the user's leg which could be adjusted to generate a variable support which ranged between zero and one body mass of the test subject. Though this device is too large to operate outside of laboratory environments, it successfully demonstrates the potential to aid stroke patients in rehabilitation, and a foundation for a semi-passive gait augmentation.

2.5 Externally Powered LADs

While most LADs discussed in the previous sections been developed to mitigate leg dysfunctions for the disabled or injured, some have been developed to augment locomotion for healthy agile people in attempts to prolong endurance or enhance strength, akin to 'The 6 Million Dollar Man'[30] [31]. Although they do aid in a target motion, powered augmenting exoskeletons may follow many of the same characteristics of normal gait orthosis since there are both specified to aid a target motion; however, powered exoskeletons explore new levels of torso support and GRF generation not seen in traditional orthosis by augmenting locomotion with instilled energy from a storage source. This blossoming field holds great opportunity for innovation and discovery.

For over 30 years, powered mobility assist exoskeletons have mainly focused on three groups: the military [32], industry [33], and the medically impaired [34]. Though each group has their own specific functional requirements, the main overall goal is to reduce the metabolic energy needed for locomotion. Unlike wheelchairs, exoskeletons allow the user to navigate terrain that a wheelchair could not be able to cross. They allow navigation in an upright position which is similar to a normal gait and therefore a desirable quality for gait augmentation, rehabilitation, sustaining tissue and bone structure, and the physically disabled [35].

Externally powered LADs, commonly called powered exoskeletons, are technically leg orthosis which generate a torso supporting GRF by creating torques about leg joints using an external power source. This torque is usually generated with an electrical or hydraulic actuator which creates the equivalent muscular work needed for an anthropomorphic gait cycle; some of the most recent developments in gait augmentation devices include the following. MIT's AI Lab developed an Actuated Ankle Foot Orthosis (AAFO) to treat a gait pathology known as foot drop using an Ankle Foot Orthosis (AFO) as a base structure (Figure 2.10A) and a series elastic

actuator to control the ankle's rotation (Figure 2.9B) [36]. MIT's Leg Lab developed a lightweight exoskeleton that has a gait controlled actuated hip and a bi-modal passive knee for augmenting the user's ability to carry loads (Figure 2.10C) [37]. Yobotics, a spin off of MIT's Leg Lab, created an actuated knee brace called Roboknee to augment or replace the muscular functions of the knee to help people who have difficult with knee flexion and extension (Figure 2.10D) [38]. Berkeley's Robotics Lab created BLEEX, a self-powered exoskeleton for strength and endurance enhancement for the ankle, knee and hip (Figure 2.10D). Using a 3 HP generator and hydraulic actuators, BLEEX is one of the most coherent lower body powered exoskeleton [39]. Moving slightly away from exoskeleton LADs, Ossur's Power Knee is designed for above-knee amputees and is one of the most advanced powered prosthetics on the market (Figure 2.10). With its battery and motor incorporated into the volume of the knee and shank, the Power Knee can "lift the user when standing from a seated position; support the user while ascending inclines; and power them up stairs" [40]. Though this prosthetic does not give superhuman performance, its success shows promising direction for what the future will bring.

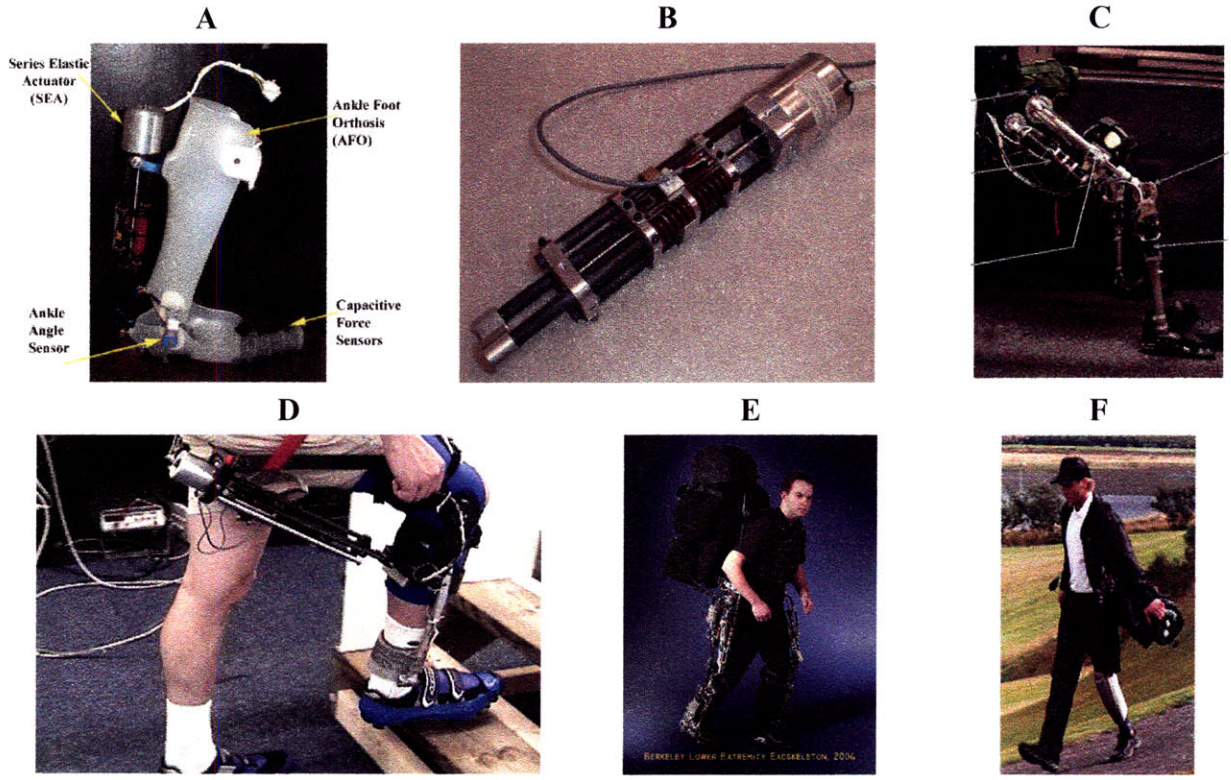

Figure 2.10: (A) MIT's AI Lab AAFO [36] (B) A Series Elastic Actuator used to instill energy into powered orthosis systems [36]. (C) MIT's Leg Lab hip actuated load carrying LAD [37]. (D) Yobotics' RoboKnee [38], (E) Berkeley's BLEEX [39], (F) Ossur's Power Knee for amputees [40].

Though powered exoskeletons are extremely useful in assisting or augmenting locomotion, the high energy demands of powered gait assist exoskeletons are their limiting obstacle. Legged walking assist systems require a considerable amount of energy to dynamically support the

motion of the user's torso against gravity while accelerating and decelerating the limbs and the body's torso [41]. Though Legrangian mechanics show that the energy cost of legged locomotion for humans is approximately 60 W [42], after factoring all losses into a physical system, a military spec powered locomotion assist device is estimated to require 600 W for full functionality [43]. Since this augmented mobility comes with a high energy demand, most solutions for these exoskeleton require a tethering umbilical cord to supply power in a laboratory environment, or a bulky internal combustion engine strapped onto the user's back [39]. As a result of these high energy costs, augmenting exoskeletons are still bound by the energy-density of their power source. Fortunately, recent jumps in emerging technological bring assistive exoskeletons closer and closer to the cusp of realization. Until portable energy sources acquire densities high enough to power these energy demanding exoskeletons, another solution needs to be investigated. When presented with such challenges, we look in nature for the simple solutions. It has been working on such problems for millions of years and routinely embodies a grace which cannot be rivaled.

2.6 Nature's Efficient Locomotion

Locomotion is a required task for all humans and other legged animals. In order to locomote, a leg must be able to extend in order to thrust the torso forwards. In order to do so, leg joints must flex prior the start of thrusting so the leg has ability to extend. Leg flexion occurs when a foot strikes the ground in order to absorb the energy of impact, decreasing the jarring effects on the body. Since metabolic energy is consumed when leg muscles both absorb the energy of impact and thrust the torso forward, a lot of energy is associated with the legs during locomotion. Fortunately all the energy associated with locomotion does not have to come directly from muscular work alone.

Torso support results from the appropriate torque generation about leg joints that is created by a force and a moment arm at the leg joint. This supporting force comes from muscles and tendons which collectively work in series to apply forces to bone structures. Muscles function as actuators which apply forces to tendons. Tendons are elastic tissue that connects muscle to bone (Figure 2.11). Applying the correct combination of muscles and tendons to the structural geometry of a leg, nature has developed many efficient legged locomotion systems. Learning what we can from nature's proven design scheme, more energy efficient LADs might be developed.

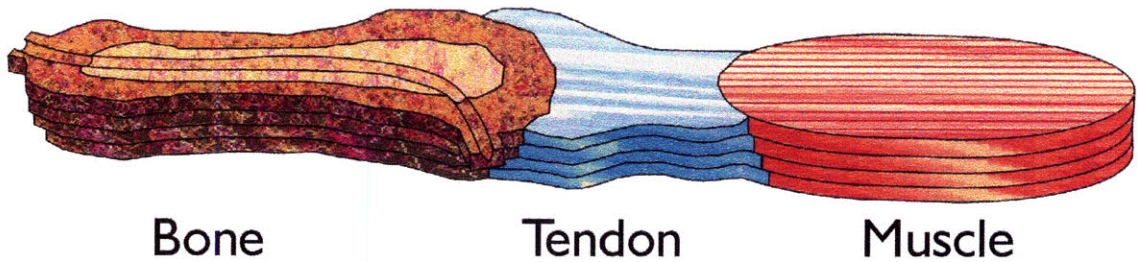

Figure 2.11: Muscles and Tendons function in series with each other to exert forces on Bones [44].

Terrestrial animals like horses, kangaroos, rabbits and dogs all share similar leg mechanics which allows a highly efficient gait cycle [45]. Their efficient locomotion results from specialized muscle-tendons fibers that span multiple leg joints (Figure 2.12). During leg compression (flexion), the long tendons elastically store strained gait energy about the leg segments in a distributed manner. During leg extension (thrusting), the stored energy is returned to the gait cycle with the appropriate torque distribution at each leg joints [46]. These organic spring-mass systems can often make effective use of these passive elastic properties to generate part of the required force for locomotion. The gait energy which could not be elastically restored by the tendons is accounted for with the specialized muscles connected in series to these elastic tendons to drive the system. This actuated spring-mass system is akin to the well known pogo stick. For periodic vertical motion, gravitational potential and inertial changes are possible by elastically storing and later releasing energy, reducing the required driving cost [1]. The musculotendinous bundles in a horse's leg are an excellent example of this design scheme. Of the seven bundles in the leg, four of them are almost entirely springy energy storing tendons that span up to four major joints. The other bundles are much shorter, composed mainly of strong specialized muscles capable of generating a large amount of thrusting force [45]. This combination of muscles and tendons results in a limb design that has a mechanism akin to a pogo stick and catapult that work together creating efficient locomotion.

Figure 2.12: The muscle-tendon anatomy of a horse's leg allows an energy efficient gait. Long tendons which span multiple joints capture and release gait energy, much like the spring in a pogo-stick. Short strong muscle thrust forwards, much like a catapult. Images from [47] and [48] respectively.

Horses are an example of efficient locomotion. In effort to create an augmenting LAD, the fundaments of an efficient gait should be understood prior building upon them. When the Wright brothers wanted to fly they didn't copy a bird and all its muscles, they first created an un-powered glider. Once they perfected it, they added power. Locomotion is a similar problem. If the core design is not seeded with the correct direction, adding energy to the system will not necessarily account for a poorly seeded design.

2.7 Dynamic Walkers

2.7.1 Passive Dynamic Walkers

Passive Dynamic Walkers (PDWs) are remarkably simple devices that are constructed from solid bodies connected by rotational joints. They can be built to walk down subtle slopes under stable conditions with motions very similar to humans even without any actuators or control system [49]. PDWs represent the simplest machine that could be built which captures the essence of stable dynamic walking. These mechanical walkers provide an elegant illustration of how proper machine design can generate stable and potentially very energy-efficient walking. Insights into the success of PDWs allow a solid basis to build upon for the development of anthropomorphic LADs.

There are a range of passive dynamic walkers which have been created to gain insight into a different quality of the human gait cycle in the quest for efficient locomotion. The variables which have been explored include the relevance of the head, arms and torso during locomotion, the width between the hip joints, the importance of a knee, relevance of an ankle, and the size and shape of foot (Figure 2.13) [49]. Passive walkers are extremely efficient at locomotion; defined as:

$$\eta = \frac{average\_forward\_kinetic\_energy}{energy\_gained\_from\_gravitationaal\_potential} \qquad \textbf{Equation 2.1}$$

As the walking slope progressively decreases to horizontal, less and less energy is gained with each step. Simulations for properly constructed walking models show that closed loop cyclic solutions exist for all negatively sloped surfaces [50]. Though physical passive walkers do have their limits, prototypes have operated remarkably close to their theoretically maximal efficiency [51].

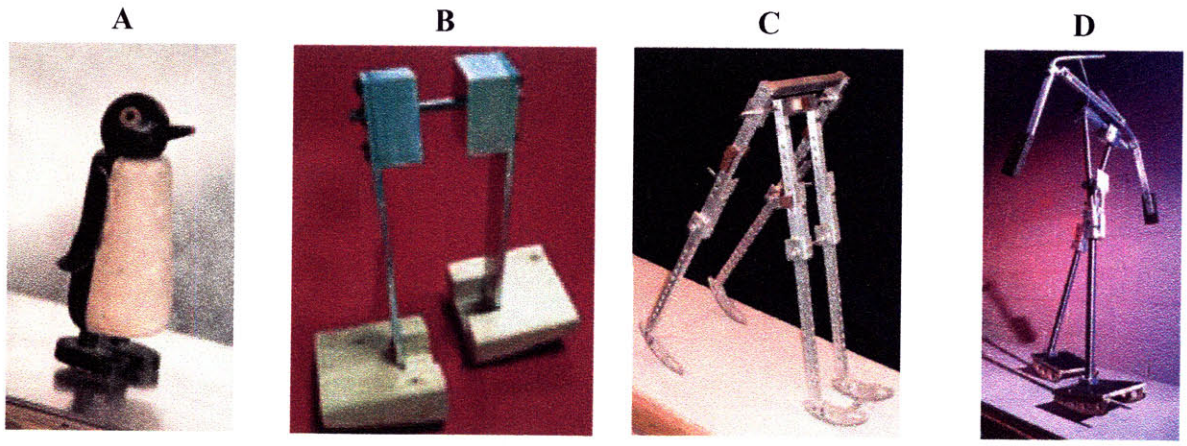

Figure 2.13: Passive Dynamic Walkers. (A) The Wilson "Walkie" [52], (B) MIT's improved Wilson "Walkie" [53], (C) Cornell's copy of McGeer's capstone design [49], (D) Cornell's kneed passive biped with arms [54].

2.7.2 Actuated Dynamic Walkers

The next step beyond the limitations which bind passive dynamic walkers (i.e. flat or inclined surfaces and frictional losses) is the addition of actuators to the legs. Actuated Dynamic Walkers (ADW) use a small quantity of stored energy to power actuators which mimic the function of muscles of the leg in order to attain further insight into the mechanics of human walking. This new class of powered dynamic walkers is at the forefront enlightening the development of augmenting LADs.

Using PDWs as a base, MIT, Delft and Cornell created functional ADWs using either batteries or pneumatics as their energy source. MIT's ADW (Figure 2.14A), while not as efficient as Cornell's, uses a clever learning algorithm to control the electric actuation for each ankle in order to find a stable gait cycle.

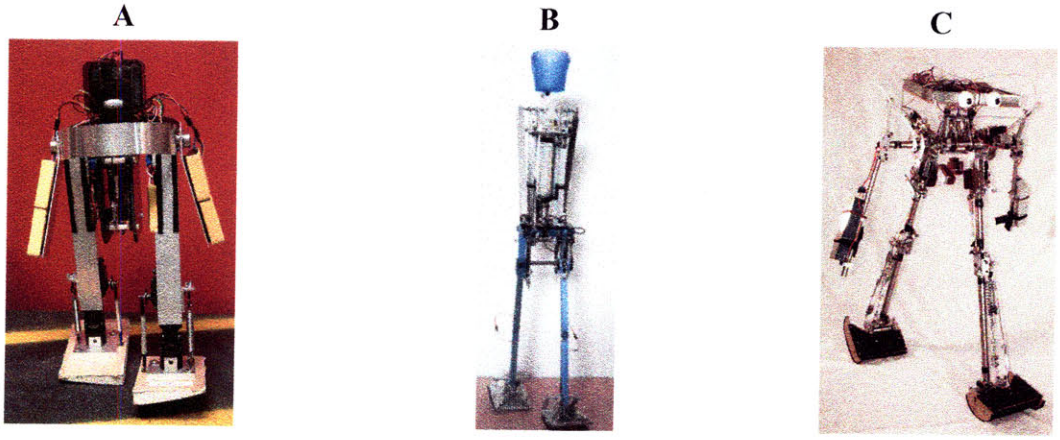

Figure 2.14: Actuated Dynamic Walkers. (A) MIT's powered biped of the Wilson "Walkie" [53], (B) Delft's pneumatic biped [49], (C) Cornell's powered biped [49].

The design of Delft's ADW (Figure 2.14B) took a different path, using pneumatics to control artificial muscle-pistons at each hip. Cornell's ADW biped (Figure 2.14C) was designed to minimize energy consumption for each step. Using motors and solenoids that control springs which provide thrust for the ankle, Cornell was able to create one of the most energy efficient and anthropomorphic walking robot to date [49].

Though research into actuated dynamic walkers is a fairly new, these energy efficient walkers are providing great insight into human locomotion [49]. Further research on these powered walkers will pave a path for more realistic ambulatory humanoid robots, new prosthetic limb designs, and powered exoskeletons allowing superhuman strengths. Only by combining our understanding of the biological components associated with human locomotion and these mechanical devices can the correct correlations between man and machine be made; allowing the development of an energy efficient LAD which is both functional and organic.

3 Analysis of Human Locomotion

While it is important to have an understanding of prior LAD development, one must also understand the human gait cycle to appreciate the different approaches. For this reason, an analysis of the human gait cycle and its associated anatomy is provided. Insights reveal simplifications to the human gait model that can be made with minimal sacrifice in anthropomorphic motion while closely matching existing mechanical locomotion devices. Only by correctly correlating the connections between man and machine can a solution be achieved which is both functional and organic.

In this chapter, the human gait cycle and its associated biological components is presented, analyzed and correlated. Using this information, a gait model which appears to exhibit anthropomorphic behavior is introduced and simulations are conducted. Using these results, new, energy-efficient, augmenting LADs are designed, built and tested.

3.1 What is Locomotion

The human body has hundreds of skeletal bones and muscles for structural support and force generation [55] [56]. Functioning together, they allow all the motions we use on a daily basis. Since everyone has their own idiosyncratic mannerisms, there is no right or wrong way to walk or run; however there is an overall theme – Energy Conservation [3]. Giovanni Borelli (1608 – 1679) realized this common characteristic and stated: "A perpetual law of Nature consists of acting with the smallest work." Extrapolating from Borelli's statement, we see that locomotion follows suit such that the integral motions of all leg segments attempt to minimize metabolic energy consumption, and that any deviation from these relationships will invariably result in an increased metabolic cost of locomotion.

Due to the physiological construction of the human skeleton, the body uses an elaborate set of energy minimizing motions in order to travel from place to place with the least amount of energy required. While some of these motions are mandatory for anthropomorphic locomotion, others have higher order effects, which smooth the trajectory of the torso, enabling a more efficient locomotion. In order to optimally design a LAD which uses these energy minimizing motions to its advantage, one must determine what actions are required for torso support, and what motions exist to generate second-order smoothing effects for the torso.

3.2 The Human Gait Cycle

The human gait cycle is defined as "the interval of time during which one sequence of regularly recurring succession of events is completed." It can be broken down into 2 phases, 6 periods and 7 events, each representative of the progression throughout one cycle (Figure 3.1) [3]. By definition, a human stride is initiated at the heel strike of one foot and continues through to the heel strike of the same foot; this is one gait cycle. To better explain the periods of a cycle, the support phase of one walking stride is broken down using a simplified model consisting of a point mass representing the torso and force vectors representing the GRF generated by the legs (Figure 3.2).

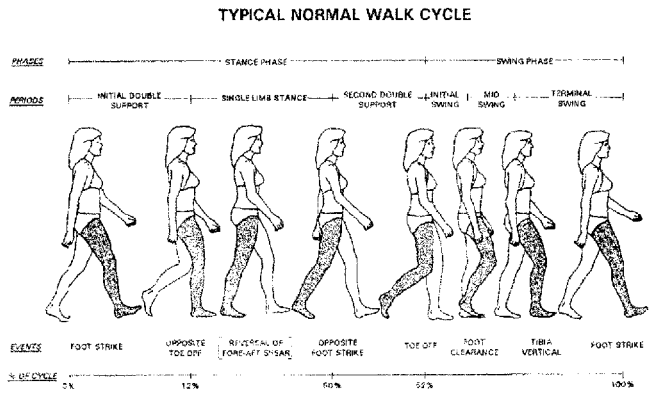

Figure 3.1: The human gait cycle can be broken down into a stance phase (where the leg supports the torso above the ground), and the swing phase (where the leg swings forward in preparation for the next step) [3].

In walking, heel strike initiates the double support phase where both legs are in contact with the ground generating a torso support force. During this double support period, weight is transferred from the old stance leg to the new stance leg. This is known as the Weight Transfer Epoch (WTE). Shortly after heel strike, the new stance leg produces a small force supporting the torso while the majority of the weight is still supported by the old stance leg. Midway through WTE, the old and new stance legs support the torso weight about equally. Near the end of the WTE, most of the torso weight is supported by the new stance leg with only a small fraction supported by the old stance leg. At opposite toe off, the old stance leg has pushed off the ground, becoming the swing leg and completing the WTE. As the new swing leg swings forward in preparation for its next heel strike, the torso is solely supported by the stance leg. At system apex, the person's hips are directly over the ankle, the system's horizontal velocity is at its minimum, and the stance leg thrust vector points directly upward. Shortly after system apex, but prior the next heel strike, the calf muscle is excited, causing the angle between shank and foot to increase and the heel to lift off the ground.

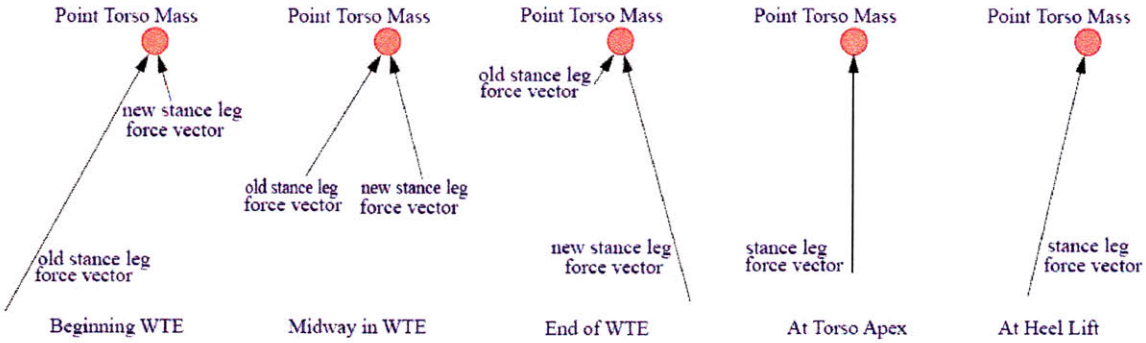

Figure 3.2: The weight transfer epoch represented with a point mass for the torso and vector forces for the actions of the legs

3.3 The Ground Reaction Force (GRF)

As previously stated, the basic requirement for locomotion is the periodic generation of a varying GRF such that the system remains in a steady state cycle. The GRF is transferred through the legs from the foot's center of pressure in contact with the ground up to the pelvis where it supports the torso (Figure 3.3).

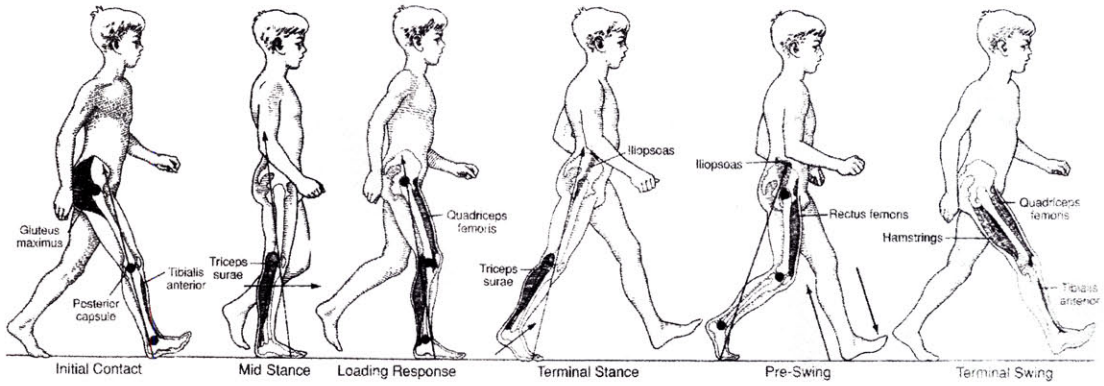

Figure 3.3: The torso supporting GRF is generated by the legs and is transferred from the foot's center of pressure in contact with the ground to the pelvis [3].

Recall that with each step, the torso falls and rises a few centimeters and its velocity decreases and increases as it passes over the support leg and foot (Figure 3.6). During walking (Figure 3.4A) in order to for the torso to maintain a consistent average height above the ground, the sum of the vertical components of the GRF must average to body weight over the gait cycle. If this were not true, then the torso would accelerate upwards or downwards and would not maintain a constant average height above the ground. Similarly, as the horizontal velocity of the torso increases and decreases, the average net horizontal force produced by both thrusting legs must be zero. If this were not the case, then there would be an average horizontal acceleration, and the system would slow down or speed up, nullifying the requirement for a steady state gait cycle.

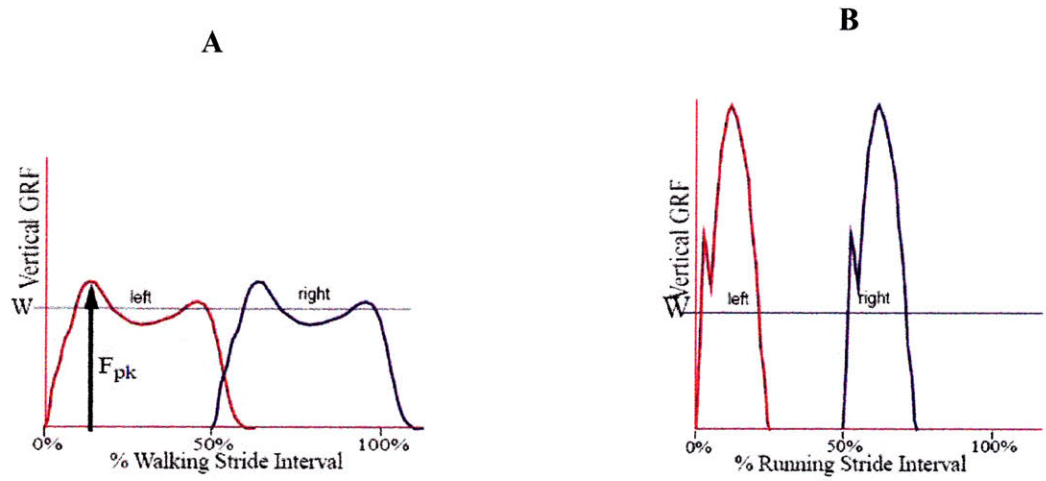

Figure 3.4: The vertical component of the GRF normalized to body weight over one gait cycle for (A) walking and (B) running.

Unlike walking, there is no WTE during running. Instead, there is an airborne phase during which neither leg is in contact with the ground (Figure 3.4B). Since the legs need to generate the same average GRF as walking, peak running GRFs must be dramatically higher since they support the torso for a shorter duration. So, since higher running velocities result in shorter support periods (Figure 3.5A), peak GRFs are directly proportional to running speed (Figure 3.5B). This is explained further in Appendix C and Appendix D.

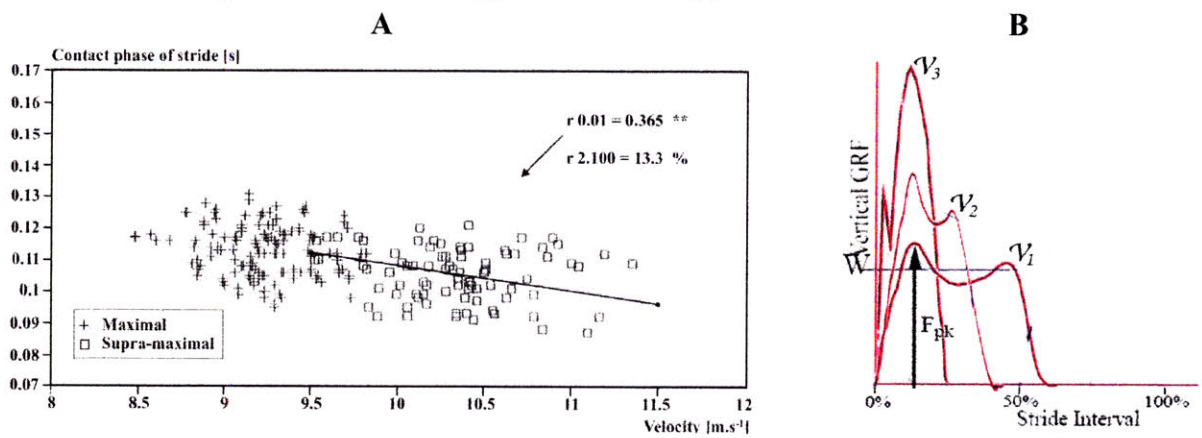

Figure 3.5: (A) Leg Contact Duration vs. Running Velocity [57], (B) The vertical component of the GRF normalized to body weight at 3 different gait velocities. Note the shorter relative support periods and higher peak forces with higher velocities.

3.4 Mechanics of Locomotion

The largest component of metabolic energy consumption during locomotion is associated with the leg's production of an upward thrust to support the torso [3]. In order to develop an energy

efficient LAD, we must first develop the simplest gait model capable of generating the closest approximation of this naturally occurring trajectory.

Though the human leg is an extremely complicated force generating mechanism composed of intricate joints, skeletal structures and organic actuators, when boiled down to the basics, in order to support the torso, the leg has to generate a GRF in order to resist buckling (Figure 3.6B). Looking at a simplified skeletal structure of the leg (Figure 3.6C), it is composed of a foot, ankle joint, shank, knee joint, thigh and hip joint. Though a foot and ankle do aid in smoothing the sinusoidal trajectory of the pelvis, any person with a flail ankle can attest that it is not mandatory for torso support generation or locomotion. If the ankle can not generate 'normal' gait torques, though the gait cycle is somewhat effected (see Appendix A for details) this case is akin to the peg-leg shank.

The knee, on the other hand, is definitely mandatory for torso support. If the knee cannot generate necessary torques, the leg will buckle and the person will collapse; there is no way around this. Knowing this, the simplest anthropomorphic walking model can be constructed from a peg-leg shank, a knee joint, a thigh and a ball and socket hip joint located at the pelvis (Figure 3.6D). This statement is later supported with simulated gait model presented in Section 5.4, and a decomposition of the ankle and foot's trajectory in Appendix A.

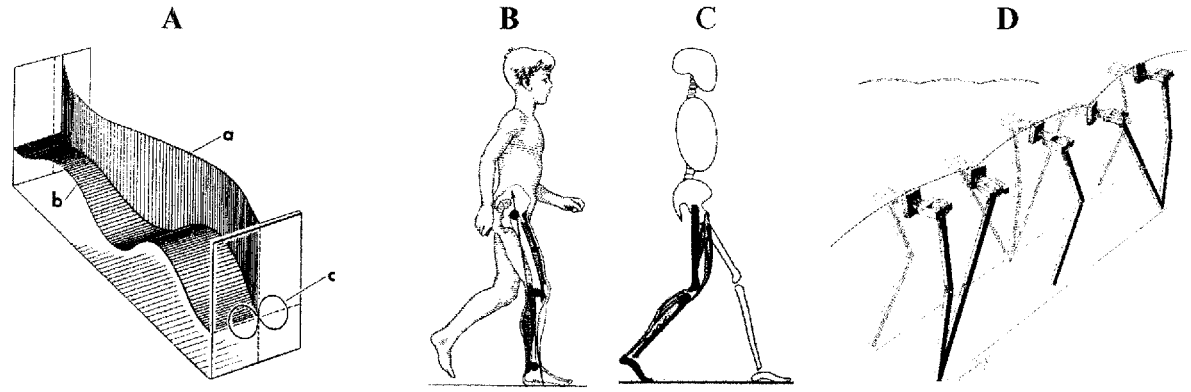

Figure 3.6: (A) The 'lazy 8' trajectory naturally traced out by the pelvic center of mass [3], (B) and (C) GRF generation by the leg and skeletal system [3], (D) the simplest anthropomorphic model capable of generating such a path [3].

3.5 Muscles and Torso Support

Muscles are the contractile tissue of the body that changes length when electrically activated in order to exert forces on bones; enabling locomotion. In order to determine appropriate methods for physically augmenting locomotion, it is important to understand the basic functionality of the muscles and their interactions with individual leg segments throughout the gait cycle.

The different muscle groups used throughout the stance phase are shown in Figure 3.7. The quadriceps muscle is associated with support and energy absorption after heel strike. The calf muscle is associated with ankle control as the body rotates about the stationary foot and the plantarflexion of the foot which aides in GRF generation by lifting the heel, pushing the body forward in preparation for the next step. Note the volume difference between the quadriceps and the calf; this strongly suggests that there is a larger muscular demand during the weight acceptance and energy absorption period of the gait cycle, implying a greater energy consumption.

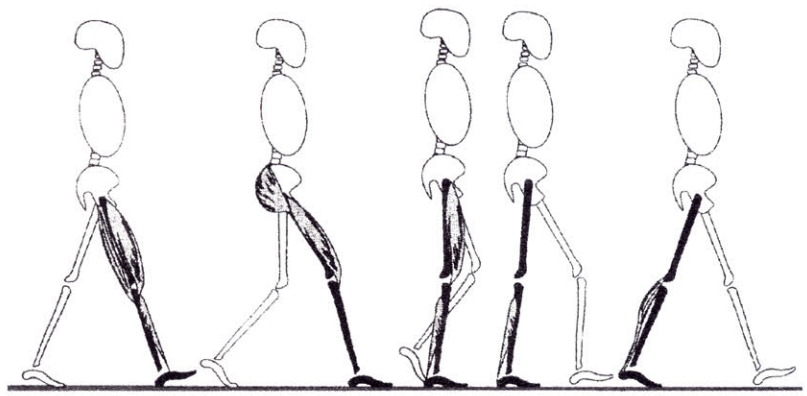

Figure 3.7: The muscles used throughout the support period to generate the GRF. Note the larger scale of the quadriceps muscle which absorbs the energy of heel strike and slows the vector velocity of the torso, in comparison to the scale of the calf muscle responsible for actions associated with the ankle such as plantarflexion of the foot [3].

Throughout the gait cycle, in order to keep the system stable, the leg must absorb energy during knee flexion and later inject it into the leg via muscular contractions. The quadriceps absorbs and injects the required energy by creating a varying torque over its rotational displacement. In order to meet this energy requirement, the knee can generate high torques about a small knee rotation, or low torques about a large knee rotation.

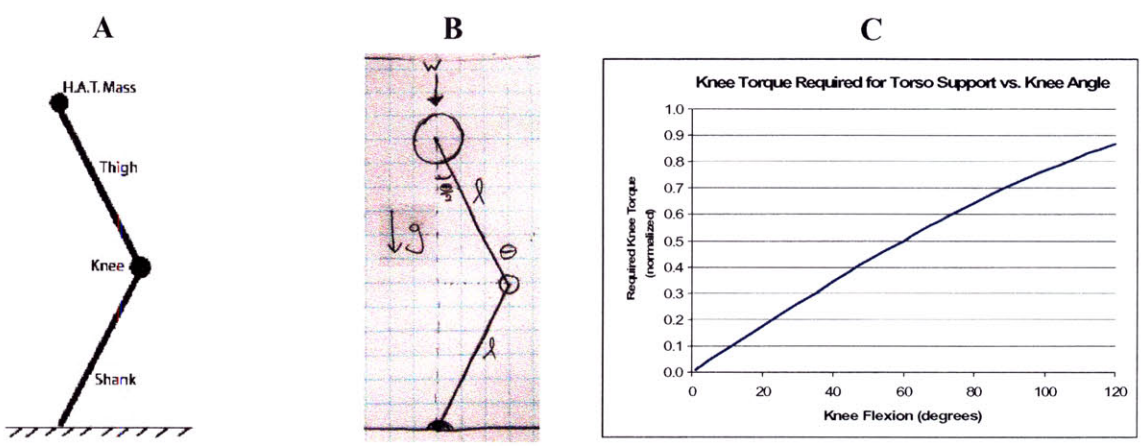

Figure 3.8: (A) A first order anthropomorphic leg model consists of a peg-leg shank, a knee, a thigh and a ball and socket hip located at the Torso point mass, (B) a Free Body Diagram of the simplified leg generating torque at the knee to support the torso, (C) the Knee Torque (normalized to body weight and leg length) required to support the torso vs. Knee Angle flexion.

Due to the geometric structure of the leg, the torque required to support the torso increases at greater angles of knee flexion. Using the simplified model of the leg, the quadriceps is

responsible for generating the varying torso support (Figure 3.8A), a free body diagram of torso support is presented (Figure 3.8B). The knee torque required to support the torso over a range of knee flexion was determined using Equation 3.1, where 'W' is the weight of the torso, θ' is magnitude of knee flexion, and 'l' is the length of the thigh assuming the shank and thigh are equal length. This torque profile, normalized with respect to body weight and thigh length, is shown in Figure 3.8C.

$$T_{knee}(\theta) = W * l * \sin\left(\frac{\theta}{2}\right) \qquad \textbf{Equation 3.1}$$

Since the maximum GRF the leg can produce is governed by knee angle, this constraint leads to the concept of a 'Critical Knee Angle'. The critical knee angle is defined as the maximum angle the knee can flex while supporting a specific force; and it is a common concern for elderly people.

As people get older, their muscles weaken, and their ability to produce joint torques decreases. Though the strength of muscles are dependent upon the person, if the torso exerts a load on the leg which is greater than the maximum GRF that can be generated at that knee angle, there will no longer be a balance in vertical support forces, and the knee will flex. As knee flexion increases, the maximum GRF the leg can generate decreases and the leg can never rebalance the vertical forces on the torso and the leg will 'give out'; thus, a person falls.

There are two types of muscles, slow and fast twitch. Slow twitch muscles act over a longer distance with a lower peak tension, and fast twitch muscles act over a shorter distance with a higher peak tension [3]. This results in lower rates of muscular contraction at higher loads, and higher rates of contraction at lower loads (Figure 3.9A). This constraint, when coupled with the geometry of the leg, is an unfortunate fact for sprinters, rowers, weightlifters, and other people involved in activities which benefit from higher force generation in short durations.

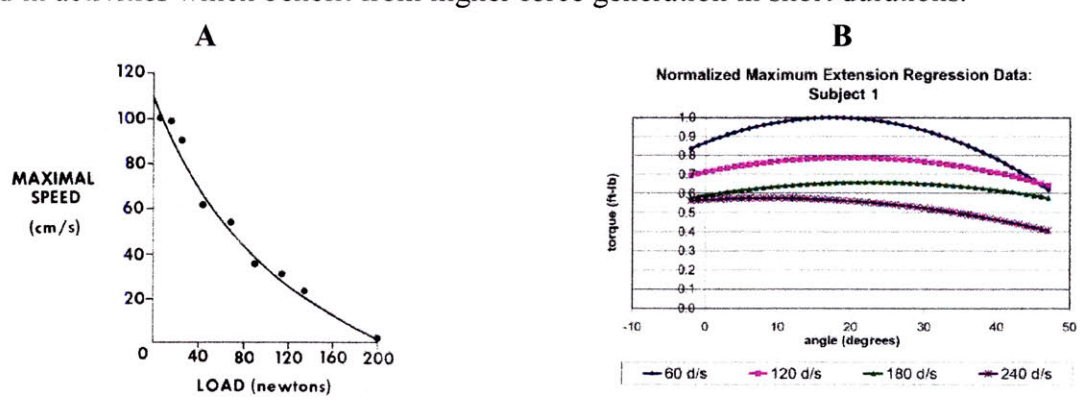

Figure 3.9: (A) Muscular Shortening Speed vs. Peak Force Generation. Faster rates correlate with lower loads [3], (B) Peak Knee Torques (normalized to body weight and leg length) vs. Knee Angle at four different rotational rates. Note that as the knee flexes, the maximum torque (and GRF) the leg can generate decreases.

Since the peak muscular forces (torques) capable of being generated by the knee decrease at higher angular rates of rotation, the ability to generate appropriate torso support also diminishes as the rate of knee flexion increases. Coupling this with the thrust limitation associate with the angle of flexion reveals that larger angles of knee flexion and higher rotational rates of flexion limit the peak torques and GRFs capable of being generated by the leg. A plot of this relationship is shown in a normalized graph (Figure 3.9B).

In summary, the leg can support larger loads when the knee is bent less or flexing at a slower rotational rate. In addition, with the geometry of the knee joint (Figure 3.11A), the leg can theoretically support extremely large loads if the knee is locked fully extended with no flexion. Unfortunately, having the knee locked for the support period is not feasible due to the high compressive loads that the knee joint and associated tissue must sustain. First, the body is an organic, living entity which will get damaged upon the impact of heel strike with a locked knee as a result of the sudden and sharp impacts. The knee must bend in order to safely absorb the energy associated with heel strike. Second, in order for the leg to generate a thrust, the knee must extend. In order to be able to extend, the knee must flex at some prior point.

3.6 Leg Kinematics of Locomotion

In order to create an anthropomorphic augmenting LAD which is as compliant with natural movement as possible, we must understand the motions associated with the human gait cycle. Since the knee joint is mandatory for GRF generation, and the gait model is composed of a peg-leg shank, knee and thigh, we focusing on the knee's characteristics.

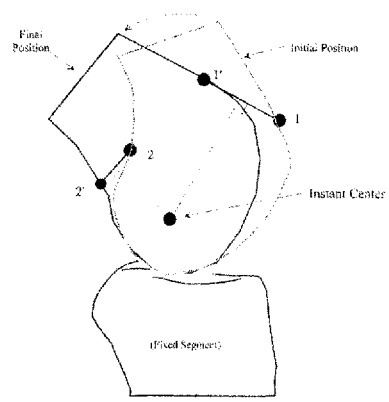

Figure 3.10: The instant center of the knee's rotation [3].

The skeletal bones of the knee joint are shown in Figure 3.10. Due to the geometric interface between the bones, the knee both slides & rolls about the joint. This complex rotation results in an instant center located at the bottom of the femur. Knee flexion throughout a gait cycle (Figure 3.11B) can be broken down by the stance and swing phase. Upon the start of the stance / support phase at heel strike, the knee is never fully extended or locked. The initial state of being slightly

bent requires further knee flexion in order to absorb the energy of impact. In walking, this flexion is approximately 20°. Upon completion of the torso supporting phase, the knee rapidly flexes approximately 60° in order to accommodate adequate foot clearance during the swing phase in preparation for the next step [3].

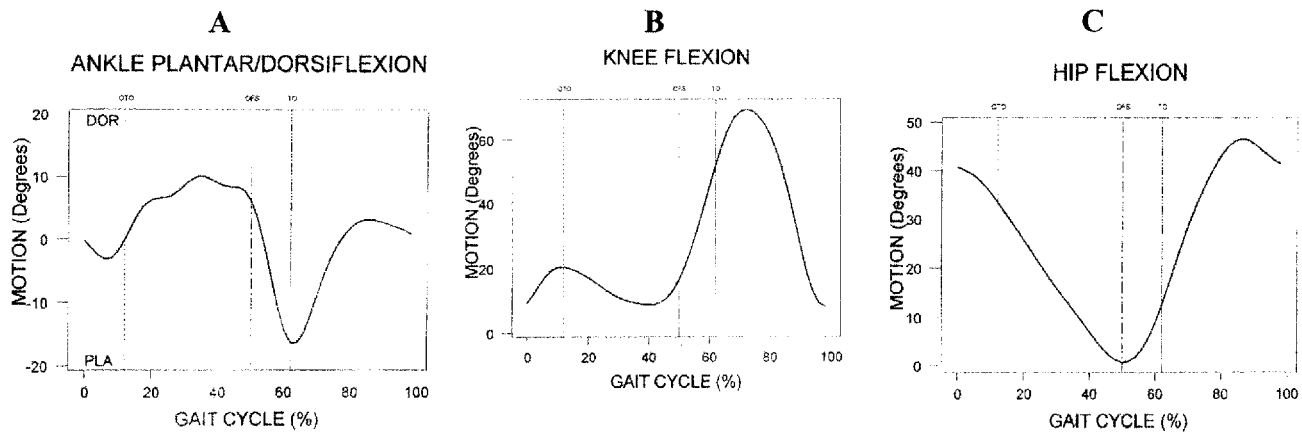

Figure 3.11: (A) Ankle plantar-dorsiflexion [3], (B) Knee flexion and extension over a gait cycle [3], (C) Hip flexion and extension [3].

Comparing knee flexion and GRF generation throughout ranges of the gait cycle (denoting the range: [$n_1 - n_2$%]) reveal insightful correlations (Figure 3.12). [0 – 12%] At the start of the support phase and weight transfer epoch, the knee flexes in order to absorb the energy of heel strike while the leg's GRF increases as support is transferred from the old support leg to the new. [9%] Peak knee flexion occurs at the end of the WTE which is also when the GRF equals 1.2x body weight. [9 – 12%] As the GRF continues to increase, the leg thrusts the torso upwards and the knee promptly begins to extend; peak GRF thrust at the end of the WTE. [12 – 40%] As knee extension continues, GRF generation slightly fluctuates, averaging to a thrust of approximately 1x body weight. [40 - 50%] Upon fully extending the leg, the ankle plantarflexes the foot; this lifts the heel, increases the GRF and initiates the second round of knee flexion in preparation for foot clearance during the swing phase. [50 – 62%] At the start of the next WTE, heel strike of the other leg, the GRF generated by the initial leg rapidly decreases and knee flexion continues. [62 – 100%] After toe-off, the stance phase becomes the swing leg, the knee continues to flex and finally extend, completing one gait cycle.

Figure 3.12: GRF and Knee Flexion throughout a gait cycle. Note that peak GRF occurs at max knee flexion of weight acceptance period of the support leg [3].

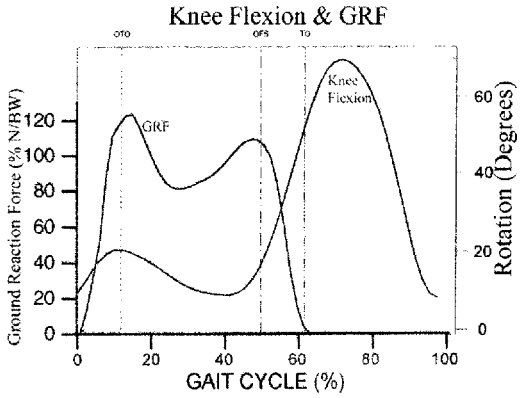

Seeing that there are two separate thrusting phases from the knee and then the ankle, since there is only one energy absorption phase by the knee and the quadriceps (the largest muscle in the body), this further justifies creating a LAD which focuses on the knee joint.

3.7 Summary

During normal locomotion, the human torso is structurally supported by the foot, shank and thigh, while the calf and quadriceps provide the muscular forces at the ankle and knee which allow movement. In a simplified view of locomotion, proper torso support can be generated by the muscular actions of the knee alone. Though the secondary actions of the ankle and foot do help to smooth the vertical displacement of the torso, they are not mandatory for torso support. In creating a first order locomotion assistive device, focusing on the actions and function of the knee alone shows strong potential for success.

4 Design Architecture

The goal of this thesis was to develop a LAD that increases performance by reducing the muscular force and metabolic energy required for human locomotion. This LAD should increase performance without impeding the user's natural motions, have a transparent interface such that it feels like a natural extension of the body, and be both comfortable and safe enough to use for extended durations without decreasing its augmentation performance. In order to do so, existing designs should be evaluated in order to draw upon draw upon what worked and avoid what did not. To reduce the complexity of the system, the design should be simple and accomplish its desired functions in an uncoupled manner. For this reason, the functional requirements and design parameters of the LAD system must be defined.

4.1 Functional Requirements:

1. Appropriate Torso Thrust
2. Organic Human Interface
3. Longevity
4. Easily Controllable

The system must be able to generate the appropriate thrust between the ground and the torso such that the body is appropriately supported throughout the gait cycles. Since the GRF requirements vary with locomotion velocity, any gait augmentation is likely to alter the cycle to some degree. Therefore, it is desired to minimize this deviation from the user's normal gait cycle.

In order to generate a torso thrust which is helpful, the system must have an interface which is compliant with the human body. The design must be both comfortable enough to wear for prolonged durations without causing discomfort or tissue damage. Tissue needs oxygen to live and will not survive if subjected to high pressures for extended durations. For this reason comfort is a primary concern.

The system must be self sufficient for prolonged durations without the need for recharging or refueling. Since thrust generation requires energy, torso thrust generation must either be highly efficient or supplied from an energy source with a very high energy density.

The system must have a transparent control interface such that the LAD feels like an extension of the body. If this is not the case, then along with being difficult to operate, it will have a

noticeable affect on the user's natural gait. Although the body can adapt and learn remarkable well to new walking conditions, it is still desirable to minimize the change that the device will have on the gait.

In addition to these functional requirements, the system should be light weight in order to minimize inertial effects during leg swing. Its design should be adjustable in order to comply with people's various sizes. It should be relatively simple and feasible to manufacture so that the cost is realistic for a consumer to purchase. The LAD must be easy to don and doff without assistance, preferably in less than 2 minutes, so that the user does not mind putting it on. Likewise, the device must be able to supplement locomotion enough to justify using the device.

4.2 Discussion

Upon consideration of existing LADs previously discussed in comparison to the stated functional requirements, a few trends emerge. Series supporting LADs have some good qualities, especially for the longevity requirement. They are compliant with the human body, their elastic mechanism harvests energy from the gait cycle, allowing extended use with no external energy source, and though there is a learning curve, they are easy to use. Unfortunately, the elastic mechanism that transfers forces between the ground and the bottom of the foot still requires the force to be transmitted through the knee, but with an altered thrust requirement. Because of this, series supporting LADs drastically alter the gait appearance and feel for the user.

Standard parallel supporting LADs, as seen in Figure 2.8, have the potential for excellent torso support. Bimodal LADs fit almost all the requirements put forth. They comply with the gait cycle and offer a transparent control interface by offering support while the foot is in contact with the ground and free rotation for the knee when the foot is in the air. However, they are deficient in generating an anthropomorphic torso thrust; they either provide no support when the foot is free to rotate or all support of applied loads when the user's foot is in contact with the ground.

Elastic joint restoring LADs combine some of the better qualities of the series and parallel supporting LADs. Like series supporting LADs, elastic LADs harvest and restore some of the energy associated with the gait cycle, giving them great potential to comply with the longevity requirement and the generation of anthropomorphic support. The major deficiency in parallel supporting elastic joint LADs is their infancy in development. At present day, since their elastic energy storing component inhibits the target joint from freely rotating during the necessary gait phase, they are only suitable for joints where free rotation is not critical. This is the primary reason that commercially available Elastic Joint Restoring LADs, such as the Flex Foot, are for the ankle and not for the knee. Though the gravity balancing exoskeleton developed at

University of Delaware does address the torso support associated with the knee, this device is presently only suitable for the laboratory environment. Though gait dynamics are not addressed for University of Delaware's exoskeleton, Ossur's ankle prosthesis were designed to accommodate different user's gait. Though these ankle LAD's are configurable for each user, since they have a set spring constant, their assistive performance diminishes as the gait strays from what the device was tuned; resulting in control difficulties at different gait velocities.

Though externally powered LADs have been researched for over 30 years, they are still in the developmental research stage. Though Ossur's Power Knee shows many signs for being the most functional powered LAD solution on the market, its interface is only compliant with above knee amputees. Aside from this shortcoming and its inability to generate the required GRFs of higher walking speeds, the Power Knee functionally addresses almost all the functional requirements. This is a common problem for powered augmenting LADs. Generating the desired thrusts profiles necessary for a varying locomotion requires relatively high powered actuators and therefore a substantial amount of stored energy. Since power density is presently their limiting throttle, any powered device that does not decrease the overall energy consumption will result in a device which is bulky, heavy, expensive and overlooks the longevity requirement. Though functional powered exoskeletons do exist, they only address three of the four functional requirements. A self sustaining solution which is capable of prolonged use requires efficiency, and therefore must be accordingly designed.

Drawing upon the pros and cons of the different LAD schemes, it appears that an energy efficient design is possible while still appropriately addressing all the functional requirements. In light of the success the Wright brothers achieved after modeling their airplane with a gliding bird, the pursuit of a nature-inspired solution is investigated.

4.3 Nature-inspired Solution

In nature, we see in horses and kangaroos that can capture and restore some of the inherent energy associated with locomotion, resulting in a more efficient gait. If we want to create an elegant LAD, a similar energy capturing and restoring system should be used when augmenting human locomotion. Antonie Bogert came to the same conclusion stating that "poly-articular elastic mechanisms are a major contributor to the economy of locomotion … it should be possible to design unpowered assistive devices that make effective use of similar mechanisms." [47] Working from nature's design, Bogert presented a passive assistive gait architecture which used elastic chords called 'exotendons' and a varying number of pulleys located at the leg joints to minimize the energy of locomotion. It was found that "exotendons could significantly reduce the muscle forces required for locomotion" and that the "results are robust and not dependent on particular details of the model and data that were used." [47] Encouraged by Bogert's pursuit of

a LAD which embodied nature's efficiency, our LAD's design architecture was solidified to consist of a shank, a tuned controllable elastic knee joint, a thigh and a point mass located at the pelvis. Though the basis of this architecture closely follows University of Delaware's gravity balancing design, accounting for the dynamics associated with locomotion requires additional insight.

In the human walking gait, the knee flexion duration is approximately half of the knee extension duration. Since springs follow the laws governing simple harmonic motions, using a simple spring mechanism to generate leg thrust will not be able to follow a true anthropomorphic gait cycle. As the gait velocity is increased to running speeds, the duration of the knee's flexion and extension converge, suggesting that the LAD developed in this paper may be better suited for faster velocities. Since the flexion and extension durations vary with gait velocity, this could result in some gait velocity constraints, however the dynamic responds may still be close enough to give justification for further development. In order to best design this LAD, the design parameters of the system must be determined in order to minimize the system's complexity.

4.4 Design Parameters:

1. Anthropomorphic Structurally Sound Exoskeleton
2. Ergonomic Force Transferring Interface
3. Tuned Energy Spring at Knee Joint
4. Kinematic Gait Control Module

A more detailed description of these modules can be found in Section 6 - Alpha Prototype Architecture.

The exoskeleton needs to comply with the human leg, its kinematic motions and the human gait cycle while it creates a supporting force for the torso. In order to do so, the LAD's exoskeleton must be strong enough to be able to withstand the forces and torques instilled by the energy spring at the knee.

In order for the exoskeleton to effectively generate a torso supporting force to catch and catapult the user in the appropriate direction, the structure must be able to transfer large forces to the human body without causing damage to the tissue. This can be accomplished by using the appropriate cross sectional area to distribute the forces applied to the leg by a saddle or sling module

The exoskeleton's thrusting force is created by the appropriate kinematic response of a spring which generates the appropriate knee torques during the gait cycle. Bogert's design architecture, based upon elastic chords stretched about multiple joints, was avoided since a mechanism which

allowed a controllable knee joint at a low energy cost could not be easily implemented. Instead, in order to maintain a decoupled system, a controllable torsion spring was implemented at the knee joint. The details design of the torsion spring for varying gait cycles is found in Appendix B.

Lastly, since the leg has two phases during the gait cycle (the stance phase and swing phase), the leg must be able to act accordingly during each phase in order to achieve desired anthropomorphic motions. During the stance phase the energy spring at the knee must be able to create torso support upon knee flexion. During the swing phase, the knee must allow free rotation so it can appropriately flex, allowing adequate foot clearance in preparation for the next step. This bimodal knee requires that a gait controlled 'Energy Spring Engaging Clutch' needs to be incorporated into the design.

After solidifying the main functional requirements and design parameters of the design architecture for our passive augmenting LAD, simulations of gait models can be performed.

5 Modeling Locomotion

In efforts to augment human locomotion with an exoskeleton, it is necessary to be able to model the human gait cycle. Since the bones in the legs are relatively stiff and the joints have low friction, a walking model that uses rigid bodies and frictionless joints can be reasonably accurate. Conducting mathematical simulations of walking allow us to easily change parameters, providing an insight and understanding one could otherwise not get.

In order to better design an augmenting LAD for humans, a gait model must be defined and simulations must be conducted. For successful gait simulations, the boundary conditions and the user controllable parameters of locomotion must be defined. Simulations allow the non-dynamic gait parameters to be tuned so the system's kinematic response best conform to the human gait cycle. From these verified and optimized parameters, a physical LAD can be constructed and tested.

5.1 Thrust Generation

In order to have an anthropomorphic gait cycle, the GRF generated between the ground and the hip must match the gait requirements (Figure 5.1A). Using a free body diagram of the simplified leg (Figure 5.1B), the GRF created by the knee torque can be determined (Equation 5.1). Where 'F_{GRF}' is the thrusting force on the torso, 'T_{knee}' is the torque generated about the knee during the gait cycle, 'θ' is the magnitude of knee flexion relative to a straight leg, and 'l' is the length of the shank or thigh. Note that all equations were calculated using radians.

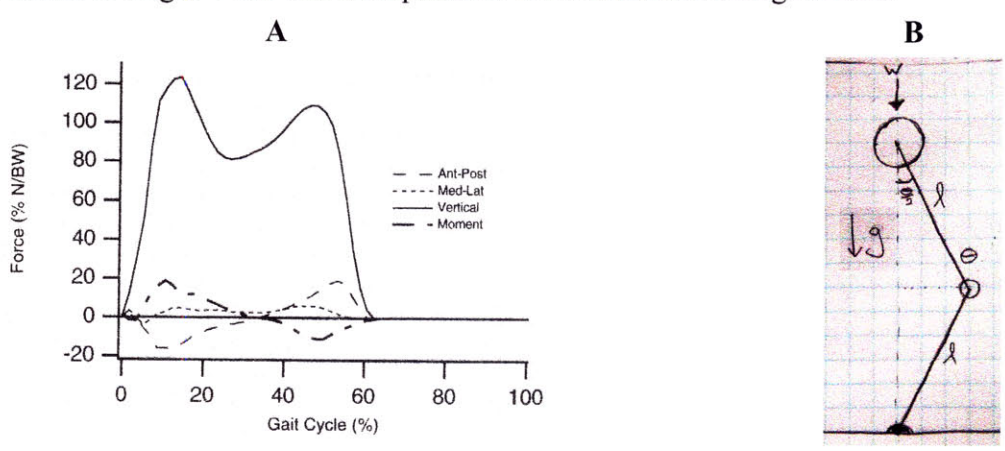

Figure 5.1: (A) The GRF throughout a gait cycle, (B) the free body diagram of the leg which creates the thrusting support force for the torso.

$$F_{GRF}(\theta) = \frac{T_{knee}(\theta)}{l * \sin\left(\frac{\theta}{2}\right)}$$ **Equation 5.1**

Since the knee of our leg is modeled as a torsion spring, there is a stiffness factor for this joint. Much like the specially tuned tendons in the legs of horses, we desire to find the appropriate spring constant for the knee which optimally matches torque requirements for the gait cycle (Equation 5.2); where 'k_{knee}' represents the spring constant of the torsion spring at the knee; from now on referred to as the 'Energy Spring'.

$$T_{knee}(\theta) = k_{knee} * \theta$$ **Equation 5.2**

Combining Equation 5.1and Equation 5.2 determines the GRF generated during flexion of the leg's torsion spring knee; where 'c_1' is a scalar multiple for the equation (equal to ½ in this case).

$$F_{GRF}(\theta) = c_1 * \frac{k_{knee} * \theta}{l * \sin\left(\frac{\theta}{2}\right)}$$ **Equation 5.3**

In order to more easily understand the kinematic response of the kneed torsion spring leg, the system is simplified further.

5.2 The Pogo Stick Model – Mapping Flexion to Compression

From Equation 5.3, we know that the thrust generated by the knee's energy spring is dependent upon the stiffness of the knee joint and the magnitude of knee flexion (Figure 5.2A). Since the torso bobs up and down as the knee flexes and extends (Figure 5.2B) (Equation 5.4), a relationship between the GRF and the linear displacement between the hip and ground 'Δ' can be made. Using this correlation, the concept of a synthetic leg (SEG] is introduced.

$$\Delta = Pelvic\_Bob(\theta) = 2 * \left(l - l * \cos\left(\frac{\theta}{2}\right)\right)$$ **Equation 5.4**

A SEG can be thought of as a massless telescoping leg that creates a thrust between the pivot point in contact with the ground (the 'ankle') and the hip (Figure 5.3). The SEG's thrust profile is dictated by the torque profile of the torsion spring at the knee and can be modeled as a non-linear compression spring. As the knee energy spring flexes, the knee torque creates a GRF between the ankle and the hip, the distance between the ankle and hip decreases, and the SEG's spring compresses, creating a restoring force exactly like a pogo stick (Figure 5.2C) (Equation 5.5) (Figure 5.3). Where 'Δ' represents the SEG's linear displacement between the ankle and hip, 'k_{SEG}' is the spring profile for the SEG's compression spring and 'c_2' is it's scalar coefficient.

Since the SEG's thrusting force is equal to the energy spring's thrusting force, and both are collinear with the GRF, we now have the means to calculate the direct mapping between the two fields.

$$F_{GRF}(\theta) = c_1 * \frac{k_{knee} * \theta}{l * \sin\left(\frac{\theta}{2}\right)} \Leftrightarrow F_{GRF}(\Delta) \Leftrightarrow SEG_{thrust}(\Delta) = c_2 * k_{SEG} * \Delta \qquad \text{Equation 5.5}$$

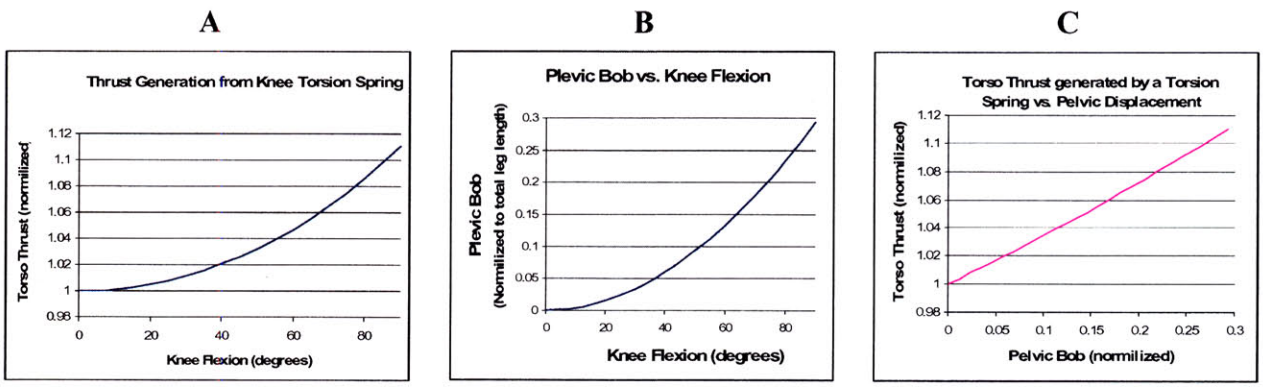

Figure 5.2: (A) Torso thrust generated by a generic torsional knee spring, (B) Vertical displacement of the pelvis as the knee flexes, (C) the Torso Thrust generated by a knee spring w.r.t. the displacement of pelvis during knee flexion.

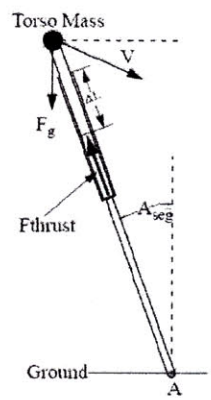

Figure 5.3: A Synthetic Leg [SEG] maps the GRF created by leg with a torsion spring at the knee to the thrust profile of a telescoping leg.

5.3 Setting up the Simulation Model

Our leg model is a spring and mass system at its core. From this basis, the main focus of these simulations is to create a lossless stable gait cycle which can maintain an average velocity on a level surface. In order to conduct relevant simulations of our elastic leg, the following constraints and boundary conditions are instilled upon each step of our gait model.

1. All gait cycles start with the same initial conditions
2. All gait cycles end with the same initial conditions
3. All body mass is located at the hip as a lump sum
4. The leg is massless

5. The point in contact with the ground (the ankle) does not slip, but can be lifted off the ground
6. No torque can be generated between the peg-leg's ankle and ground
7. The average horizontal velocity equals the target speed
8. The sum of all vertical force averages to the weight of the human body
9. All GRFs are transmitted through the leg in contact with the ground
10. At initial ground impact, the torso is moving forwards & downwards

In addition, it is assumed that the left and right legs have identical behavior, resulting in symmetric behavior for each step, and the system has no friction or any losses.

As stated, for both walking and running, at the start of each gait cycle, the torso is moving forwards (+X velocity) and downwards (-Y velocity) relative to the ground. When the leg strikes the ground, the SEG creates a torso supporting GRF between the ankle and the hip. In order to simulate the kinematics of the SEG, the three gait parameters which can be controlled by the user must be defined (Figure 5.4):

1. The SEG's angle from vertical at heel strike: 'A_{SEG_Strike}'
2. The torso's velocity at heel strike: 'V_{HS}'
3. The torso velocity's angle relative to horizontal at heel strike: 'A_{tilt_HS}'

Where 'A_{SEG}' is the SEG strike angle, 'A_{SEG_Strike}' is the torso velocity at heel strike, and 'A_{tilt}' is the torso tilt angle. These three initial conditions will be further explained in the Simulations section; Appendix D verifies that a gait cycle can be accurately modeled using these modeling parameters.

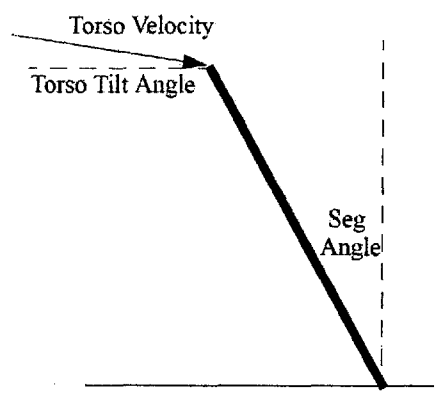

Figure 5.4: The three critical initial conditions for modeling locomotion upon heel strike. (1) SEG strike angle relative to vertical, (2) the magnitude of the torso's velocity, (3) the angle of the torso's velocity relative to horizontal.

The torso velocity and its tilt angle define the torso's energy and its vector trajectory, while the SEG strike angle defines the initial direction of torso support. These gait parameters in conjunction with the SEG's thrust profile allow simulations to be conducted and the average horizontal velocity throughout the entire gait cycle to be determined. This average horizontal is defined as 'v_{tread}' since it is the same as one would have on a treadmill.

Locomotion can be split into two groups with differing characteristics according to the gait velocity. At walking velocities there is a weight transfer epoch during which torso support is

transferred from one leg to the next. At running velocities, there is no WTE, but instead an airborne period during which neither foot is in contact with the ground to generate torso support. During this airborne period, the only force acting upon the body is gravity. This fact implies that the torso's horizontal velocity does not change throughout the airborne epoch (ignoring wind drag), and is the same as the horizontal velocity at heel strike. Likewise, the vertical velocity at the start of the airborne epoch is equal but opposite of the vertical velocity at the end of the airborne epoch which corresponds to heel strike. Since the WTE associated with walking velocities muddies the clarity of which leg is supporting what fraction of the torso for what duration; the simulations will be modeled after a running gait cycle that has an airborne epoch, since it more closely matches the constraints and requirements for our system.

In order to generate an appropriate GRF, the simplified leg has a torsion spring at the knee and the equivalent SEG has a compression spring in the telescoping slider that is mapped to produce the same thrust. Since the spring-mass system will compress and extend with a symmetric time response, in order to keep the system in a stable cycle that complies with all the system requirements, the kinematic response of the energy absorption epoch must be symmetric to the thrusting epoch. Observing one running step, heel strike starts the stance epoch and the energy absorption epoch. The stance leg SEG produces an upwards and backwards force which decelerates the vertical and horizontal velocity of the torso, transferring the torso's kinetic energy to the SEG spring's potential energy. As the SEG compresses, the torso also rotates about the SEG's grounded pivot. In order to keep the system symmetric, maximum spring compression must occur over system apex. This requirement introduces the concept of the 'Critical SEG Strike Angle'. The critical SEG strike angle is the SEG strike angle that results in maximum SEG compression at system apex; this is required for a symmetric and stable gait cycle. The variables which dictate the critical SEG strike angle are: the SEG thrust profile, the torso mass, and the torso velocity its tilt angle at heel strike.

Provided that the spring constant is sufficient to support the torso, given a spring constant and any two of the three initial conditions, we can find the third initial condition which results in a stable cycle. If the torso has not fully rotated to system apex by the time of maximum spring compression, the spring will begin to thrust the torso upwards and backwards opposed to upwards and forwards, destroying the symmetry which allows for a stable cycle. Likewise, if the torso has rotated past system apex upon maximum spring compression, the end conditions will not match the required initial conditions and a stable cycle will not occur. If the optimal initial conditions are used for a particular spring, maximum spring compression will occur directly over system apex.

As the SEG rotates past system apex, the spring will extend, thrusting the torso forwards and upwards in a symmetric manner to the energy absorption epoch. The airborne epoch begins just

after maximum spring extension, when the SEG has finished supporting the torso. During the airborne epoch, the horizontal velocity does not change and the vertical velocity is governed by the initial velocity and the gravitational force. Following these kinematics, the end conditions will equal the initial conditions which meet the requirements for a stable lossless system. Figure 5.5 details the distance between the ankle's point of pivot on the ground and the torso point mass during the compression, thrusting and airborne epochs. From this, it is easy to see that the correct initial conditions produces a symmetrical horizontal and vertical velocity profiles with respect to the time at which apex occurs.

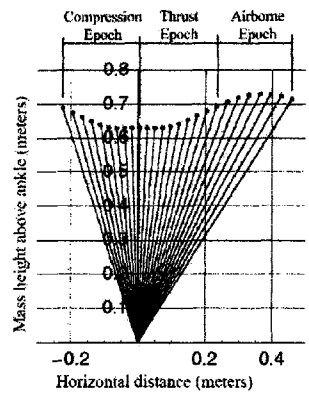

Figure 5.5: Point mass distance from grounded pivot: Compression, Thrust and Airborne epoch.

5.4 Gait Simulation

The goal of this section was to create a gait model which matched the GRF associated with an anthropomorphic gait cycle such that stable locomotion was possible. In doing so, the model should facilitate the realization of a LAD which could both mimic and augment the motions in a human gait cycle. We started with a simplified leg model consisting of a peg-leg shank, a torsion spring knee, a thigh and a point mass torso located at the pelvis. To keep things as simple as possible, a linear torsion spring was initially used at the knee. The torsional rotation of the knee spring was mapped to the compression of the SEG spring. Knowing the spring profile and two of the three initial conditions, simulations were conducted to obtain the remaining initial conditions that resulted in a stable gait cycle. Once it was determined that stable gait cycles could be modeled, two additional simulations were conducted at a slow velocity and then again at a high velocity. In order to attain a more anthropomorphic GRF for the gait cycle, the simulations were repeated using a non-linear hardening spring.

We are attempting to create a simulated LAD model capable of lossless locomotion over a realistic range of velocities. Recapping, the three gait parameters which can be controlled by the user are the SEG strike angle, the torso tilt angle and the velocity the torso at heel strike. Since we desire the gait cycle to be as anthropomorphic as possible, we correlate the torso tilt angle and the velocity at heel strike to the average locomotion velocity since they are not as natural to change. This leaves the SEG strike angle and the spring constant as the two remaining variables.

Once one is chosen, the other has to be a certain value in order to attain closed loop solutions. Since it is not practical to change the spring constant during walking, the user will need to adjust their SEG strike angle based upon their velocity.

With a single energy spring for each round of simulations, the torque and thrust profile does not change. With the spring profile locked in, an initial loop function varies the torso velocity and tilt angle initial conditions, while another loop function determines the SEG strike angle from a calculated estimation. In order to simplify this process, the torso's vertical velocity at SEG strike is fixed and the torso velocity tilt angle is varied. This varies the magnitude of the torso velocity as its tilt angle changes (Equation 5.6).

$$Torso\_Velocity = \frac{y\_vertical\_velocity@HS}{\sin(torso\_velocity\_tilt\_angle)}$$ **Equation 5.6**

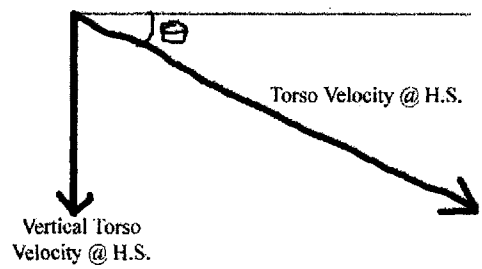

Figure 5.6: In all simulations, the torso velocity at heel strike was determined using the fixed vertical velocity and varying the torso tilt angle at heel strike.

With a method for finding the initial conditions necessary for a stable lossless gait cycle over a range of velocities given an energy spring profile, all other desirable parameters of the gait cycle can be determined. The simulation results can be compared to an actual gait cycle, and the energy spring profile can be adjusted to more optimally fit a natural step.

The system dynamics for the model were created and computed using Mathematica 5.0 and an application packaged called "Dynamics Workbench". The Dynamics Workbench package was used to create a system of bodies linked together with joints, and their equations of motion. The non-linear and time dependent functions of the SEG were created in Mathematica, and later solved using its differential equation solver. All the systems and their solutions obey Lagrangian mechanics, where the total system energy remained constant throughout the gait cycle.

5.4.1 Linear Torsion Spring Simulations

The first round of simulations used a linear torsion spring at the knee joint to generate the torque required for torso support. Seeded from the peak vertical GRF found in a walking gait cycle, the initial energy spring's torque profile was chosen such that it produced a thrust of 1.3x torso weight at a knee flexion of one radian (Figure 5.7).

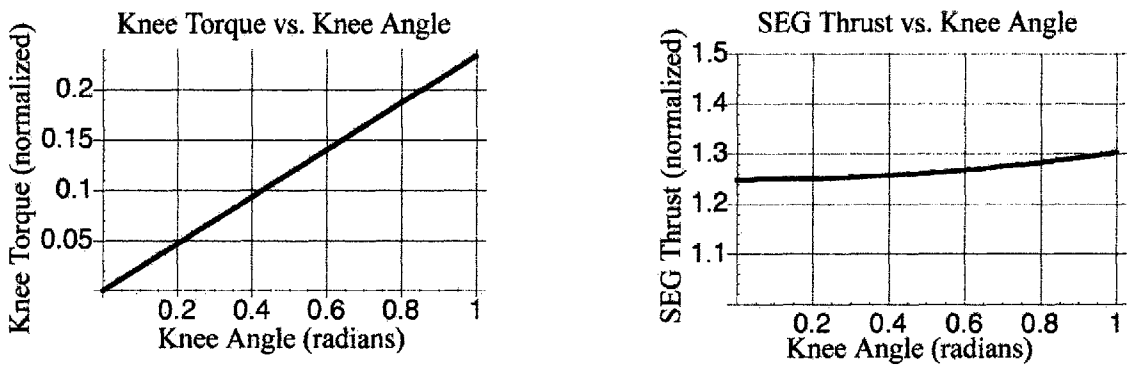

Figure 5.7: Linear Torsion Spring – Normalized Knee Torque and SEG Thrust vs. Knee Flexion.

Fixing the vertical component of the torso velocity at heel strike to 0.3 m/s, the torso velocity tilt angle was varied from 4.3° - 35° in order to adjust the magnitude of the torso velocity at heel strike. Knowing the springs profile and having two of the three initial conditions, the SEG strike angle was determined for 31 intervals. With a compete set of initial conditions for the range of velocities, the average velocity and the gait associated parameters could be determined (Figure 5.8).

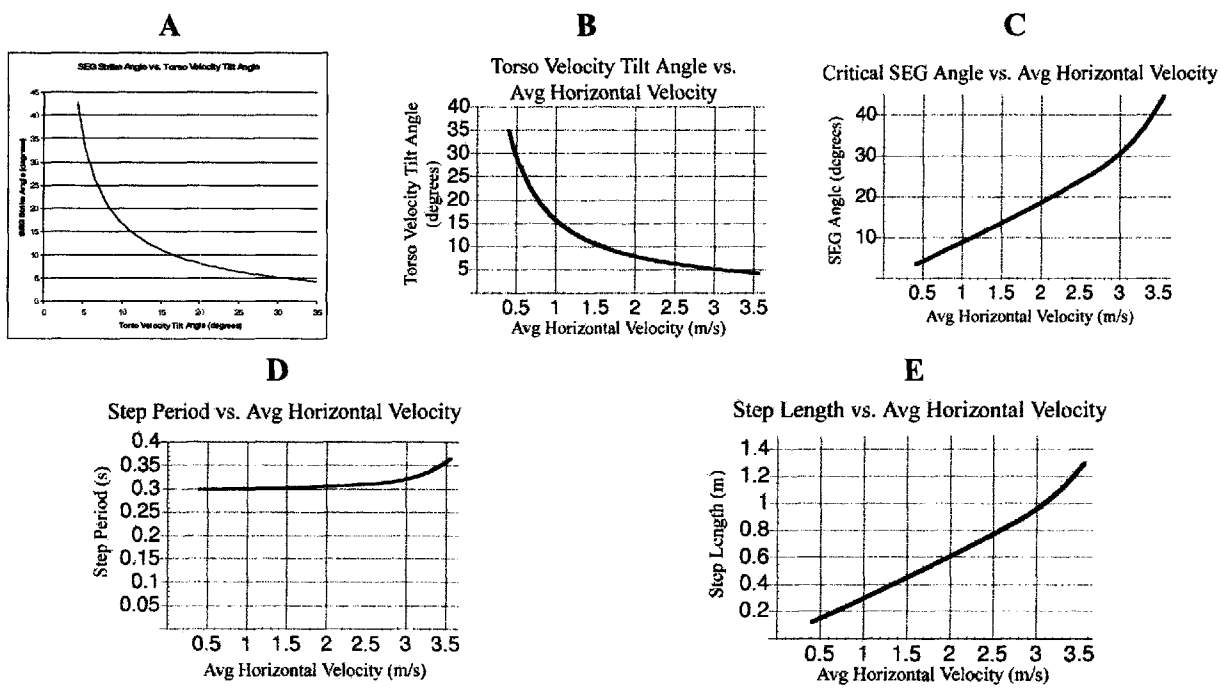

Figure 5.8: Linear Torsion Spring – Gait parameters over a range of locomotion velocities

Observing these data, Figure 5.8 reveals that the torso tilt angle at heel strike and the SEG strike angle are inversely related. This indicates that as the initial horizontal velocity increases, the torso velocity tilt angle needs to decrease and the SEG strike angle needs to increase in order to achieve a sable gait. Satisfied that a lossless gait cycle could be successfully modeled using a

single energy spring for a range of locomotion velocities, two additional simulations were conducted at a slow and fast velocity.

5.4.1.1 Linear Simulation 2 – Slow

Using the same linear spring profile, the torso kinematics, the GRF and the gait cycle parameters were determined (Figure 5.9) (Figure 5.10) (Table 1) using the following initial conditions:

Initial Horizontal Velocity at Heel Strike	1.2 meters / s
Initial Vertical Velocity at Heel Strike	-0.6 meters / s
Torso Velocity Tilt Angle at Heel Strike	26.5651°
Critical SEG Strike Angle	16.2982°

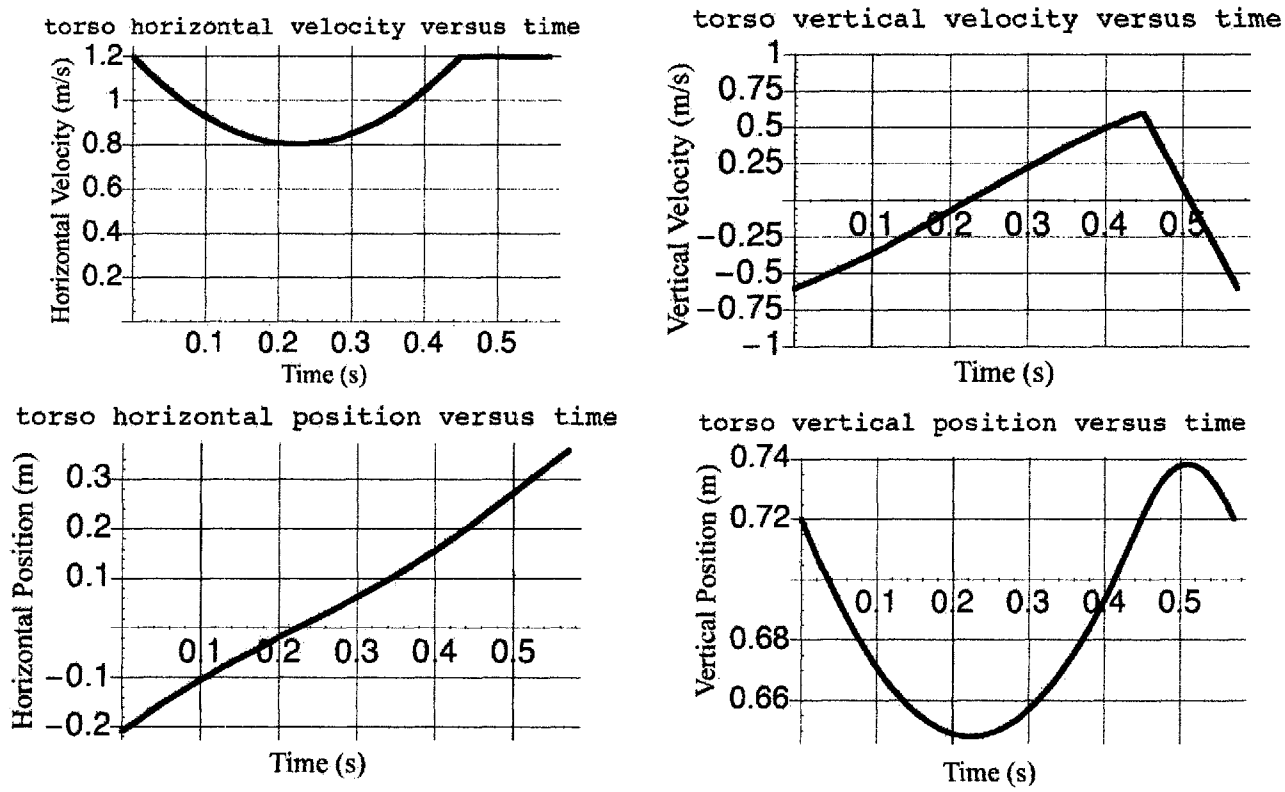

Figure 5.9: Linear Torsion Spring. V_{ih} = 1.2 m/s V_{iv} = -0.6 m/s. Torso kinematics during a gait cycle

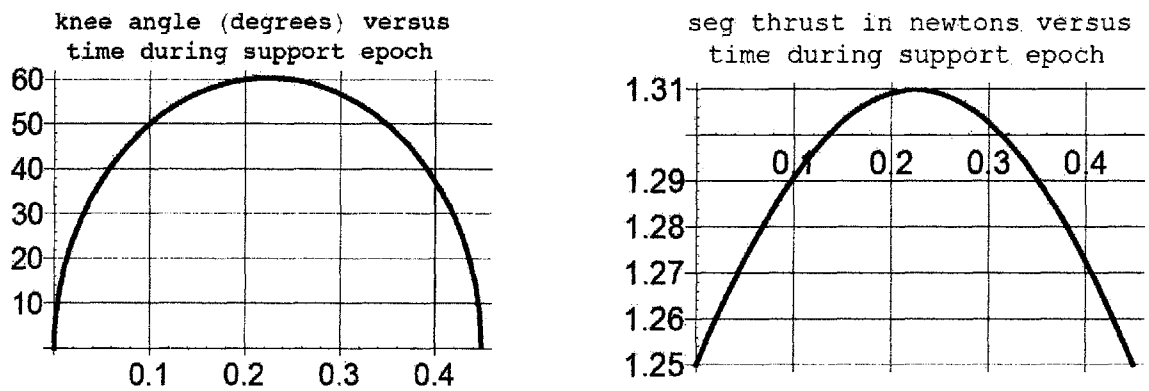

Figure 5.10: Linear Torsion – GRF Parameters. V_{ih} = 1.2 m/s V_{iv} = -0.6 m/s.

Average Horizontal Velocity	0.99423 meters / s
Vertical Velocity at End of Step Period	-0.599995 meters /s
Simulation Error	0.000833%
Maximum Angle of Knee Flexion	60°
Step Period	0.570927 seconds
Step Length	0.567743 meters
Average Vertical GRF during Support	1.27268 x Body Weight

Table 1: Linear Spring - Gait Parameters. V_{ih} = 1.2 m/s V_{iv} = -0.6 m/s.

The average vertical GRF for the support epoch was calculated in order to verify that the vertical support thrust during the support phase averaged to body weight for the entire step. These calculations all had a direct correlation with the simulation error. Observing four successive steps further confirmed that lossless stable gait solutions are both feasible and capable of mimicking an actual gait cycle with close similarity (Figure 5.11).

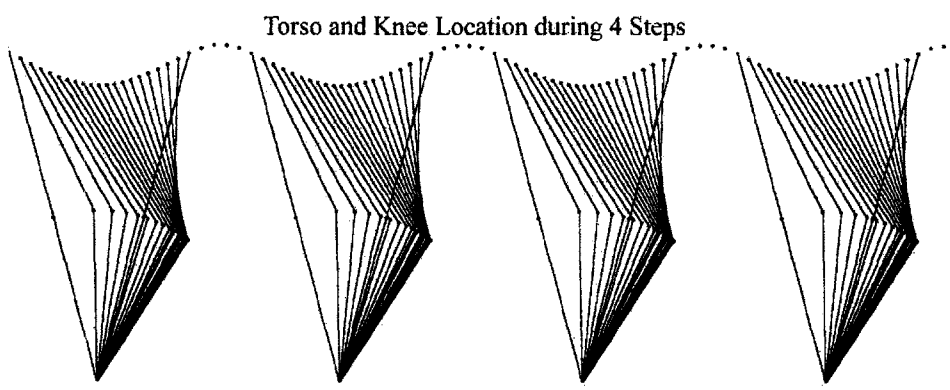

Figure 5.11: Linear Torsion Spring. V_{ih} = 1.2 m/s V_{iv} = -0.6 m/s. Three successive steps.

Comparing the simulated hip's displacement to the actual displacement revealed very encouraging results. The only unnatural aspect of this simulation was that the torso bob was almost 2.75 inches, where normally this would only be about one inch (Figure 5.12) [3]. This

larger displacement was the result of a larger maximum knee flexion angle for that velocity which was cause by a knee spring that had a thrust profile which was lower than necessary.

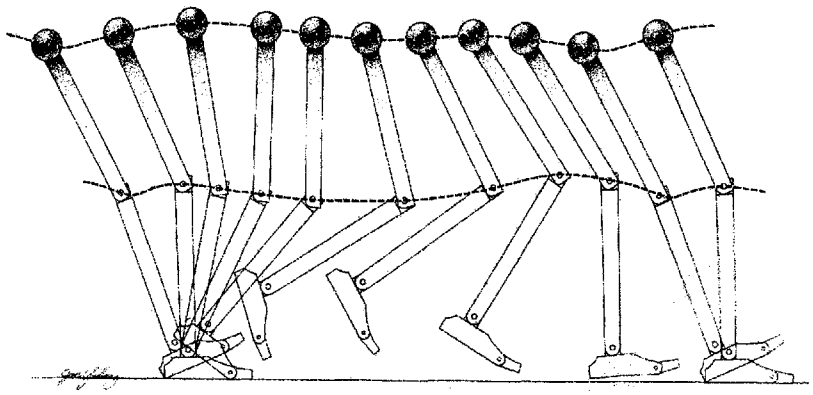

Figure 5.12: Natural torso bob is around one inch.

Verifying that the system complies with Legrangian mechanics, the kinetic and potential energy of the torso and the energy stored in the spring reveal that the total system energy remains constant at every instant throughout the simulation (Figure 5.13).

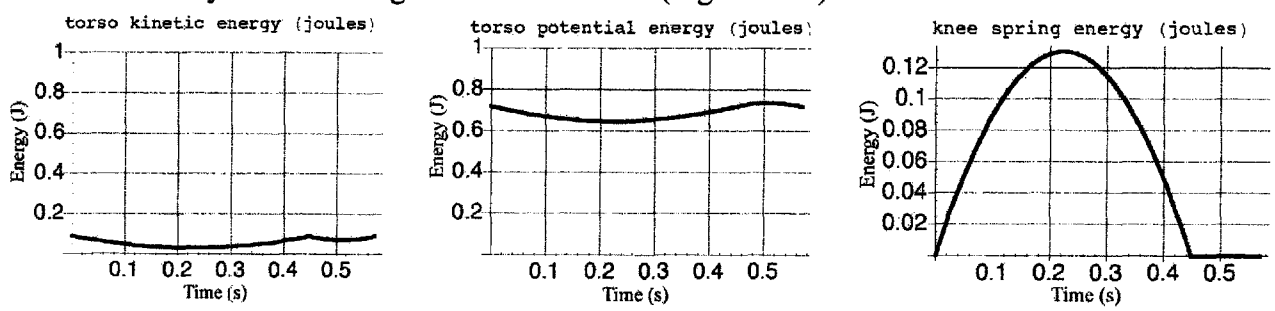

Figure 5.13: Linear Spring. V_{ih} = 1.2 m/s V_{iv} = -0.6 m/s. The total energy in the system remains constant throughout each step.

5.4.1.2 Linear Simulation 3 – Fast

For the third round of simulations, the same linear spring profile was used, the torso kinematics, the GRF and the gait parameters were determined (Figure 5.14) (Figure 5.14) (Table 2) using the following initial conditions:

Initial Horizontal Velocity at Heel Strike	4.4 meters / s
Initial Vertical Velocity at Heel Strike	-0.26 meters / s
Torso Velocity Tilt Angle at Heel Strike	3.38173°
Critical SEG Strike Angle	46.2615°

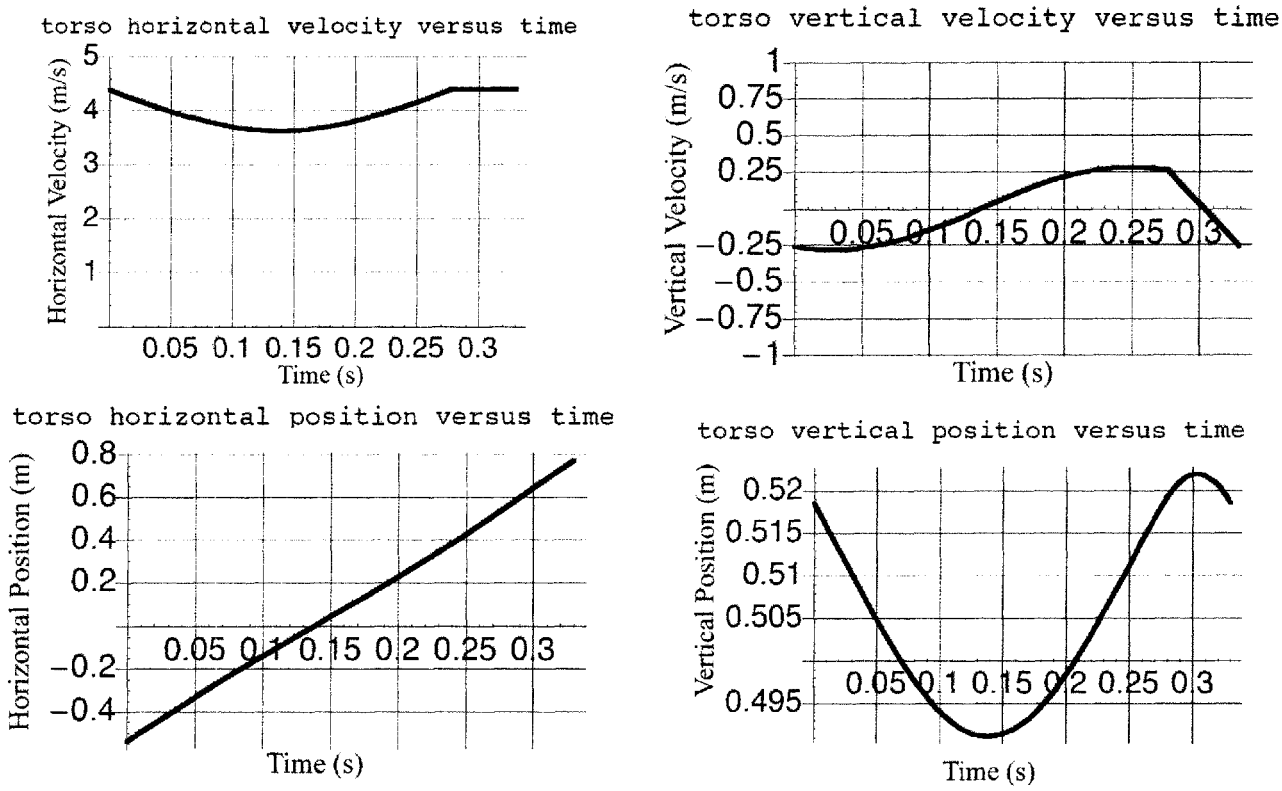

Figure 5.14: Linear Torsion Spring. V_{ih} = 4.4 m/s V_{iv} = -0.26 m/s. Torso dynamics during a gait cycle.

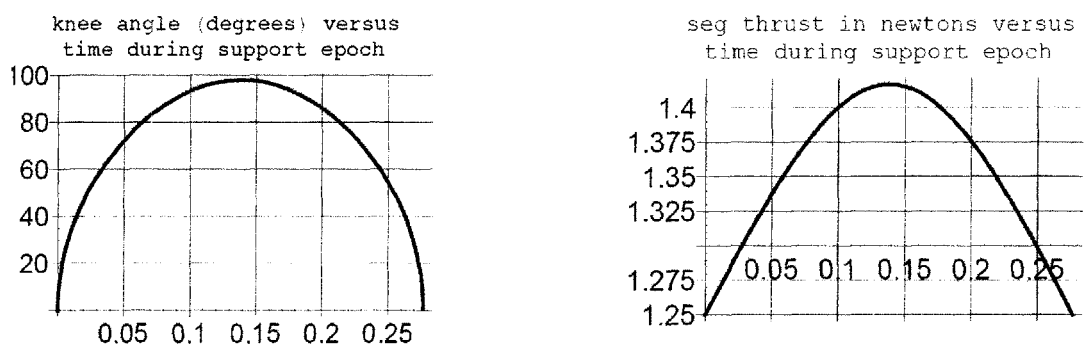

Figure 5.15: Linear Torsion – GRF Parameters. V_{ih} = 4.4 m/s V_{iv} = -0.26 m/s.

Average Horizontal Velocity	3.99267 meters / s
Vertical Velocity at End of Step Period	-0.25999 meters /s
Simulation Error	0.00384%
Maximum Angle of Knee Flexion	97°
Step Period	0.329851 seconds
Step Length	1.31698 meters
Average Vertical GRF during Support	1.19148 x Body Weight

Table 2: Linear Spring - Gait Parameters. V_{ih} = 4.4 m/s V_{iv} = -0.26 m/s

Observing three successive steps, though the torso bob was much only around one inch, the leg kinematics were not desirable (Figure 5.16). Having a SEG strike angle of 46° and a maximum angle of knee flexion of almost 100°, the average torso height from the ground is more than 10 inches lower than standing straight up. This higher velocity clearly verifies that the spring profile was too low and needs reevaluation.

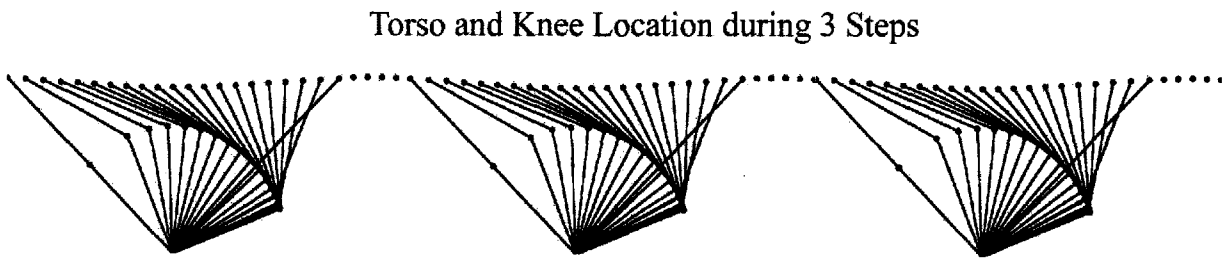

Figure 5.16: Linear Torsion Spring. V_{ih} = 4.4 m/s V_{iv} = -0.26 m/s. Three successive steps.

Verifying that the system complies with Legrangian mechanics, the kinetic and potential energy of the torso and the energy stored in the spring reveal that the total system energy remains constant at every instant throughout the simulation (Figure 5.17).

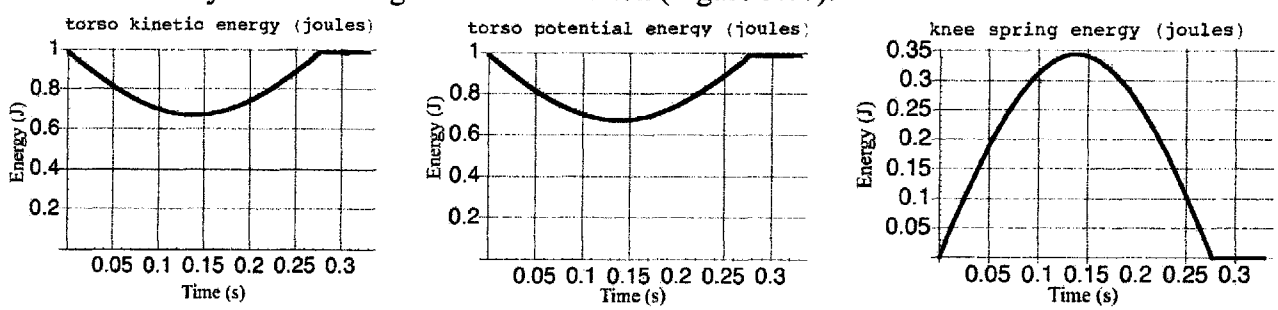

Figure 5.17: Linear Spring. V_{ih} = 4.4 m/s V_{iv} = -0.26 m/s. The total energy in the system remains constant throughout each step.

Though lossless gait solutions are theoretically possible for any gait velocity as long as the spring can generate a torso thrust greater than body weight, not all solutions have realistic initial conditions. Recall that, for linear springs, as the horizontal velocity increases, in order to attain a stable gait, the torso tilt angle must decrease and the SEG strike angle must increase. As the velocity increases, the step period decreases; meaning that the leg must swing faster and faster in preparation for the next step as the velocity increases. Since there is a limit for how quickly a human can feasibly rotate their leg, this rotational rate limits the horizontal velocity the user can locomote at using that specific spring. Having this constraint for linear springs, we investigate a knee spring that has a non-linear torque profile.

5.4.2 A Better Knee Spring

Recall that GRF is related to knee flexion (Figure 5.18A), and that the magnitude of GRF increases dramatically at higher locomotion velocity (Figure 5.18B) due to decreased ground contact duration (Figure 5.18C). Running at higher speeds requires significantly different demands on the spring since the magnitude of GRF increases with velocity, and the overall energy of the system increases as the square of the velocity. Ideally, the LAD could have a torso thrusting spring selection mechanism which could select or adjust the spring constant so it generates the correct thrust for each step for a stable gait. Unfortunately, this is easier said than done, especially if energy conservation is a primary objective for the device. Though an array of springs could allow combinations which approximate solutions, the thrust demands for the spring still hold a larger concern.

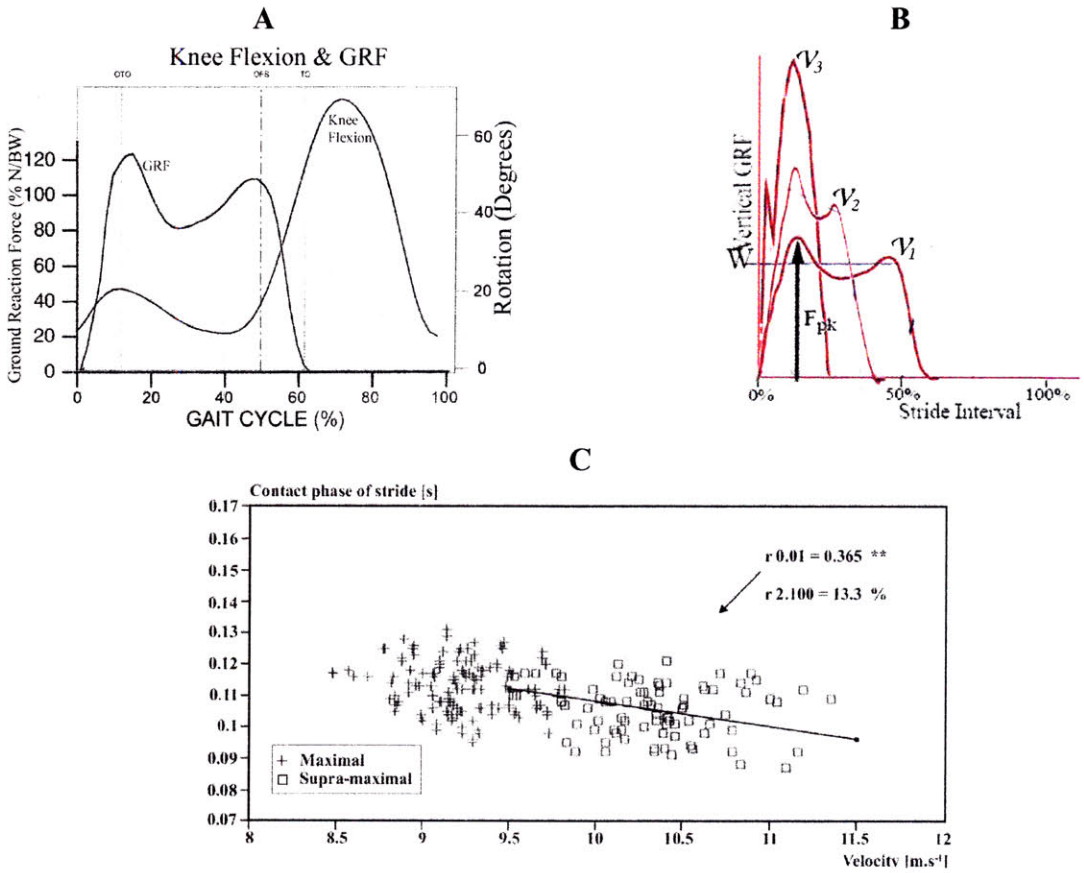

Figure 5.18: (A) GRF and Knee Flexion throughout a gait cycle [3], (B) Higher peak GRFs are required at higher locomotion velocities, (C) the leg has a shorter duration to generate these thrusts at higher velocities [57].

Due to the geometric construction of the leg, if the knee uses a linear torsion spring to generate the torque required for thrust generation (Figure 5.19A), the GRF remains fairly constant, independent of knee flexion magnitude (Figure 5.19B). Although a linear torsion spring for the

knee would be very useful for squat thrusts (a task requiring a constant vertical thrust during knee flexion), recalling Figure 5.18A&B, the GRF required for locomotion is anything but constant.

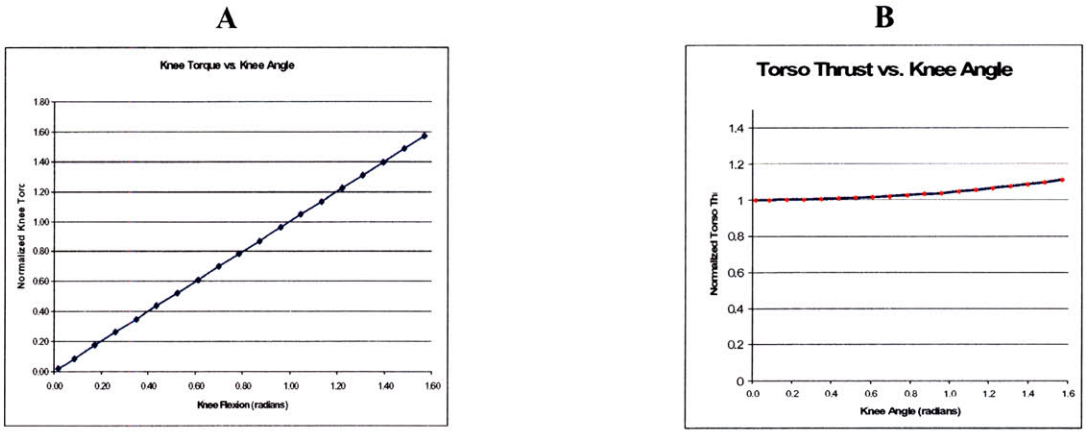

Figure 5.19: Generic Linear Torsion Spring (A) Knee Torque vs. Knee Flexion Angle, (B) Torso Thrust vs. Knee Flexion Angle

If a spring is to be used to absorb the energy of heel strike and generate the appropriate GRF, analyzing the data in Figure 5.18 and Figure 5.19 reveals that the thrust profile for the spring system must be non-linear. Unlike the difficulties which arose when a single linear spring was used at both low and high velocities, investigation into the kinematic response of non-linear springs reveal that the thrust demands for a realistic range of gait velocities and initial conditions can be attained with the careful design of a single non-linear torsion spring. The detailed design of the knee's energy spring is described in Appendix B.

5.4.3 Non-Linear Torsion Spring

Nature developed efficient locomotion by tuning the tendons and corresponding geometry in the spring-mass leg such that its GRF generation and time response optimally matched the desired gait cycle. In order to develop a LAD which embodies the efficiency and grace found in nature, the thrust producing spring must follow suite for the human gait cycle.

Since the leg is modeled as a spring-mass system, the torque profile of the spring is critical to the dynamics of the gait cycle. Observing the GRF and knee flexion of a normal gait cycle (Figure 5.20A), it is obvious that a linear torsion spring can not generate the correct thrust profile necessary for an anthropomorphic gait (Figure 5.20B).

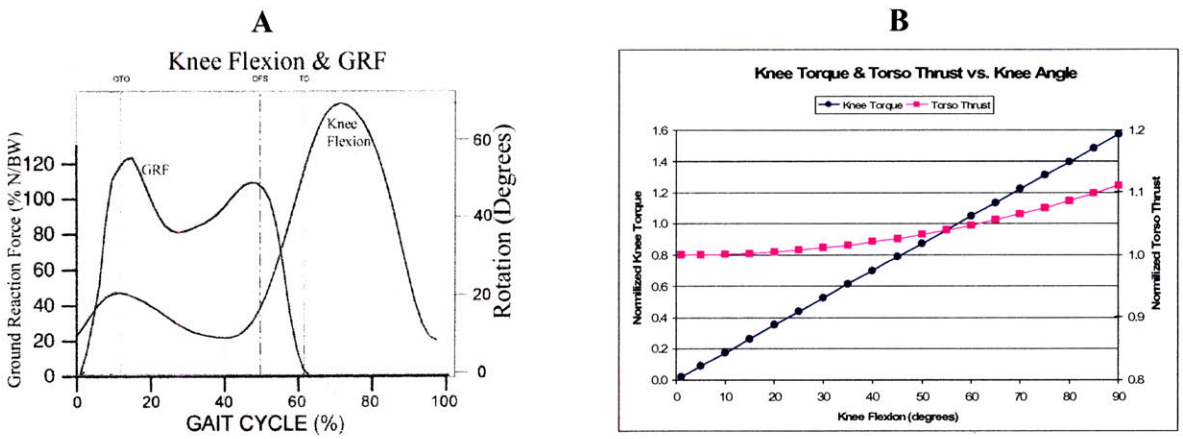

Figure 5.20: (A) The torso thrust generated the human leg as the knee flexes throughout the gait cycle [3], (B) the torso thrust generated by a linear torsion spring.

In walking and running, the peak GRF is dependant on velocity and typically varies from between 1x and 4x body weight. It would therefore be beneficial if the thrust profile of the LAD increases in a similar manner. In order to generate the large range of varying GRFs required for locomotion, the torque profile of the knee is altered from a linear torsion spring to a non-linear hardening torsion (Figure 5.21A). Only by using this flavor of torsion springs can the thrust profile attain a positive slope (Figure 5.21B).

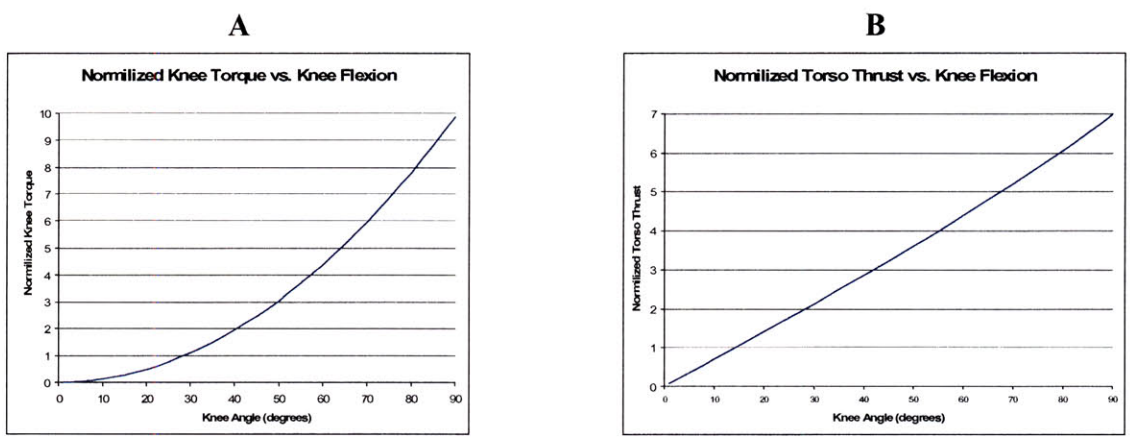

Figure 5.21: The (A) torque, and (B) thrust profiles of a generic 2nd order Non-Linear Hardening Torsion Spring.

Unlike a linear torsion spring, a non-linear hardening torsion spring requires more and more torque to rotate a defined increment. It can be mathematically described by Equation 5.7; where 'k_1', 'k_2' and 'r' are engineering parameters used to construct the desired knee torque, and 'c_1' is a scalar constant.

$$T_{knee} = c_1 * k_1\theta * \left(1 + k_2\theta^r\right) \qquad \textbf{Equation 5.7}$$

Using this torque profile in Equation 5.1 leads to the thrust profile in Equation 5.8.

$$F_{GRF}(\theta) = c_1 * \frac{k_1\theta * (1 + k_2\theta^r)}{l * \sin\left(\frac{\theta}{2}\right)}$$ **Equation 5.8**

Since the natural frequency of a system is determined by its poles, unlike the single poled linear springs, non-linear hardening springs have an infinite number of poles, this spring scheme can be mathematically engineered so its time response can match the period of the gait cycle at varying velocities.

As the gait velocity increases, the leg must generate a higher peak force in a shorter amount of time. This implies that the thrust profile of the LAD's non-linear hardening spring should have a positive convex slope (Figure 5.22B). In order to do so, the spring must have a third order torque profile since this geometry allows for a larger GRF to be generated with smaller and smaller increases in knee flexion (Figure 5.22A) (Equation 5.9). A spring with these characteristics is highly desirable since it allows higher peak thrusts to be generated in shorter durations; exactly the same requirements that the gait cycle demands of the leg at higher velocities.

$$T_{knee} = 2\theta^3 + \theta^2 + 0.1\theta$$ **Equation 5.9**

A **B**

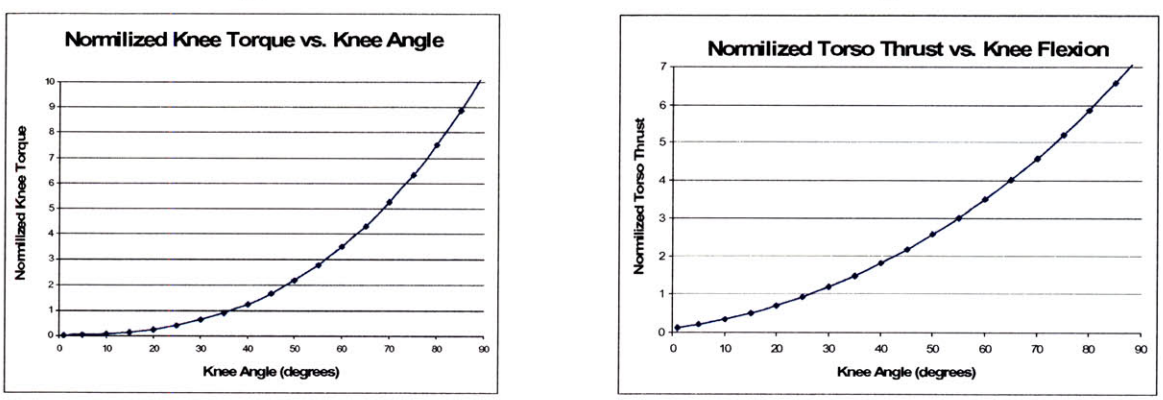

Figure 5.22: The (A) torque, and (B) thrust profiles of a generic 3rd order Non-Linear Hardening Torsion Spring.

Since non-linear hardening torsion springs are designed using engineering parameters, this suggests that the correct profile can generate the appropriate GRF required throughout the knee flexion of a specific gait cycle. Figure 5.23 demonstrates a sampling of the wide range of potential thrust profiles that a non-linear hardening torsion spring could generate.

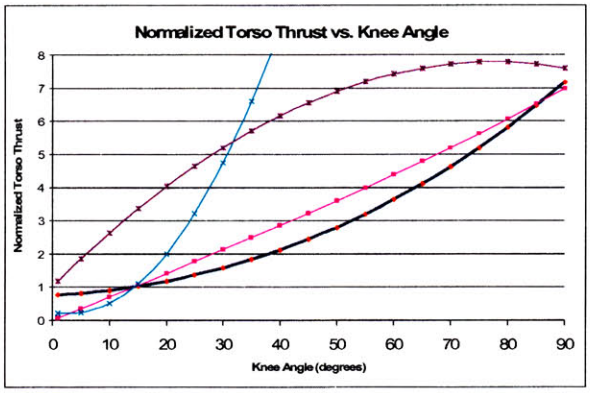

Figure 5.23: Four different normalized thrust profiles of differing non-linear hardening springs demonstrating the possible range of thrust profiles capable of being created.

Mapping the thrust profile created by the torsion spring leg to the thrust profile of the compressive SEG (Equation 5.10), the simulations were repeated using the non-linear hardening torsion spring; where 'Δ' is the linear displacement along the SEG's telescoping support strut, and 'b_1' 'b_2' 'b_3' and 'b_4' are engineering parameters used in describing the thrust profile of the non-linear compression spring.

$$F_{GRF}(\theta) = c_1\left(\frac{k_1\theta * (1 + k_2\theta^r)}{l * \sin\left(\frac{\theta}{2}\right)}\right) = F_{GRF}(\Delta) = c_2\left(b_1\Delta^3 + b_2\Delta^2 + b_3\Delta + b_4\right) \qquad \textbf{Equation 5.10}$$

5.4.4 Non-Linear Torsion Spring Simulations

The second batch of simulations used a non-linear torsion spring at the knee joint to generate the torque required for torso support. Seeded from a conservative estimation of the peak vertical GRFs required at varying locomotion velocities, the initial non-linear energy spring's torque profile was chosen such that it produced a 3x body weigh thrust at a knee flexion of 1 radian (Equation 5.11) (Figure 5.24).

$$SEG_{Thrust\_non-linear} = \frac{0.5\Delta^3 + 0.5\Delta^2 + 0.5\Delta + 0.75}{2} \qquad \textbf{Equation 5.11}$$

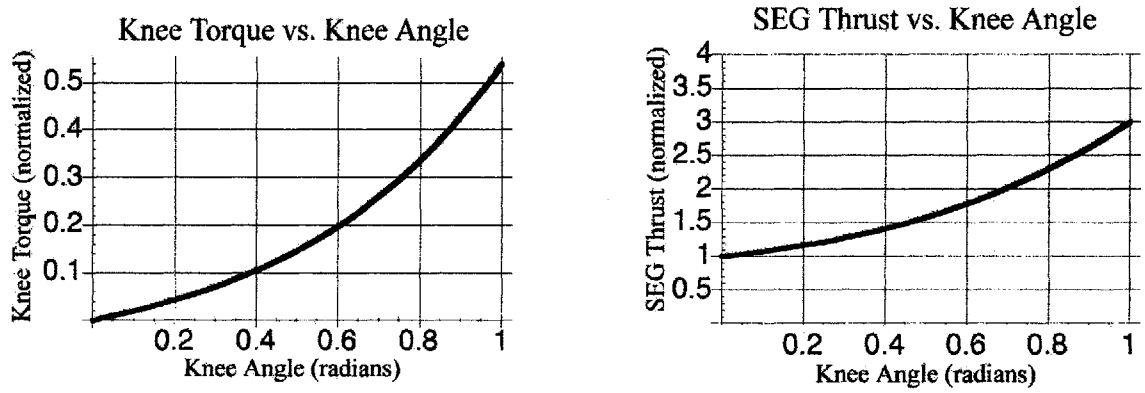

Figure 5.24: Non-Linear Hardening Torsion Spring – normalized torque and thrust profile.

Following the same simulation protocol, the vertical component of the torso velocity at heel strike was set to 0.3 m/s while the torso velocity tilt angle is varied from 4.3° - 35° in order to vary the torso velocity. Again, the SEG strike angle was determined for the 31 incremental velocities. With a compete set of initial conditions for the range of velocities, the average velocity and the gait parameters associated with them were determined at each incremental set of initial conditions (Figure 5.25).

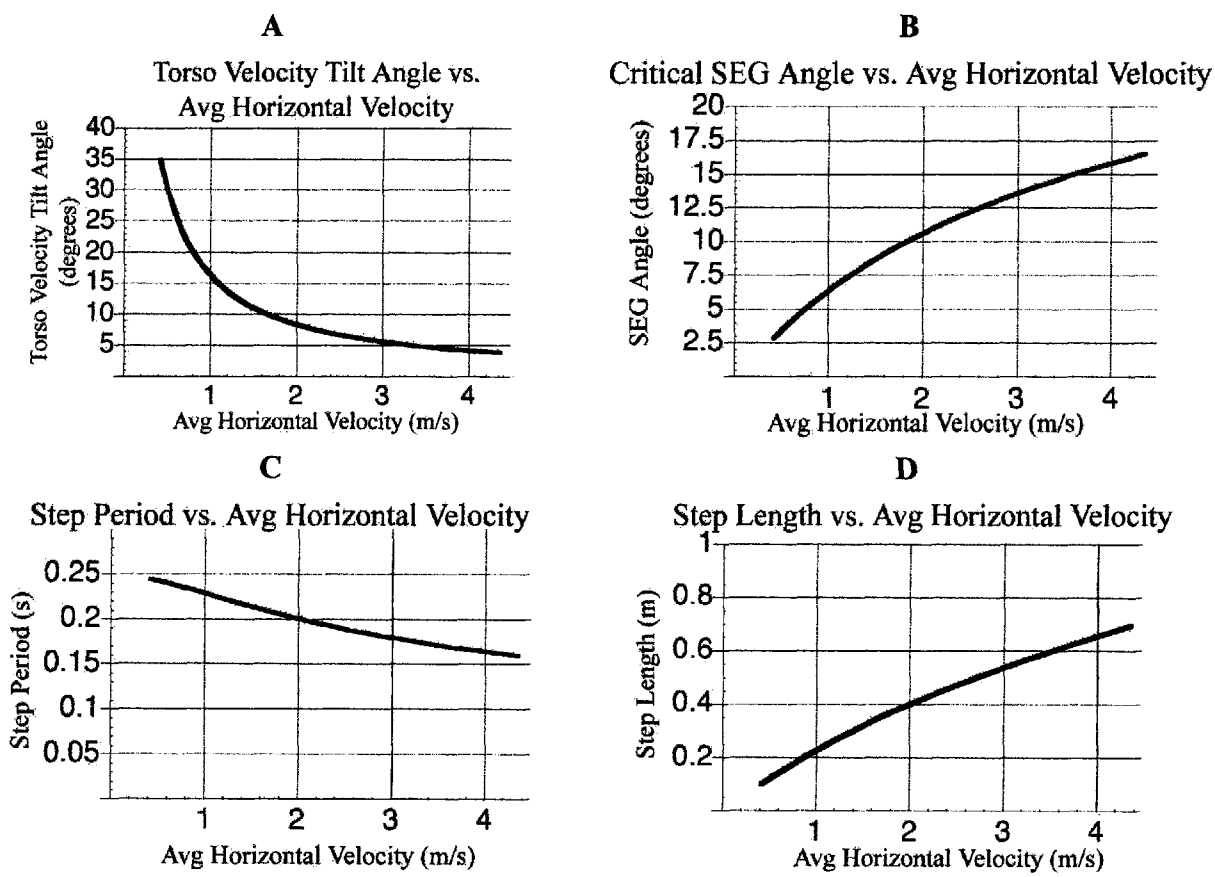

Figure 5.25: Non-Linear Torsion Spring – Gait parameters over a range of locomotion velocities.

Comparing these results to those of the linear spring shows that the response of the non-linear spring is far more desirable. Recall that for linear springs, as the gait velocity increased, the step period duration remained fairly constant with only a slight increase at higher velocities. However, as predicted, using non-linear torsion springs, at higher velocities the step period decreased. Likewise, for linear springs, the critical SEG strike angle and the step length both have an increasing rate of growth at higher velocities. This indicates that the sensitivity to the error in these parameters increases at higher velocities. Fortunately, for non-linear springs, both the critical SEG strike angle and the step length have a decreasing rate of growth. This indicates that the sensitivity to error in these parameters decreases at higher velocities, a very desirable quality for generating stable gait cycles. Satisfied that lossless simulations could be accurately conducted using non-linear torsion springs, the slow and fast gait simulations were conducted.

5.4.4.1 Non-Linear Simulation 2 – Slow

Using the same non-linear spring profile as before, the torso kinematics, the GRF and the gait parameters were determined (Figure 5.26) (Figure 5.27) (Table 3) using the same initial conditions as used in the slow linear simulation 2:

Initial Horizontal Velocity at Heel Strike	1.2 meters / s
Initial Vertical Velocity at Heel Strike	-0.6 meters / s
Torso Velocity Tilt Angle at Heel Strike	26.5651°
Critical SEG Strike Angle	8.17829°

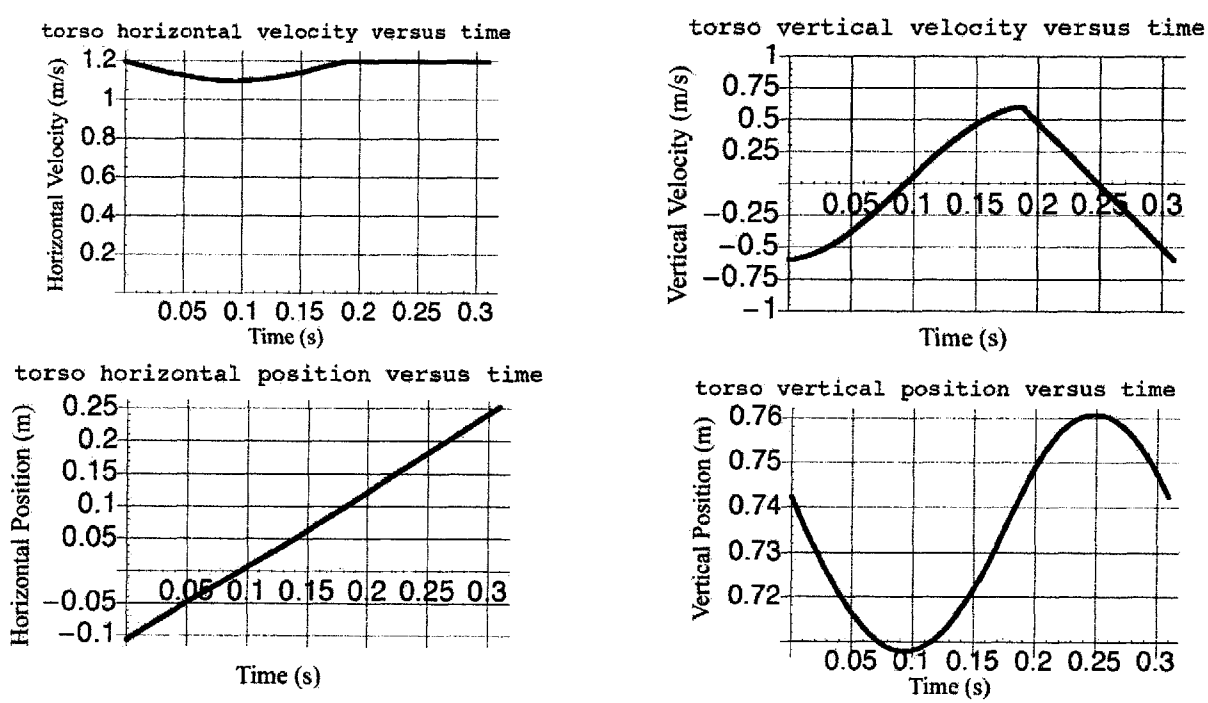

Figure 5.26: Non-Linear Torsion Spring. V_{ih} = 1.2 m/s V_{iv} = -0.6 m/s. Torso dynamics during a gait cycle

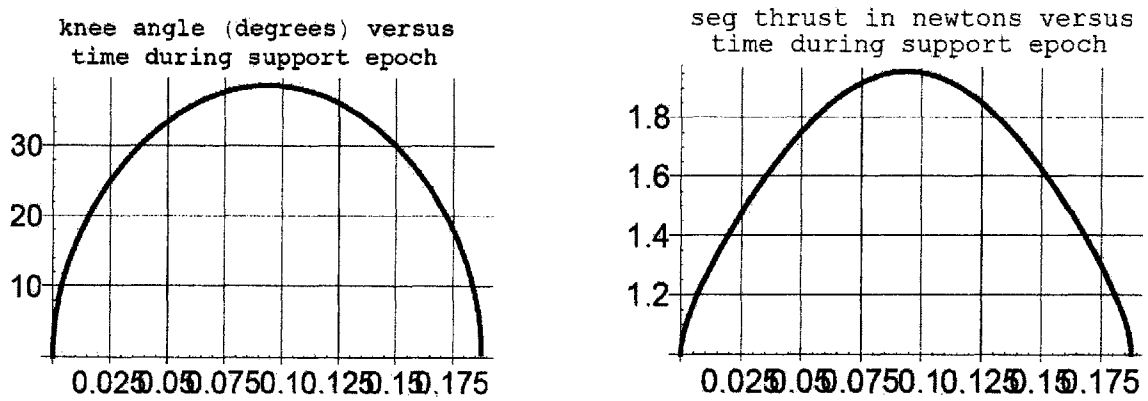

Figure 5.27: Non-Linear Torsion – GRF Parameters. V_{ih} = 1.2 m/s V_{iv} = -0.6 m/s.

Average Horizontal Velocity	0.99423 meters / s
Vertical Velocity at End of Step Period	-0.599995 meters /s
Simulation Error	0.000833%
Maximum Angle of Knee Flexion	39°
Step Period	0.570927 seconds
Step Length	0.567743 meters
Average Vertical GRF during Support	1.652 x Body Weight

Table 3: Non-Linear Spring - Gait Parameters. V_{ih} = 1.2 m/s V_{iv} = -0.6 m/s.

Recalling the gait response from the linear spring, comparing the two simulations, the non-linear allowed a much closer response to that of a normal gait cycle. With the same torso velocity tilt angle at heel strike, though the step period was the same, the non-linear SEG strike angle was reduced (as expected), and the maximum knee flexion angle was also decreased. Observing four successive steps further confirming that lossless stable gait solutions are feasible and can vary accurately mimic an actual gait cycle (Figure 5.28). The non-linear simulated a pelvic bob or approximately 1.2 inches; a very close match to a natural gait.

Torso and Knee Location during 4 Steps

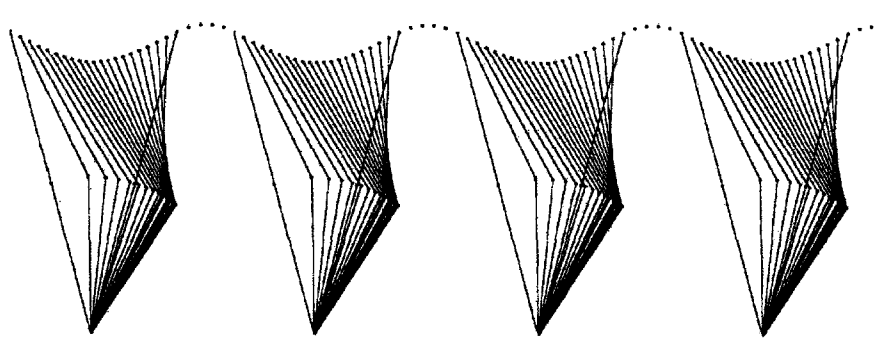

Figure 5.28: Non-Linear Torsion Spring. V_{ih} = 1.2 m/s V_{iv} = -0.6 m/s. Four successive steps.

Verifying that the system complies with Legrangian mechanics, the kinetic and potential energy of the torso and the energy stored in the spring reveal that the total system energy remains constant at every instant throughout the simulation (Figure 5.29).

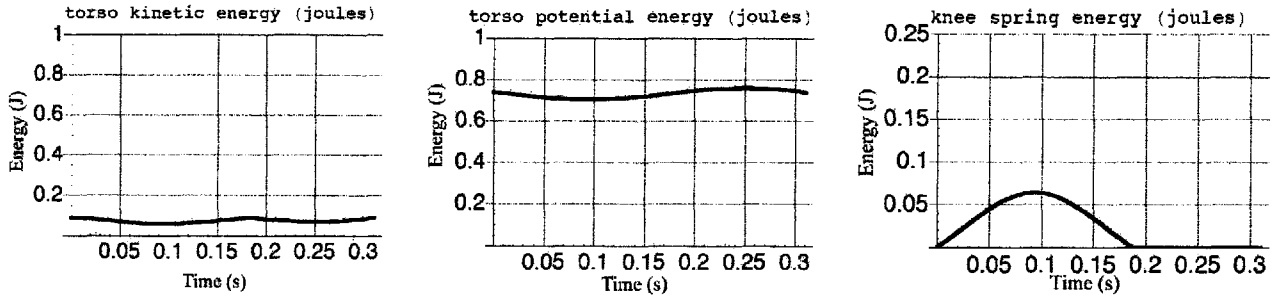

Figure 5.29: Non-Linear Spring. V_{ih} = 1.2 m/s V_{iv} = -0.6 m/s. The total energy in the system remains constant throughout each step.

5.4.4.2 Non-Linear Simulation 3 – Fast 1

Using the same non-linear spring profile, the torso kinematics, the GRF and the gait parameters were again determined (Figure 5.30) (Figure 5.31) (Table 4) using the same initial conditions as used in the fast linear simulation 3:

Initial Horizontal Velocity at Heel Strike	4.4 meters / s
Initial Vertical Velocity at Heel Strike	-0.26 meters / s
Torso Velocity Tilt Angle at Heel Strike	3.34173°
Critical SEG Strike Angle	15.7583°

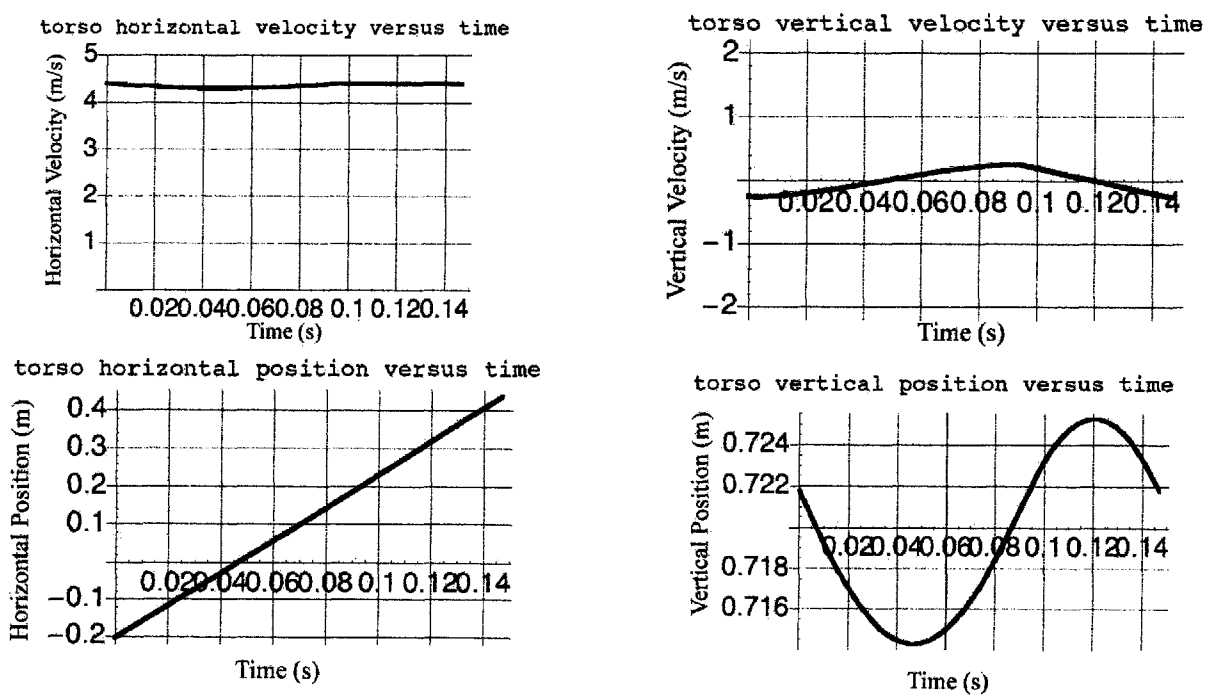

Figure 5.30: Non-Linear Torsion Spring. V_{ih} = 4.09 m/s V_{iv} = -0.26 m/s. Torso dynamics during a gait cycle

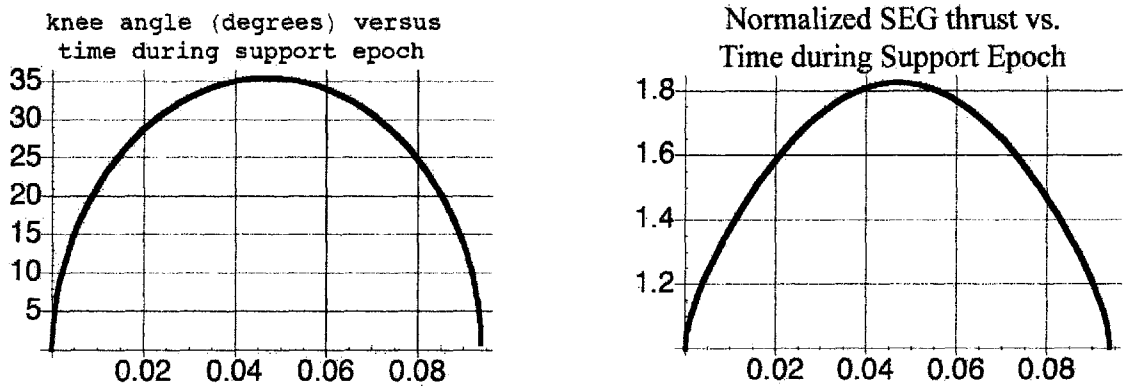

Figure 5.31: Non-Linear Torsion – GRF Parameters. V_{ih} = 4.09 m/s V_{iv} = -0.26 m/s.

Average Horizontal Velocity	4.36248 meters / s
Vertical Velocity at End of Step Period	-0.260003 meters /s
Simulation Error	0.0011%
Maximum Angle of Knee Flexion	36°
Step Period	0.146843 seconds
Step Length	0.640602 meters
Average Vertical GRF during Support	1.56489 x Body Weight

Table 4: Non-Linear Spring - Gait Parameters. V_{ih} = 4.09 m/s V_{iv} = -0.26 m/s.

Again, we immediately see a desired improvement using the non-linear spring in comparison to the linear spring. The maximum knee flexion is reduced to a realistic magnitude, the SEG strike angle is decreased to a more desirable angle, and the support duration was shorter. The downfall to this simulation is that the step period was reduced to a duration in which it is not possible for humans to swing their leg forward in preparation for the next step. Observing four successive steps, though the simulated torso and knee trajectories are far more appealing than those of the linear spring under the same conditions, the airborne epoch duration was too short (Figure 5.32).

Torso and Knee Location during 4 Steps

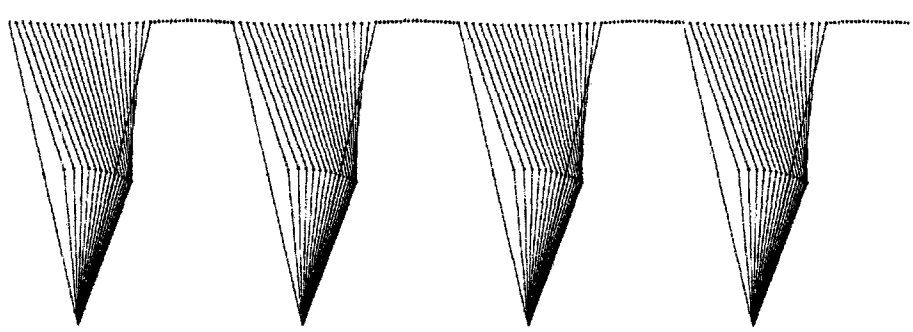

Figure 5.32: Non-Linear Torsion Spring. V_{ih} = 4.09 m/s V_{iv} = -0.26 m/s. Three successive steps.

Verifying that the system complies with Legrangian mechanics, the kinetic and potential energy of the torso and the energy stored in the spring reveal that the total system energy remains constant at every instant throughout the simulation (Figure 5.33).

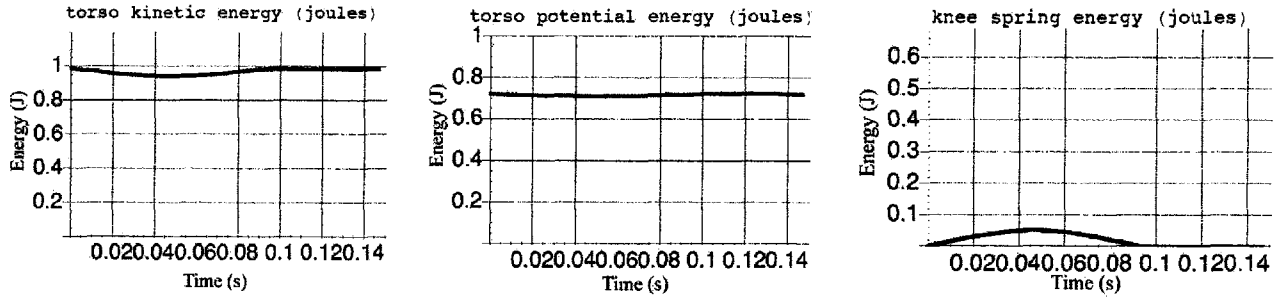

Figure 5.33: Linear Spring. V_{ih} = 4.09 m/s V_{iv} = -0.26 m/s. The total energy in the system remains constant throughout each step.

5.4.4.3 Non-Linear Simulation 4 – Fast 2

Unsatisfied with the short step period of the non-linear simulation 3, a fourth simulation was conducted with an increased initial vertical velocity at heel strike in order to increase the step period so it is more appropriate for humans. Using the same non-linear spring profile, the torso kinematics, the GRF and the gait parameters were determined (Figure 5.34) (Figure 5.35) (Table 5) using the following modified initial conditions:

Initial Horizontal Velocity at Heel Strike	4.09 meters / s
Initial Vertical Velocity at Heel Strike	-2 meters / s
Torso Velocity Tilt Angle at Heel Strike	26.0585°
Critical SEG Strike Angle	24.7029°

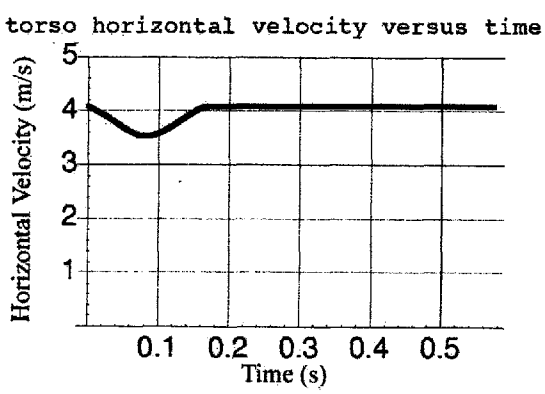

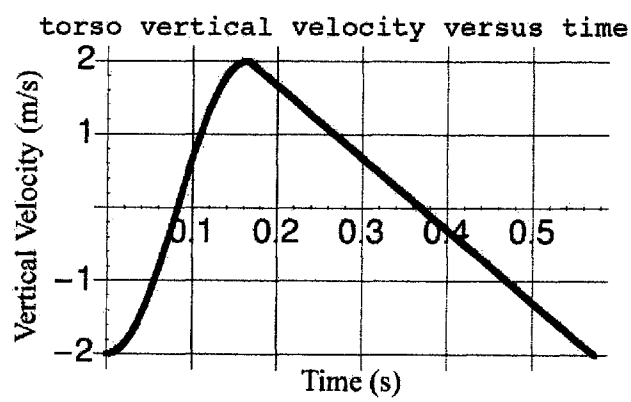

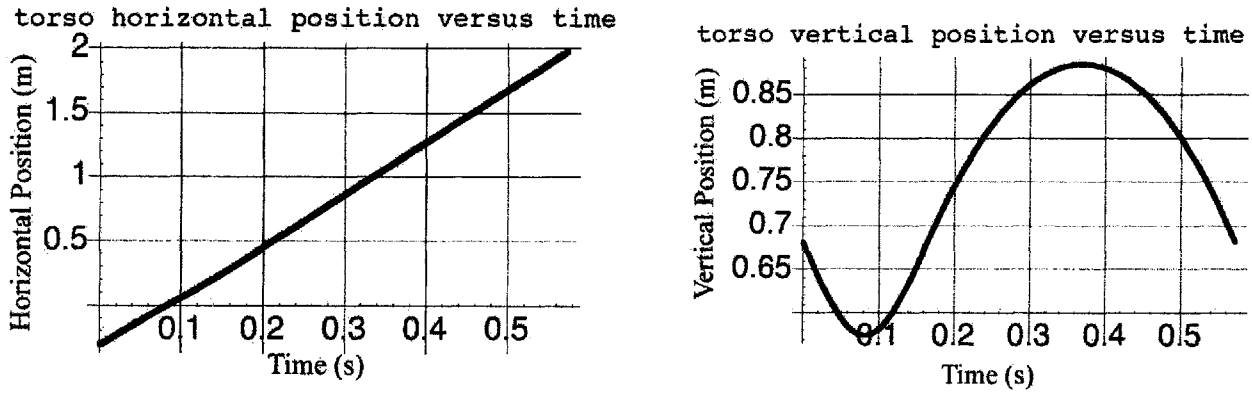

Figure 5.34: Non-Linear Torsion Spring. V_{ih} = 4.09 m/s V_{iv} = -2 m/s. Torso dynamics during a gait cycle

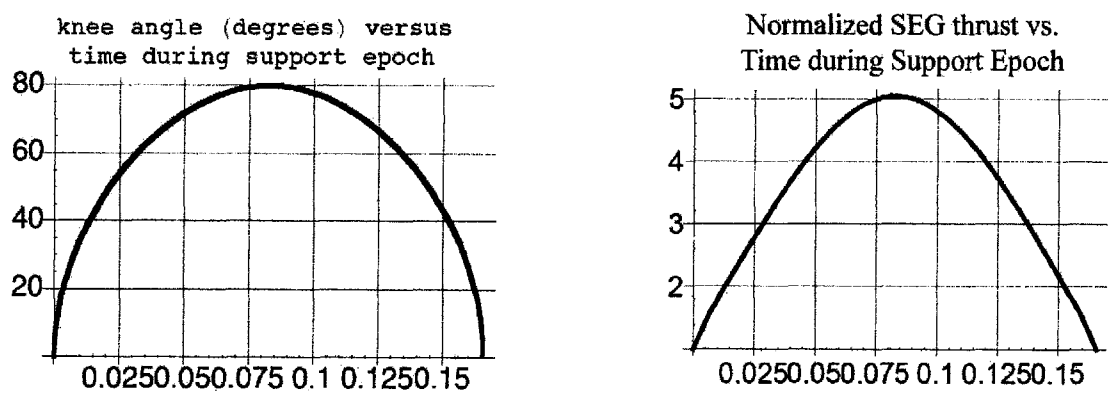

Figure 5.35: Non-Linear Torsion – GRF Parameters. V_{ih} = 4.09 m/s V_{iv} = -2 m/s.

Average Horizontal Velocity	4.00177 meters / s
Vertical Velocity at End of Step Period	-2.0 meters /s
Simulation Error	0%
Maximum Angle of Knee Flexion	80°
Step Period	0.573384 seconds
Step Length	2.29455 meters
Average Vertical GRF during Support	4.13223 x Body Weight

Table 5: Non-Linear Spring - Gait Parameters. V_{ih} = 4.09 m/s V_{iv} = -2 m/s.

With an increased vertical velocity and torso tilt angle at heel strike, we immediately see significant improvement. The SEG angle at heel strike, though increased by 9° to 24.7°, still remained very realistic. The support period increased by 173%, allowing enough thrust generation for a relaxed 0.408 second airborne hang time for step preparation. The higher velocity at heel strike clearly demonstrated the potential associated with using a non-linear spring, however the large magnitude of knee flexion indicated that the rate of growth for the springs thrust profile should be increased at larger knee flexion angles. Observing three successive steps, though the torso bobbed almost four inches due to an overly large maximum

angle of knee flexion, and the simulated step length was longer a normal human's, the torso overall trajectory was still elegant (Figure 5.36).

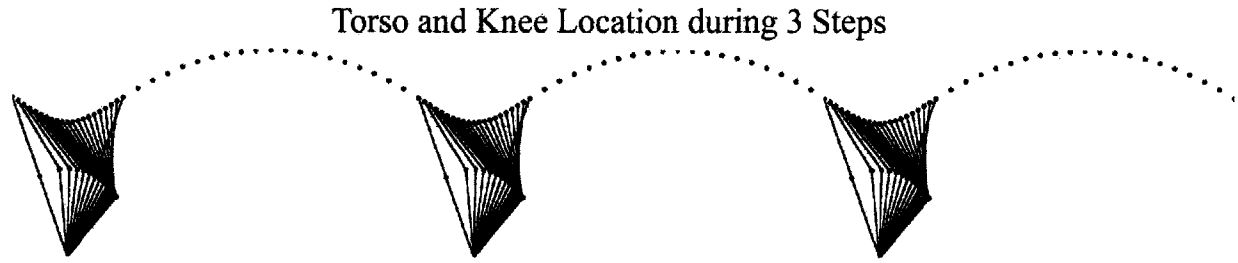

Figure 5.36: Non-Linear Torsion Spring. V_{ih} = 4.09 m/s V_{iv} = -2 m/s. Three successive steps.

Verifying that the system complies with Legrangian mechanics, the kinetic and potential energy of the torso and the energy stored in the spring reveal that the total system energy remains constant at every instant throughout the simulation (Figure 5.33).

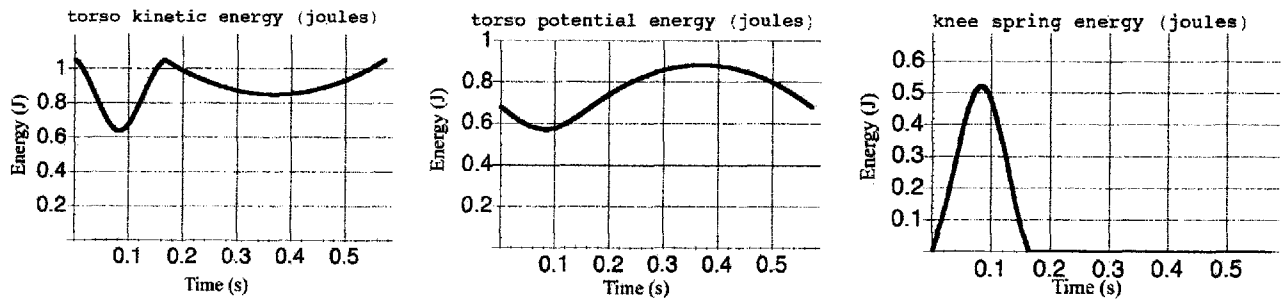

Figure 5.37: Linear Spring. V_{ih} = 4.09 m/s V_{iv} = -2 m/s. The total energy in the system remains constant throughout each step.

5.4.5 Simulation Conclusion

In order to a construct an energy efficient LAD which can desirably support the torso at various velocities, using a single engineered torsion spring, for a range of velocities, its kinematic response must be able to generate the required thrust while appropriately flexing the energy spring such that the maximum angle of flexion and the step period are realistic for the human leg at that velocity.

Observing the linear and non-linear simulations, it is clear that a non-linear torsion spring can generate far more anthropomorphic and desirable responses. Using realistic initial conditions for the non-linear spring, the gait parameters from the slow and fast simulations showed very encouraging results. Though the maximum angle of knee flexion was about twice what it should have been for the slow velocity and around 2.5x for the second fast simulation, the first fast simulation (Figure 5.31) had a very desirable knee flexion but a step period that was too short. This indicates that the non-linear spring's rate of growth for the thrust profile must be increased,

and with further tuning, shows very strong potential to anthropomorphically comply with the human gait cycle, aiding in locomotion as advertised.

Recalling the GRF thrust profile of the human leg during knee flexion (Figure 5.38A) and its diminishing ability to do so at higher rates of knee flexion, if a LAD is to augment the thrust generation of the leg with SEG thrust (Figure 5.38B), at higher velocities, the LAD must generate more thrust in shorter durations. Since this is counter to the performance of human muscle in the leg, the LAD's thrust geometry would ideally complement the thrust capability of the human leg (Figure 5.38C); generating stable torso support over a range of gait velocities. Note that at lower angles of knee flexion (i.e. lower velocities), the human leg has a larger ability to influence torso thrust, while at larger angles of knee flexion (i.e. higher velocities), the SEG generates the majority of torso thrust. This SEG supplementation works elegantly since slower gait velocities need more control (hence influenced primarily by humans) and higher velocities require more thrust (hence generated by the SEG, which has a lower thrust error at higher velocities).

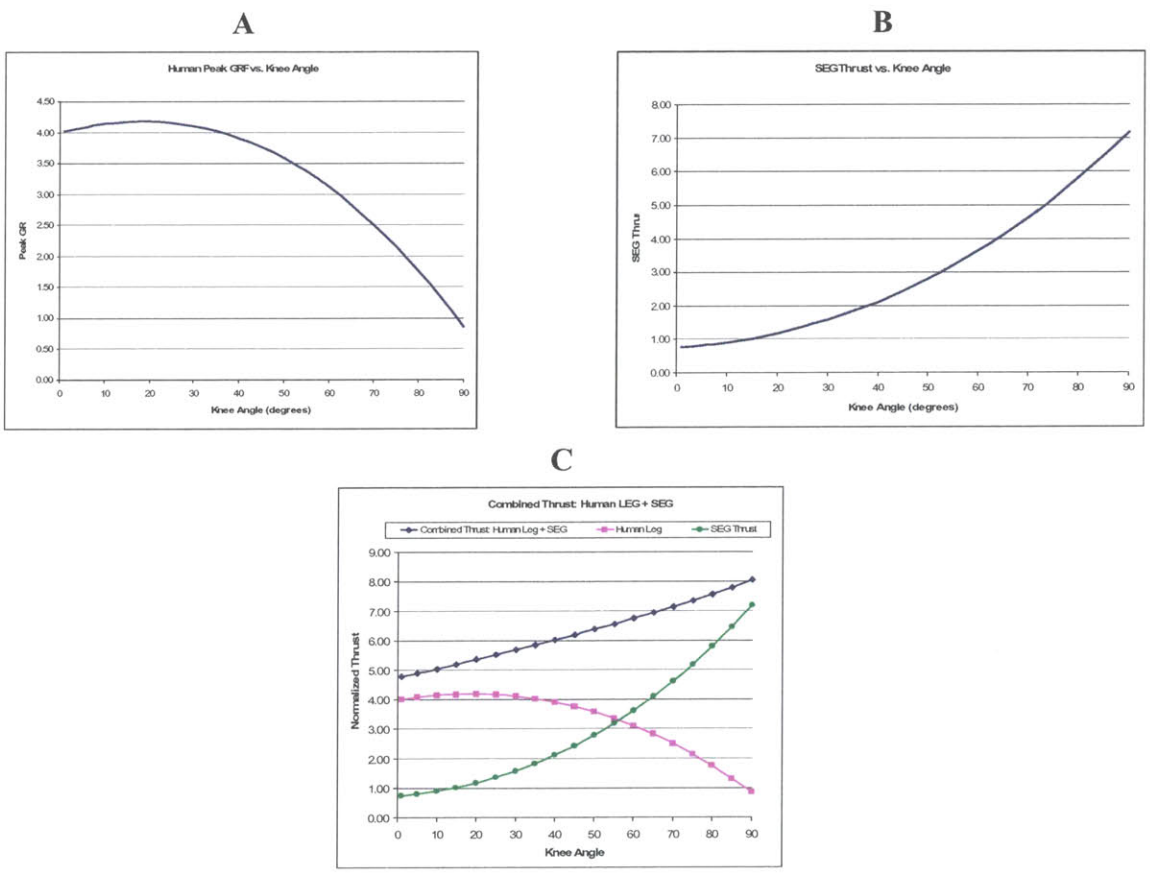

Figure 5.38: (A) Peak Thrust generated by the human leg at one rotational rate, (B) Thrust generated by the SEG, (C) The combined thrust of both the Leg and the SEG

Since we are attempting to engineer a single knee spring which creates an anthropomorphic torso thrust for varying velocities, the real question is how it feels to the user. Though the human body can adapt to different gait cycles, the only method of figuring out if something has a compliant human interface is by trying it out with human test subjects.

6 Alpha Prototype Architecture

In order to address the requirements needed for the proper implementation of the walking assist device, an architectural layout is presented in order to structure the design. Recalling from Section 4 - Design Architecture, the functional requirements and the design parameters presented were as follows:

Functional Requirements

1. Appropriate Torso Thrust
2. Organic Human Interface
3. Longevity
4. Easily Controllable

Design Parameters

1. Anthropomorphic Structurally Sound Exoskeleton
2. Ergonomic Force Transferring Interface
3. Tuned Energy Spring at Knee Joint
4. Kinematic Gait Control Module: Energy Spring Engagement Clutch

From the design parameters, four high-level modules emerge:

1. Structural Exoskeleton
2. Saddle, Cushioning and Straps
3. Torsional Energy Spring at Knee Joint
4. Control for Bimodal Spring Engaging Clutch

A simplified representation of the LAD and the design used to transfer the GRF to the human body is shown in Figure 6.1.

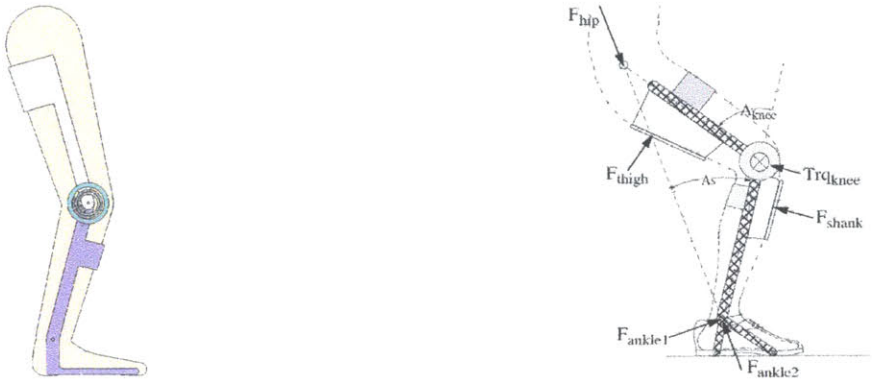

Figure 6.1: The physical architecture of the LAD and its support forces transferred to the human leg.

6.1 Structural Exoskeleton

As defined in the leg model used in the gait simulations, the leg was modeled as a peg leg shank connected to a thigh with a gait controlled bimodal torsion spring at the knee joint. Though this model was only intended to simulate a simplified leg, its physical embodiment needs additional elements. The LAD's exoskeleton is composed of the following elements:

- Shoe Frame with ankle pivot
- Shank Strut
- Thigh Strut
- Knee Joint which allows rotation between shank and thigh strut

It is assumed that the LAD user has both feet. A shoe frame with ankle pivot is used to transfer strut GRFs to the ground. Though the shoe frame's ankle pivot is the rotational point for the shank struts, the simulations still remain accurate since the shoe frame can be modeled as the ground. Though any human instilled ankle torques or heel lift will affect the response of what was modeled, these two additional influences can be thought to be additional control elements for the gait cycle.

The shank and thigh struts must be rigid enough so they do not deform upon torque loading, while at the same time light in weight so minimize inertial interference. In order to ensure that the inside and outside struts both move and rotate in unison, the two must be rigidly attached in order to keep the system symmetrically balanced.

Much like a human knee, the LAD's knee joint must have minimal friction; hence the need for ball bearings. Since the shank and thigh struts must be free to rotate while transferring loads as large as four times the user's body weight, the housings and bearings for the struts axis of rotation should utilize a dual support design in order to minimize internal bearing torques. In order for the inner and outer struts to rotate together, they must share a common axis of rotation about the knee joint. This can be guaranteed by using parallel strut segments above and below the knee joint that are rigidly connected. The struts can have any desired contouring bends above the knee joint, and require the shank struts to be concentrically attach to bearings at the ankle joint on the shoe frame.

Since the physical exoskeleton of the LAD acts as the base platform to upon, it must also be able to accommodate the other modules. There must be attachment points for the thigh saddle, the shank cushion, and all straps used to secure the device to the user. The SEG thrust is generated by a torsion spring which requires a constraining housing in order to develop its non-linear profile. Since the energy springs housing must also be allowed free rotation about the knee joint, the bearings in the struts at the knee joint must account for this. In order for the LAD to have a

bimodal knee joint which allows thrust generation and free rotation, a spring engagement clutch is needed in order to couple and uncouple the shank struts, the spring and the thigh strut. Fortunately, the spring housing eases the execution of this task.

6.2 Saddle –Cushioning – Attachment Straps

By itself, the LAD can easily create an upwards thrust from the ground to the hip, however in order to be useful for humans, the LAD must be able to transfer these GRFs to the human body. In order to ensure these forces are transferred correctly, attachment straps for the shank and thigh are used to secure the LAD to the user. Analyzing the reaction forces perpendicular to the upper and lower struts shown in Figure 6.1, we can determine the magnitude of these forces (Figure 6.2). Note that for these graphs 'A_s' is actually half the magnitude of knee flexion.

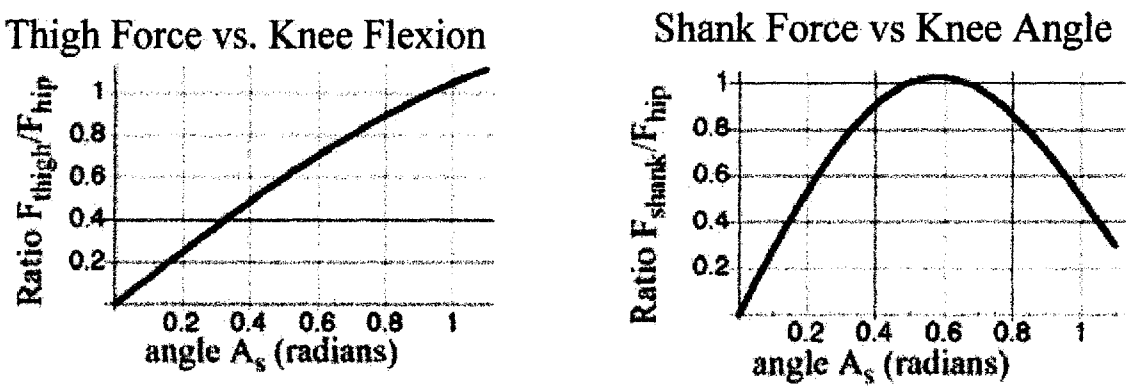

Figure 6.2: The LAD support forces transferred to the back of the thigh and the front of the shank – normalized to total SEG Thrust.

These support forces may be fairly large, so it is best for them to be exerted onto a location which can accept them without tissue damage or discomfort. Since humans can easily sit for prolonged durations, it seemed logical to transfer the thigh supporting forces through the same tissue area that one sits on. Pertaining to the shank support force, since the front of the shank is mostly bone, there is not much tissue to absorb forces. Fortunately, anyone who has played soccer knows that shin guards are extremely effective at cushioning direct shank force impulses.

6.3 Energy Spring

One non-linear torsion spring will be used on both the inside and outside of the knee joint to generate the SEG thrust for the gait cycle. In efforts to minimize the overall weight of the LAD and the required volume for the spring housing, it is desired to have a spring that has a high energy storage to weight ratio. Springs can be made from a wide range of materials. While composite springs have the highest energy storage density, in order to keep the initial design simple and inexpensive, spring steel was chosen for the energy spring material.

In order to attain the non-linear thrust profile required by the spring, the physical geometry of the spring and its housing are engineered such that upon knee flexion, when the spring starts to deform it makes contact with its housing. This interference essentially changes the boundary conditions that determine the spring's elasticity, allowing almost any torque profile to be engineered (Figure 6.3).

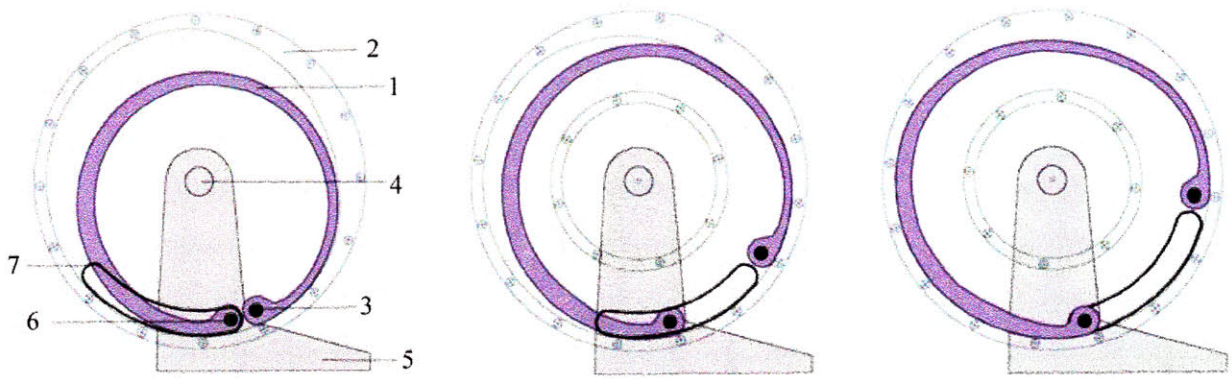

Figure 6.3: The Energy Spring and its Housing interfere upon knee flexion. This changes its effective torque profile.

6.4 Energy Spring Engagement Clutch

In order for the energy spring and its housing to allow both free rotation and thrust production, the spring must be able to be coupled and decoupled from the shank and thigh struts; ideally with a low toggle energy. The method used to accomplish this is simple –notations in the first image of Figure 6.3 will aid explanation. The construction of the knee joint is such that the shank (5) and thigh (not shown) struts are free to rotate about the common pivot (4) of the spring housing (2). One end of the spring (1) is rigidly attached to the shank strut with the 'spring strut pin' (6) that rotates along the spring housing slot (7); the other end is anchored to the inside of the spring housing (3). Since the shank strut is attached to the spring which is fixed to its housing, rotation of the shank results in the free rotation of the all three elements, independent of any thigh strut rotation.

In order to generate a SEG thrust, the thigh strut must become couple to the spring, so upon knee flexion, both struts flex the energy spring. This results when the energy spring engagement clutch activates and rigidly couples the thigh strut to the outside of the spring housing. Since the shank strut is rigidly attached to the spring which is anchored to the spring housing, the shank and thigh struts are now connected with the energy spring between them. During knee flexion, the thigh strut and spring housing remain rigidly attached. As the shank strut rotates about the

knee joint, the spring strut pin rotates along the spring housing slot, deforming the spring which creates a SEG thrust.

Assuming that a 100 kg person flexes their knee 25° during their gait cycle, this correlates to a required knee torque of 125 foot*pounds in order to support the torso. This means that the energy spring engagement clutch must also be capable of resisting that torque in order to ensure the thigh strut is secured to the spring housing. Since it is desired to have a minimal engagement and disengagement actuation force, the spring engagement clutch must be able to generate a large mechanical advantage. In order to simplify the design, it is assumed that at heel strike, the knee is in the same rotational position for every step. Since only a single solution is required for the spring engagement clutch, an easily actuated rotational interference will suffice. In order to ensure that the energy spring engagement clutch is controlled according to the gait cycle, so it is coupled to the thigh struts during the support phase and free to rotate during the swing phase, the actuation device for the rotational interference is attached to the bottom of the shoe frame. Moments prior heel strike, the pressure sensitive mechanism will contact the ground, compressing and engaging the rotational interference which is necessary between the thigh strut and the spring housing. While the leg supports the body, the actuator remains engaged. Upon heel lift, the actuator leaves the ground disengaging the interference between the spring housing and the thigh strut, and the leg is free to rotate in preparation for the next step.

7 Alpha Prototype

Having solidified the design of the modules required for the construction of an energy efficient LAD, a solid model was created and an alpha prototype was built for testing on the right leg of the author of this thesis. Due to frictional losses and other energy sinks associated with the gait cycle, the physical embodiment can not create lossless gait cycles; however it does demonstrate encouraging results for the gait augmentation community.

7.1 CAD Model

A solid model of the LAD is shown in Figure 7.1 and breakdowns of the modules can be seen from Figure 7.2 to Figure 7.5.

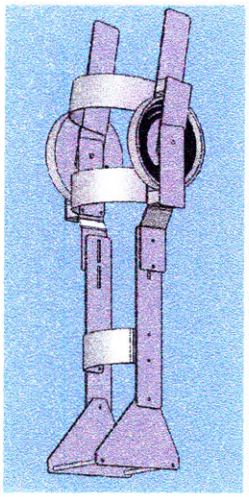

Figure 7.1: Solid model of energy efficient LAD – excluding attachment straps and thrusting saddle.

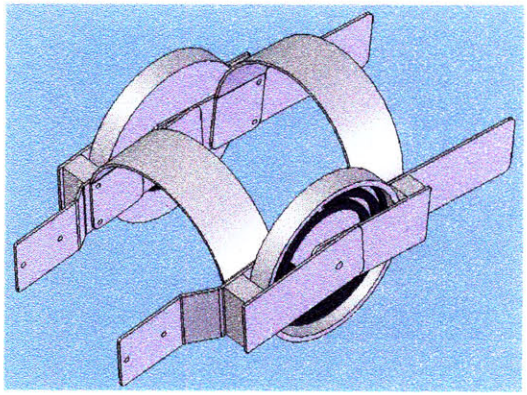

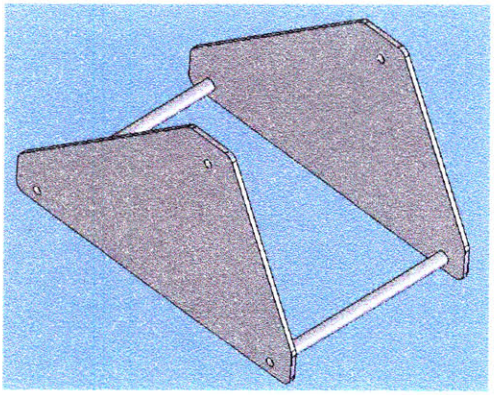

Figure 7.2: Structural Exoskeleton and Shoe Frame

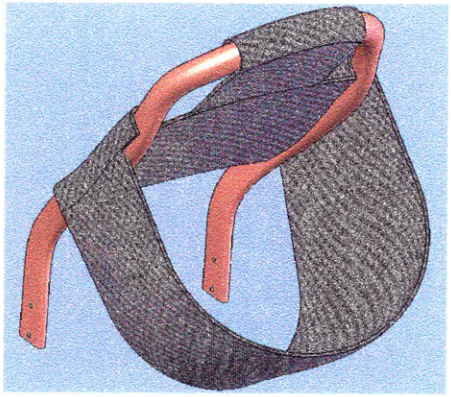

Figure 7.3: Saddle used to transfer forces to the back of the thigh.

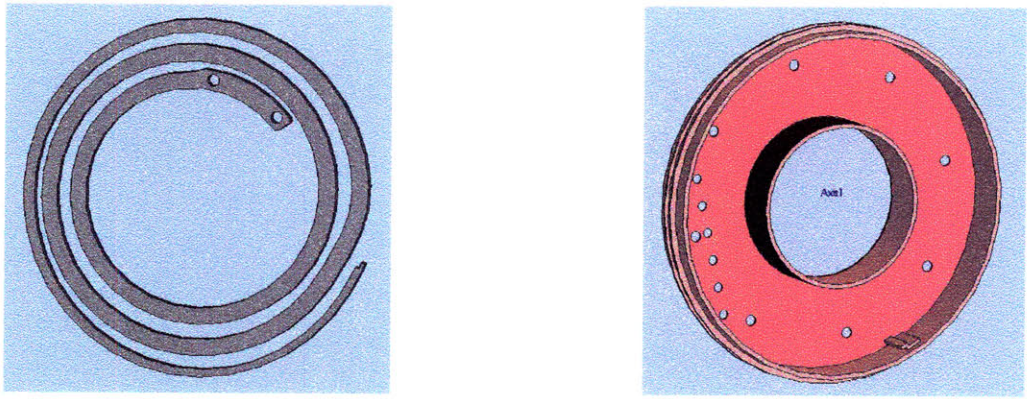

Figure 7.4: Energy Spring and Housing.

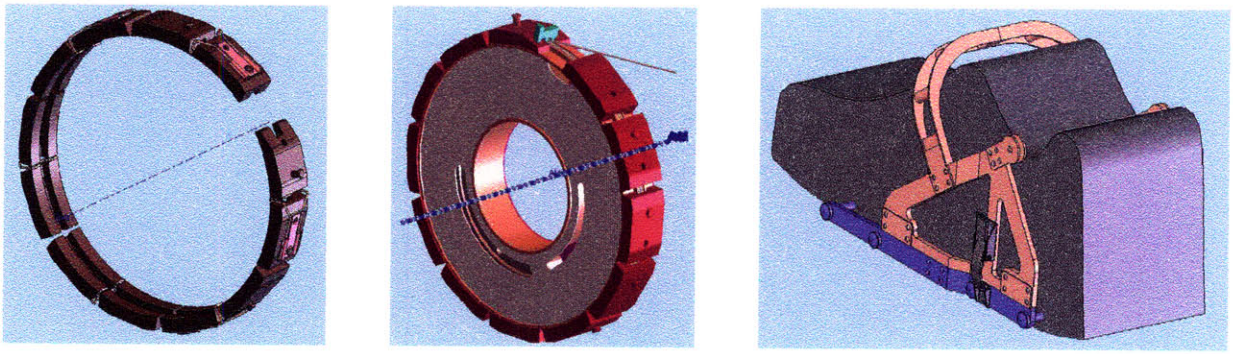

Figure 7.5: Energy Spring Engagement Clutch and Shoe Frame Actuator.

With a solid model constructed, using gait parameters acquired from the simulation with faster initial conditions, a finite element analysis was conducted on the exoskeleton and energy spring. It was determined that a steel exoskeleton constructed from 0.093" thick and 2.00" wide sheet metal is fully capable of withstanding the torques, forces and cyclic strains associated with the range of gait velocities (Figure 7.6).

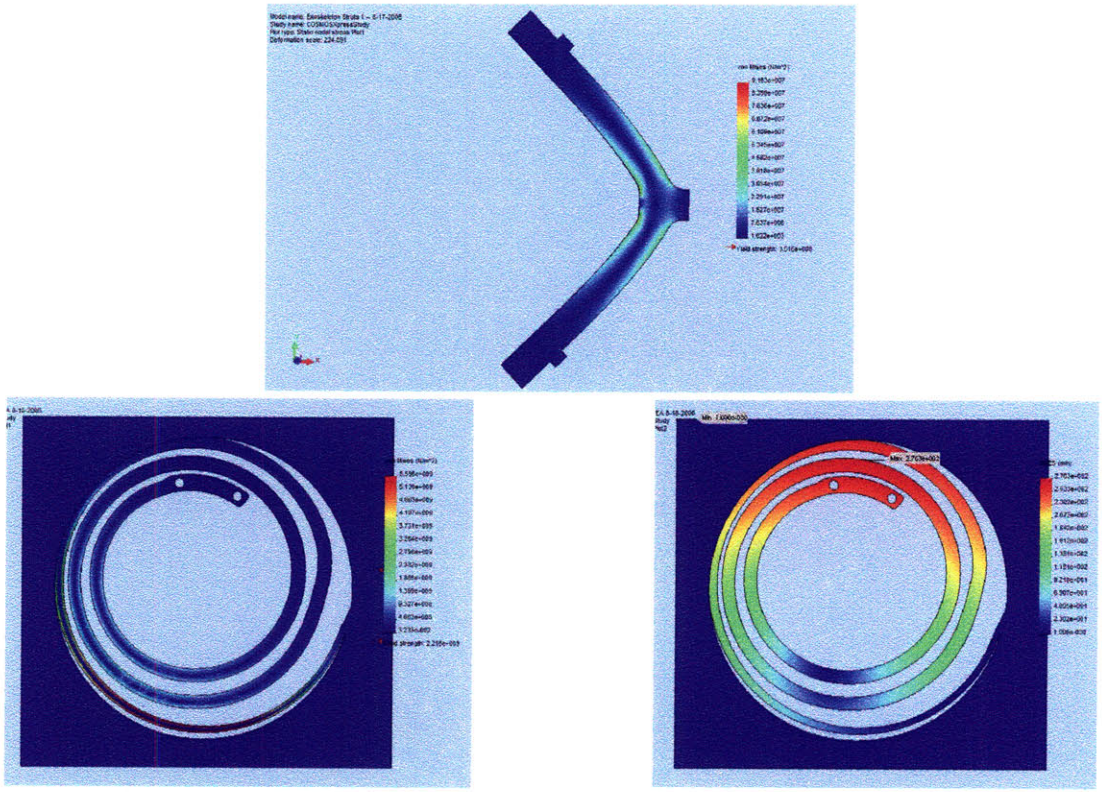

Figure 7.6: FEA of Exoskeleton and Energy Spring under maximum torsional conditions.

Unfortunately, a preliminary FEA of the energy spring was not able to give conclusive evidence of its performance since the simulation was conducted using a simple linear displacement model. This is because a non-linear FEA algorithm is necessary to analyze the collision and deformation as it occurs with the drum housing. Though the initial torsional FEA was not of aid, satisfied that structural exoskeleton was robust enough to survive the forces and torques of the simulated gait cycles, a physical prototype was constructed.

7.2 Physical Construction

The physical construction of the LAD was customized for its initial tester, the author of this paper. The Alpha Prototype and a breakdown of its modules can be seen from Figure 7.7 to Figure 7.11

7.2.1 Structural Exoskeleton

For the exoskeleton for the Alpha prototype, though the structural FEA testing concluded that steel would be the ideal material for the exoskeleton, allowing a generous safety factor, additional FEA tests also concluded that sheet aluminum could also be used; but with initial conditions that are not as aggressive and a lower safety factor. In light of this information, and

for ease of prototyping, the exoskeleton was constructed from 0.093" thick sheet aluminum and aluminum honeycomb.

Figure 7.7: The Alpha Prototype Exoskeleton and Shoe Frame.

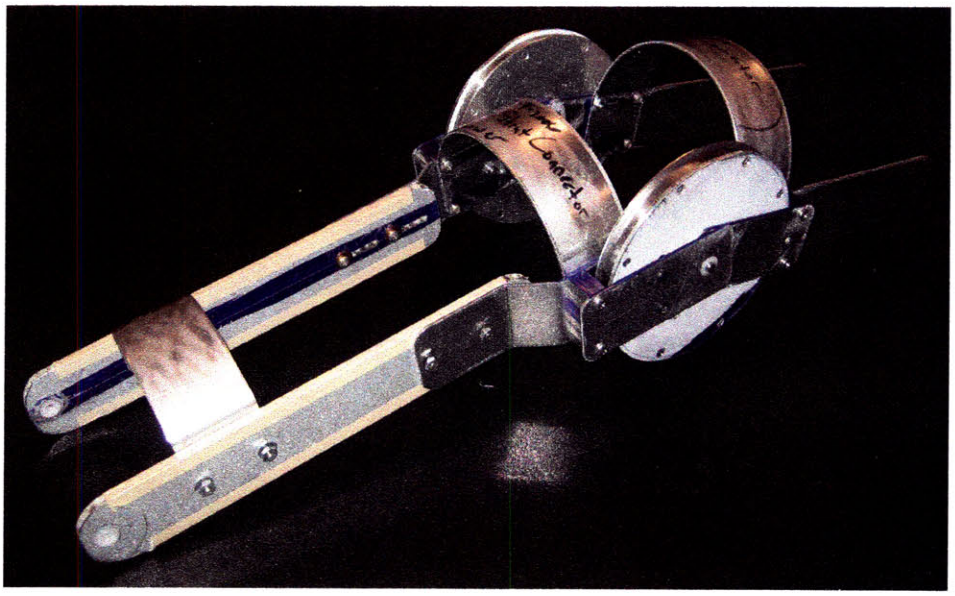

Figure 7.8: The knee torque generation mechanism with shank and thigh struts.

7.2.2 Saddle – Cushioning – Attachment Straps

In order to transfer the exoskeleton support forces to the human body, a larger surface area is desirable in order to decrease the relative applied load to body tissue. The saddle, the primary mechanism used to provide thrust to the back of the thick and butt, was molded using fiberglass.

This allows for a large surface area which is semi-compliant to the user's body. Attachment straps were used to secure the brace and saddle to the user's leg in order to minimize sliding or other undesired motion. The saddle was designed to apply force to the back of the leg over a region similar to what is sat upon in a chair. This region starts approximately 6" above the knee's pivot and extends to almost the top of the butt region. Though the inner upper strut has to stop prior interfering with the groin region, the outer upper strut can extend upwards further, generating better support for the saddle. The saddle wraps approximately 180° around the back of the thigh and attaches to the inner and outer upper struts, as seen in Figure 7.9.

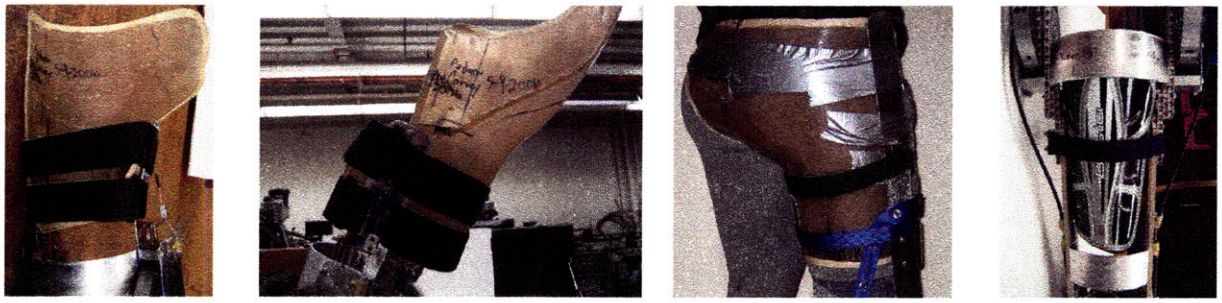

Figure 7.9: The thrust saddle, securing straps and shank cushioning.

Recalling Figure 6.2, forces are not only applied to the back of the thigh, but also the front of the shank. Without a means to secure the lower struts to the shank, the brace would slide down the leg, and the two would not follow the same trajectory, debilitating the function of the brace. To account for this, semi-structural compliant padding was secured between the lower struts for the front of the shank, while adjustable elastic straps wrap around the calf in order to secure the brace to the leg. The shank padding starts below the knee cap, approximately 3" below the knee pivot and extends downwards 8", complying with the changing contour of the shin. For the initial prototype, the shank padding consists of a modified soccer shin guard and an elastic strap with Velcro® for adjustable termination.

7.2.3 Energy Spring

The energy spring located at the knee joint is the basis for all thrust generation. Initial non-linear gait simulations were conducted using an energy spring which generated a peak thrust of 3x body weight at a knee flexion of 1 radian. Since the spring's non-linear characteristic is developed from the interference between the spring and its housing, and it was desired to develop a brace which minimally interfered with the kinematics of the leg or the lower strut shank padding, the drum housing was constrained to have an outer diameter less than or equal to 6".

Following the path of least resistance for material selection, the drum housing was selected to have an ID of 5.11". Using 1095 spring steel as the material for the energy spring and a very conservative yield strength of 85kpsi, the knee's energy spring was engineered to comply within this geometry. Unfortunately, the desired 3x body thrust at one radian of rotation resulted in a spring which had a thickness which was larger than desired, resulting in a bulky knee joint. In order to ease fabrication, the spring's peak thrust was reduced to 1.7x body weight at 1 radian of knee flexion (the detailed design of the energy spring can be found in Appendix B). This resulted in a knee spring which had a thickness of 1.5".

In order to keep a balanced design for the knee joint, the energy spring was split into two halves; one on the inside of the knee, and the other on the outside of the knee joint, both acting in parallel on the exoskeleton. Each spring was 0.75" thick, and was manufactured from four 3/16"thick plates of annealed 1095 steel. To attain the spring's non-linear hardening torque profile, the 8 springs were constrained inside a drum housing which constructively interferes with the spring's deformation upon rotation, changing the effecting stiffness of the spring with respect to rotational displacement.

In order to achieve a yield strength of 85 kpsi from the annealed 1095 spring steel, each spring was heat treated. After consulting different heat treatment charts and conducting sample test experiments, the desired hardness was achieved after firing each spring at 850 °C for an hour, quenching it in water and tempering at 500 °C for an hour. In order to maintain planar flatness of the springs, they were fixture in a holding jig during the process. One energy spring, its housing and an assembled flexural knee joint is shown in Figure 7.10.

Figure 7.10: The energy spring, its housing and a torsional knee joint.

7.2.4 Energy Spring Engagement Clutch

The energy spring engagement clutch allows the bi-modal knee to change from free rotation to a torsional elastically restoring joint. Since the functionality of the knee joint is required to match the user's gait cycle, the engagement clutch is controlled by the state between the foot and the

ground. Using a contact actuator on the bottom of the shoe frame, when the foot is in the air, the clutch is not engaged and the knee is free to rotate; as required in preparation for the next step. When the foot is on the ground, the contact switch actuates the clutch and engages the energy spring with the exoskeleton; this creates a torsional elastic knee joint. Figure 7.11 shows the energy spring engagement clutch and the shoe frame's contact actuator.

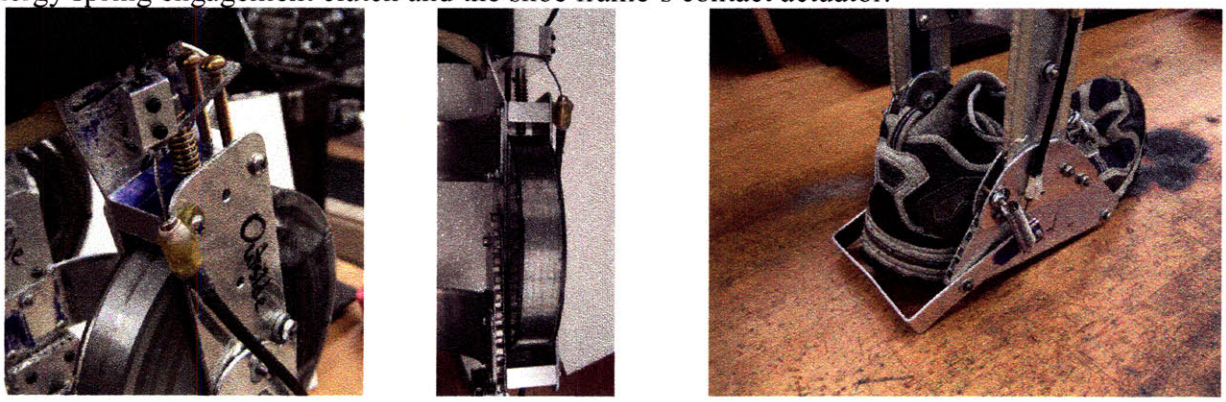

Figure 7.11: -Energy Spring engagement clutch and shoe frame actuator mechanism.

7.3 Prototype Testing and Results

Two rounds of testing were conducted to determine the performance of the LAD. The first round tested the torque generation capability of the manufactured knee energy spring in comparison to its theoretical performance. The second round of testing was conducted to determine the LAD's ability to assist with generating torso support necessary to aid locomotion. It was determined that the energy springs' physical toque profile averaged very closely to the expected theoretical torque. While the initial Alpha prototype of the LAD was too bulky and heavy to gather useful locomotion results, using EMG sensors, it was determined that the exoskeleton does assist the human leg in generating torso support by reducing the metabolic energy required to perform squat thrust.

7.3.1 Energy Spring

In order for the LAD to assist with locomotion, it must be able to generate the appropriate knee torques. To determine how accurately the physical energy spring matched the theoretical torque profile, a torsional testing jig was created in order to determine its response. Incremental weights were attached to the test fixture moment arm while the fixture's rotational displacement was recorded. The test fixture and the response for the energy spring are found in Figure 7.12. Though the spring's torque profile had a very desirable response (with an averaged error of +0.33%), the thrust error was less than desirable (having a corresponded average thrust error of -

15.72%). This increased thrust error was prominently due to the sin error's increase of the moment arm as the knee increased with flexion.

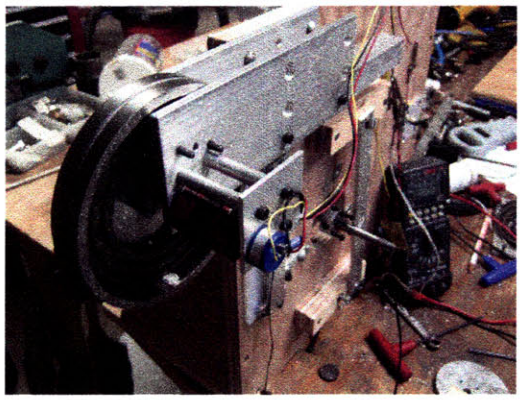

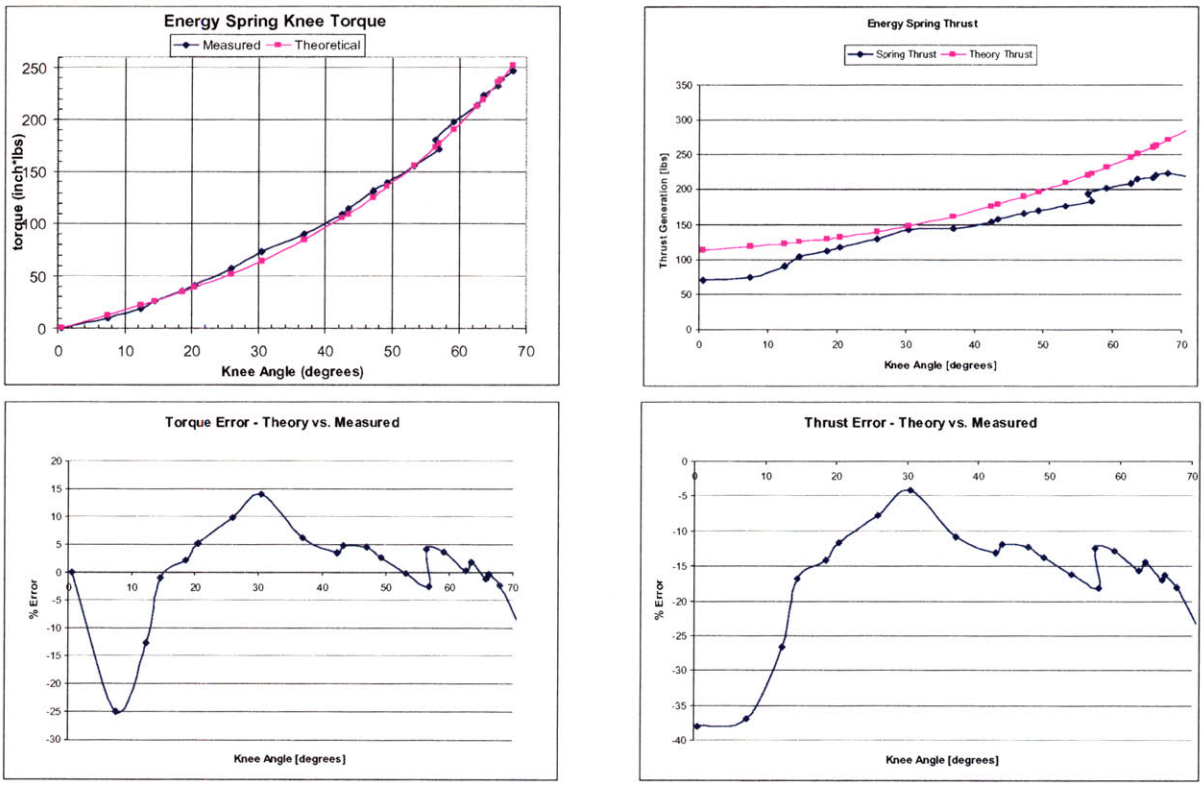

Figure 7.12: The Energy Spring's torsional testing jig. Theoretical and Measured Energy Spring Torque and Thrust generation with the corresponding error beneath.

Since the energy springs will be stressed every step, its cyclic lifespan is an important factor for its design. An average human takes approximately 2 million steps each year [58]. Assuming a six month duration between servicing the LAD with a 1.5x safety factor, the energy spring require a cyclic lifespan of roughly 1.5 million cycles. Two rounds of cyclic testing were conducted on batches of energy springs. The first round tested the springs at maximum load, having a torsional rotation of 60°. The high stresses broke the springs after approximately 5,000

cycles. The second round of testing showed much more encouraging results. Decreasing the applied stress so only 40° of rotation occurred, the energy springs were tested over 50,000 cycles without any cracking, deformation or creep. Though further testing needs to be conducted, initial results demonstrated that the energy springs could be functionally implemented into the LAD for use with human testing.

Adaptive Spring Model

Since the thrust profile of the knee spring was engineered to follow the least square fit for varying velocities, and since not all gait steps will match the optimal initial conditions, not all assisted steps will have maximum spring compression at system apex. This can result in thrusting forces which are directed backwards and upwards, opposed forwards and upwards. Since this will maliciously alter the anthropomorphic gait cycle, a preventative solution needs to be further investigated. Though it was not implemented into the physical Alpha prototype, Mathematica simulations and a more advanced solid model embody a knee freezing clutch which can freeze the knee spring at its maximum compressed state until the torso rotates about the ankle to the appropriate SEG angle such that releasing the knee spring will generate a support profile which is symmetric about system apex. Though briefly freezing the knee at maximum knee compression for an instance would disrupt the anthropomorphic motion of the knee joint, in physical application, the user's ankle joint may be able to generate torques necessary to accommodate for the error of the initial conditions at heel strike. If so, this could simplify the system design while lightening the physical structure.

7.3.2 LAD Torso Support Assist

In order to determine its assistive torso supporting performance benefit, similar tasks were conducted without the LAD and then with the LAD while the leg's metabolic effort was determined with a muscular electromyography (EMG) sensor. Unfortunately, at 10.7 pounds, the Alpha prototype LAD was too bulky and heavy to assess its aid potential during the dynamic condition of locomotion. For initial results, simplified squat thrust tests were conducted while an EMG sensor recorded the muscular effort exerted by the quadriceps muscle without and with the LAD.

The test subject was the author and developer of the Alpha prototype LAD; a healthy young adult male with no lower limb dysfunction. The torsional knee springs were engineered to generate full body support at approximately 45° of angular rotation, however due to error during the manufacturing of the torsional knee spring, full body support was achieved at a knee flexion of 55°. Three differing rounds of squat thrusts were conducted, starting from a fully erect stance to a knee flexion of 55° and back to the starting position. During each test, three squat thrusts

were conducted repetition while EMG data was recorded, without the brace, with the brace but without support assistance, and with the brace conducting support assistance; the quadriceps's EMG sensor data was compared for each test.

Figure 7.13 shows the absolute amplified voltage of the EMG sensor on the quadriceps of the support leg during the three rounds of squat thrusts. Knowing that there is a fairly linear relationship between the EMG voltage and muscular effort, for following observations are seen. First, bracing the leg reduced the required metabolic effort to support the body to 69% of normal conditions. This difference exists because the brace physically constrains lateral motion of the leg; creating the support that stabilizer muscles would normally have to generate. Since the thigh has a large cross sectional area and the surface EMG sensor captures an averaged signal of the measured area, we observe the decreased muscular efforts required of a semi-constrained braced leg. Second, when the brace was donned, conducting squat thrusts with the energy support spring engaged reduced the required metabolic effort to 43% compared with without assistance. Third, support of the assisted braced leg required only 30% as much effort to conduct the same

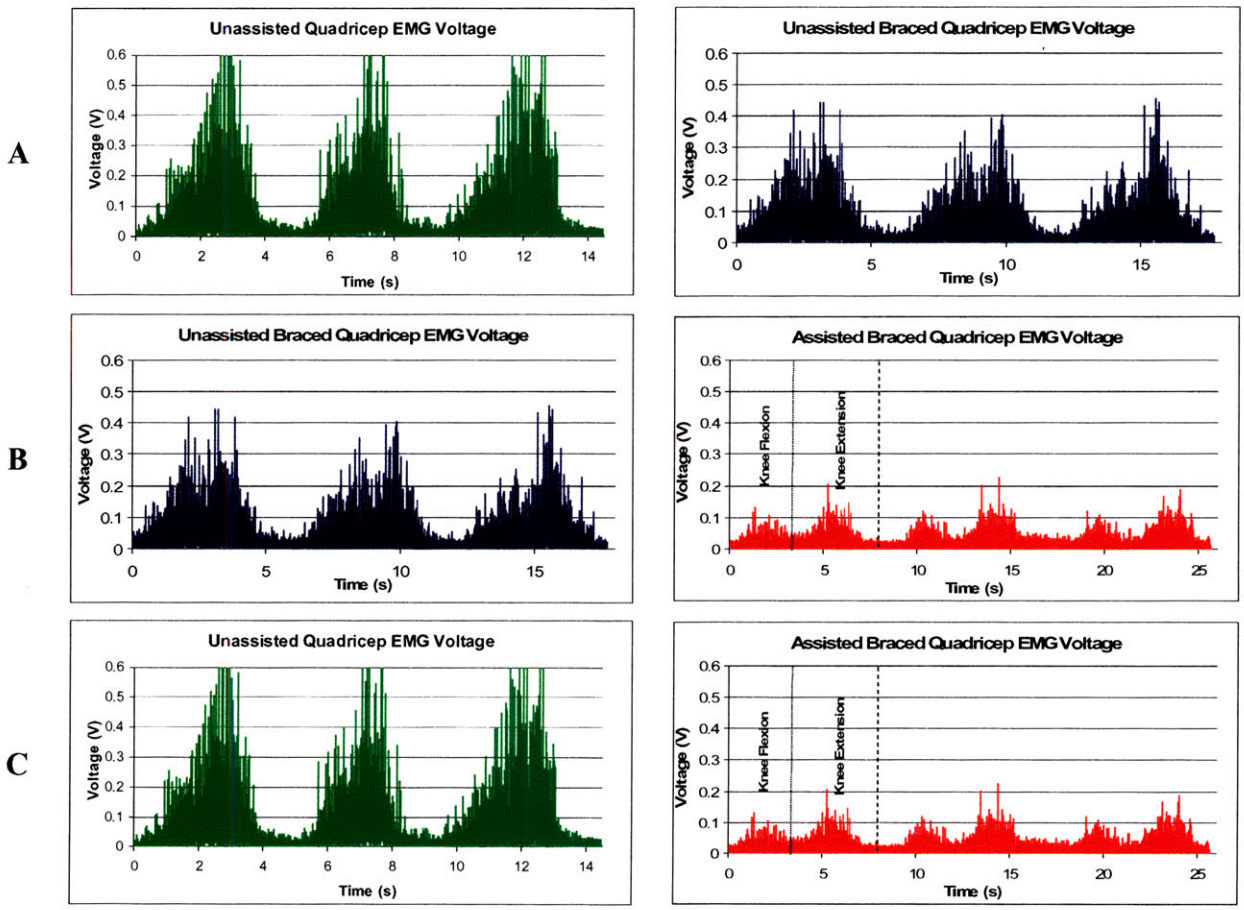

Figure 7.13: The absolute amplified EMG signal of the quadriceps muscle during three rounds of squat thrust tests: without the brace, with the brace (but no assistance), and with the brace (and support assistance).

tests as a normal unbraced leg. Forth, a discrepancy in the brace's performance is shown in the data from the assisted braced squat thrust test. While both unaided test cases showed fairly symmetric muscular effort during knee flexion and extension, the assisted leg's data revealed different muscular effort during knee flexion and extension; knee extension required approximately 36% more effort than knee flexion. This indicates that the frictional losses in the leg brace's knee joint have a dominant effect at knee angles where the torsion springs do not generate much vertical thrust.

7.3.3 Alpha Prototype Test Summary

The Alpha prototype had two test components: the physical behavior of the torsion spring which assists the knee joint and quadriceps, and the LAD's ability to assist humans in torso support. The energy springs' physical response matched the desired theoretical torque curves with extremely promising accuracy. Though the spring's lifespan needs further investigation, initial testing demonstrated a functional lifespan for preliminary LAD testing. Using the energy springs, the LAD demonstrated an encouraging decrease in metabolic effort required for torso support on humans. Though the brace was too large and bulky to conduct dynamic locomotion, the physical apparatus performed as theory predicted; justifying further development of the LAD to assess its beneficial aid during various gait velocities.

8 Conclusion

This thesis presented a KAFO containing a gait-tuned torsion spring at the knee joint which harvests the dynamic energy associated with the human gait cycle in order to assist in torso support and reduce the metabolic energy required for locomotion in patients with lower leg dysfunction. The locomotion assist device (LAD) was inspired by the efficient energy harvesting gait architecture found in some large bodied terrestrial animals. The presented LAD is passive and does not have a power supply or actuators to assist in thrust generation; only the torsion spring at the knee. Upon developing a theoretical model, simulations demonstrated that: 1) Closed loop lossless gait cycles are fully attainable over a range of locomotion velocities using a single design architecture without a need for parameter variation. 2) Appropriately altering the engineering parameters of the LAD's torsion spring can better tune the KAFO's dynamic response to better suite different use's gait cycle. Using the results from the simulations, a prototype LAD was constructed and tested. The LAD's measured torsional response of the knee spring had an average error of +0.33%, while the corresponding thrust had an average error of -15.7%. The evaluation of the exoskeleton's ability to assist with torso support on humans was conducted by comparing the quadriceps muscular EMG data during squat thrusts for one healthy human subject. The results showed that the LAD reduced the quadriceps required metabolic effort during torso support by 43%. Though the initial exoskeleton was too bulky and heavy to conduct useful dynamic gait data, the initial results strongly imply that further development of a lighter and more streamlined KAFO of this architecture could greatly assist individuals with lower leg dysfunction, or healthy people wishing augment their locomotion performance.

9 Appendix – Synthesis of the Energy Spring

It is necessary to thank my father Phil Carvey and my brother Matthew Carvey for their aid in the creation of this Mathematica Spring Synthesis Algorithm. I couldn't have done it without them. Thank you both!

Torso Support and Knee Torque

As previously indicated, after analyzing the data on GRF generation and torso support, the initial normalized Torso Thrust vs. Knee Angle estimate should follow a non-linear relationship which can be generically described as:

$$Thrust = k_1 + k_2\theta + k_3\theta^2 + k_4\theta^3 \qquad \textbf{Equation 9.1}$$

Where the torso thrust is normalized to body weight and the knee angle is in radians.

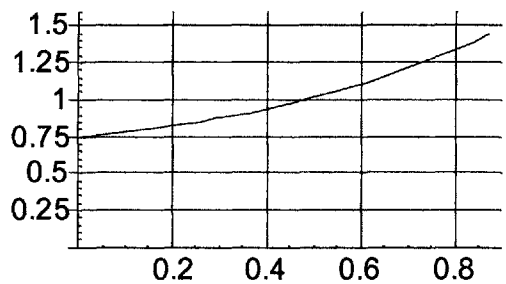

Figure 9.1: Normalized torso thrust profile vs. knee angle

Assuming a balanced design having two springs, one on the inside of the knee joint, and the other on the outside, each spring must supply half the torque required to generate a thrust corresponding to 92% of the body weight; since each leg corresponds to 8% of the body weight and the thrusting leg does not have to life itself.

$$Torque = \frac{1}{2} \cdot 0.92 \cdot Body\_Weight \cdot Thrust \cdot Femur\_Length \cdot Sin\left(\frac{\theta}{2}\right) \qquad \textbf{Equation 9.2}$$

This equation allows a mapping between the desired torso thrust vs. knee angle and required knee torque vs. knee angle.

$$Torque = k_5 + k_6\theta + k_7\theta^2 + k_8\theta^3 \qquad \textbf{Equation 9.3}$$

Where knee torque is in Newton*meters and knee angle is in radians (Figure 9.2).

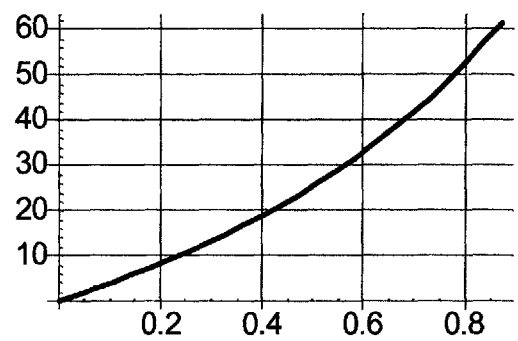

Figure 9.2: Energy Spring Knee Torque vs. Knee Angle Function.

Torsion Knee Spring Fundamentals

Since our torsion spring generates the support energy via bending deformation, in order to determine an initial 'best case' size of the torsional energy spring, we first determine the energy stored during its maximum rotational deformation.

$$Energy = \int_0^{\theta_{Max}} Torque\_Function \cdot d\theta \qquad \textbf{Equation 9.4}$$

$$Strain_{Max} = \frac{Stress_{Max}}{Young's\_Modulous} \qquad \textbf{Equation 9.5}$$

Assuming a safety factor of 2x to account for unequal stress distributions inside the spring during bending, the max energy storage capability of steel is reduced by ½.

$$Energy_{1m^3 steel} = \frac{1}{2} \cdot \frac{1}{3} Stress_{Max} \cdot Strain_{Max} \qquad \textbf{Equation 9.6}$$

Knowing the maximum energy capacity of a cubic meter of steel and how much energy we need to store in the spring, the volume of the spring is determined:

$$\frac{Required\_Stored\_Energy}{Energy\_in\_1m^3\_Steel} = \frac{Spring\_Volume}{1m^3} \qquad \textbf{Equation 9.7}$$

Taking the density of steel, we can determine its mass:

$$Spring\_Volume \cdot \rho_{steel} = Mass_{spring} \qquad \textbf{Equation 9.8}$$

In order to make progress, we need to get an initial guess of the physical characteristics of the spring (i.e. thickness, length, width, etc). In order to create the non-linear torque profile of the energy spring, 'N' mechanical stops physically constrain the spring against the internal housing drum as it rotates. This allows less and less of the spring to flex, which changes the effective bending length; increasing the spring's torsional stiffness. So, as the spring bends due to increased torque, more and more of the spring is contacting the wall (Figure 9.3).

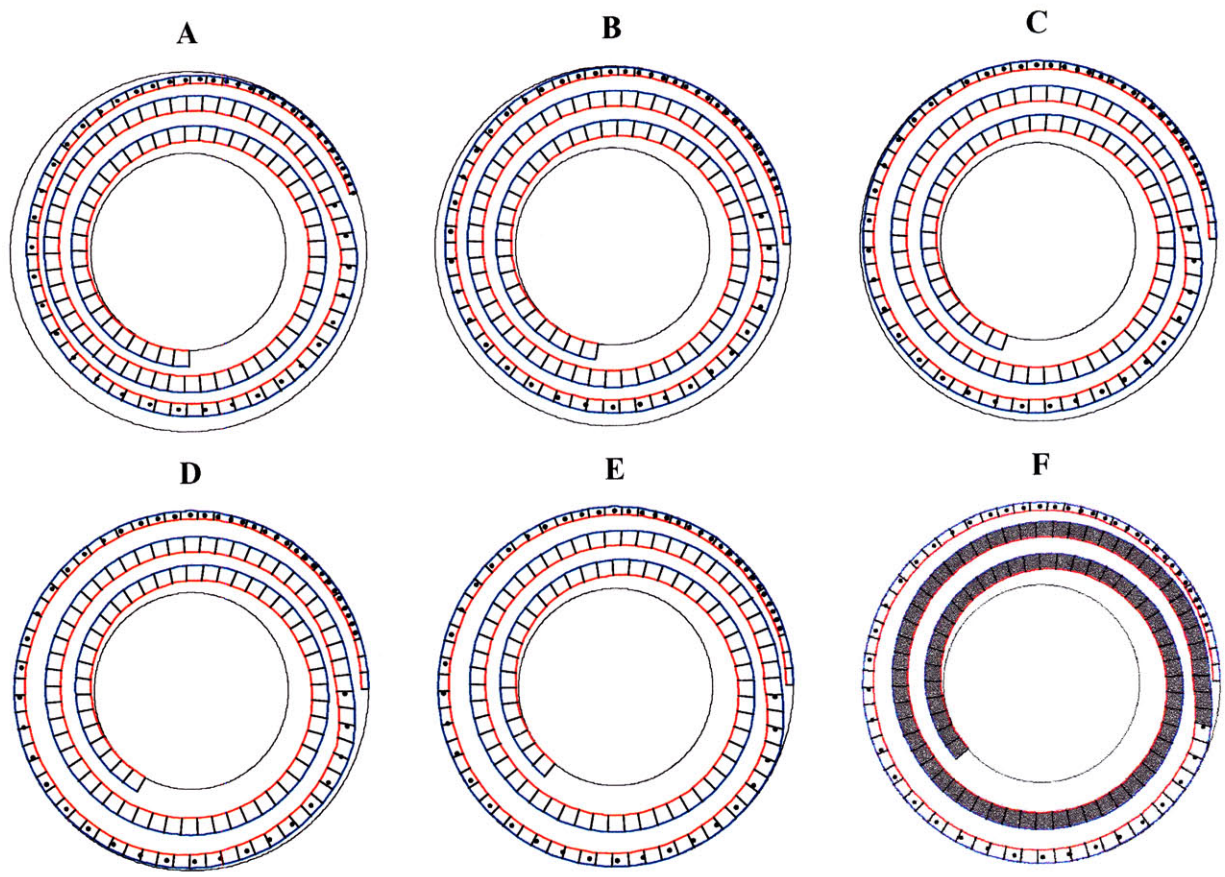

Figure 9.3: The Energy Spring is segmented into many pieces during the synthesis. The black dotes on the spring are the 'stops' where the spring will make contact with the inner wall of the housing drum to change the spring's stiffness and effective torque profile. (A) The Energy Spring with zero applied torque only contacts the wall at its termination point. (B - E) As knee and spring rotation increases, more and more of the spring contacts the spring housing wall. (F) The Energy Spring at maximum torque and rotation with all 'stops' engaged, making contact with the inner wall of the housing drum; the Primary Segment is shaded.

At maximum torque and rotational displacement, the shaded spring segment not in contact with the wall is called the Primary Segment (Figure 9.3F).

Since the shape of the spring plays a determining factor in the spring's bend performance, attempting to design the spring's geometry from zero flexion to maximum flexion state poses many difficulties; this is because altering the spring's geometry at larger angles of flexion affects past performance. Instead, since we know the system state at max torque, we work backwards.

First Order Spring Approximation

In beam bending, when a torque or moment is applied to a beam or segment, an angular rotation at the measured tip occurs.

$$\Delta\theta = \frac{Moment}{k} \qquad \textbf{Equation 9.9}$$

The angular displacement is governed by how large the applied bending moment is and the stiffness of the material 'k'. Though the stiffness of something is dictated in part by the Young's Modulus (E) of the material, the stiffness of a solid body also depends on the shape and boundary conditions. For example, the axial stiffness of a material in tension or compression is governed by its cross sectional area 'A', its Young's Modulus 'E' and the length of the element 'L'.

$$k_{axial} = \frac{A \cdot E}{L} \qquad \textbf{Equation 9.10}$$

For our energy knee spring, in order create the non-linear torque profile, the stiffness of the spring is engineered to be a specific value as the spring bends more and more. For each rotational displacement unit, the stiffness of each segment is governed by its moment of inertia (governed by its thickness), its length, and its interference boundary conditions. By decomposing the spring into N_{Seg} segments, previously described as stops, each with its own relative stiffness, the problem can be broken down into manageable bit sized segments. For segments $0 <= N < N_{Seg}$ the spring must support a torque:

$$Torque\_Function\left[N\Delta\theta + \frac{\Delta\theta}{2}\right]$$

From this required support torque, the maximum stress on the spring is:

$$Stress_{Max} = \frac{6 \cdot BendingMoment}{width \cdot thickness^2} \qquad \textbf{Equation 9.11}$$

We desire to minimize the weight of the spring. In response to this, each segment of the spring is constructed to be at its maximum allowed stress in order to maximize its energy density. Since the required support torque of the spring varies non-linearly with the angle of flexion, the effective stiffness must also change accordingly; this is governed by the thickness and total length of each flexing element, and how it interacts with the housing drum wall. Shorter and thicker flexing segments are stiffer and can undergo higher stresses. Whereas longer and thinner flexing segments are less stiff and can support lower stresses.

In order to minimize spring weight, all bend segments for the chosen material are kept at the minimum thickness required to support torque for that rotation without buckling. Starting from the zero torque state, the initial required support torques are relatively small. As angular rotation increases, the support torques increase at an exponential rate. In order to generate the initial lower support torques, the spring should be longer and can be thinner. At larger rotational angles, the higher support torques should be generated with a shorter and thicker flexing element.

We used this to our advantage for the spring synthesis by creating physical interferences with the spring housing drum as the spring bends to decrease the effective flexing length, increasing its

stiffness. By increasing the spring's thickness as the flexing length decreases, we can attain the desired non-linear torque profile. The spring segments which contact the housing wall store the energy associated with previous bent segments. Since they are constrained against the wall, they no longer affect future potential bending characteristics. Any future bending will only be conducted by the free floating spring section not against the wall, and it will only have to support the energy differential associated with the spring's torsional displacement. In effect, we have created a variable stiffness torsion spring where each flexing spring section can be thought of as being composed of many linear compression springs connected in series with different stiffnesses.

Springs in Series - Elasticity

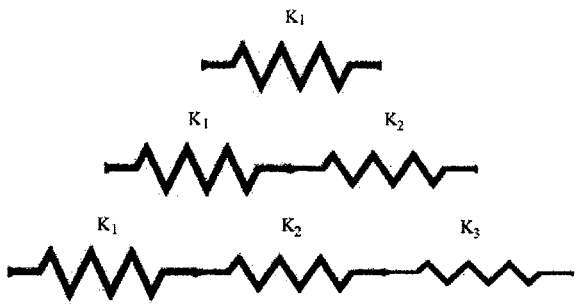

Effective Spring Constant

$$\frac{1}{k_{Seg\_1}} = \frac{1}{k_1}$$

$$\frac{1}{k_{Seg\_2}} = \frac{1}{k_1} + \frac{1}{k_2}$$

$$\frac{1}{k_{Seg\_3}} = \frac{1}{k_1} + \frac{1}{k_2} + \frac{1}{k_3}$$

Where K_1, K_2, K_3 … K_N correspond with the spring segment's effective spring constant and $K_1 > K_2 > K_3 \ldots > K_N$. K_1 is the Primary Segment's corresponding spring constant.

Since the geometry of the spring is engineered to follow a specific torque profile, the effective stiffness of the spring must also vary appropriately with rotational displacement. As the spring unbends, the required support torque decreases along with the effective spring stiffness. To account for this, the spring segments supporting this torque can be thinner. Since the previous spring element can't be changed, but the effective stiffness must decrease, the spring is lengthened with a thinner segment. This allows a spring geometry to be engineered that follows the desired torque profile function. This new combined spring constant which incorporates the bending elements' thickness into it is defined to be the compliance of the spring. It can be thought of as one over the difference in applied torque for a rotational displacement.

Springs in Series – Compliance

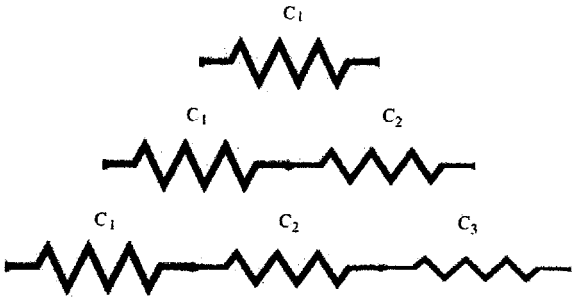

Effective Spring Compliance * Length

$$c_{Seg\_1} = c_1$$

$$c_{Seg\_2} = c_1 + c_2$$

$$c_{Seg\_3} = c_1 + c_2 + c_3$$

The compliance of each segment can be approximated as:

$$Compliance[Seg_N] = \frac{1}{Torque_{Applied}'[Seg_N]} - \frac{1}{Torque_{Applied}'[Seg_N + \Delta\theta]} \qquad \textbf{Equation 9.12}$$

Where '$\Delta\theta$' is chosen to be the maximum flexural angle divided by the number of segment stops used in the spring calculations:

$$\Delta\theta = \frac{\theta_{Max}}{N_{Segment\_Stops}} \qquad \textbf{Equation 9.13}$$

Using this relationship, as the number of spring elements increases, the compliance asymptotically approached a common compliance function. From differential calculus, the compliance function is defined as:

$$Compliance[\theta] = \frac{Torque\_Function''[\theta]}{(Torque\_Funtion'[\theta])^2} \qquad \textbf{Equation 9.14}$$

Using the torque profile previously defined, the compliance of each spring segment with respect to its rotational displacement can be visualized as:

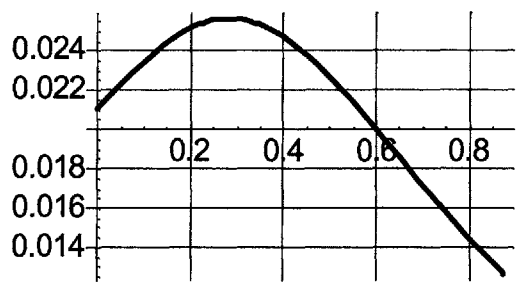

Figure 9.4: Compliance of each spring segment in Torsional Energy Spring with respect to its rotational displacement.

The torque requirement and the bending equation can be correlated to show that the length of segment N times its compliance (giving the inverse of the segment's stiffness) times the change in torque equals the change in angle contributed by that segment:

$$\Delta\theta_{Segment_N} = Length[Seg_N] \cdot Compliance_N \cdot \Delta Torque \qquad \textbf{Equation 9.15}$$

In order to determine the physical parameters of each segment, the maximum stress applied to the flexing section of the spring due to the corresponding applied torque is used to calculate the required thickness of the support element. The width of the spring is defined by choice. To calculate the length of the spring's Primary Segment, we then need to determine how much the applied torque changes if we back off the Max Torque a minute amount. To do this, we differentiate the applied knee torque function and calculate its value at the Max Torque. Assuming a uniform applied bending moment throughout the spring, the first order length estimate of the Primary Segment is calculated by:

$$length[N_{Primary}] = \frac{E \cdot moi[N_{Primary}]}{Knee\_Torque'[Max]}$$ **Equation 9.16**

Where 'E' is the Young's Modulus of the material and 'moi' is the moment of inertial of the segment. Continuing with this train of thought, an initial theoretical synthesis for the rest of the spring can be conducted; determining the thickness and length of each spring segment.

$$length[N] = compliance[N] \cdot E \cdot moi[N] \cdot \Delta\theta$$ **Equation 9.17**

The first order approximation uses 51 spring segments; one primary segment and fifty 'wall-contacting' segments. At zero degrees rotation, only the first segment contacts the drum housing. At maximum rotation, the first 50 segments contact the wall and the Primary Segment free floats at until its termination at the drive end shank strut. The following three graphs show the thickness, length and starting point along the spring for the 50 spring segments. Note that a minimal spring thickness requirement was instilled into the design in order to prevent the spring segments from buckling at higher loads.

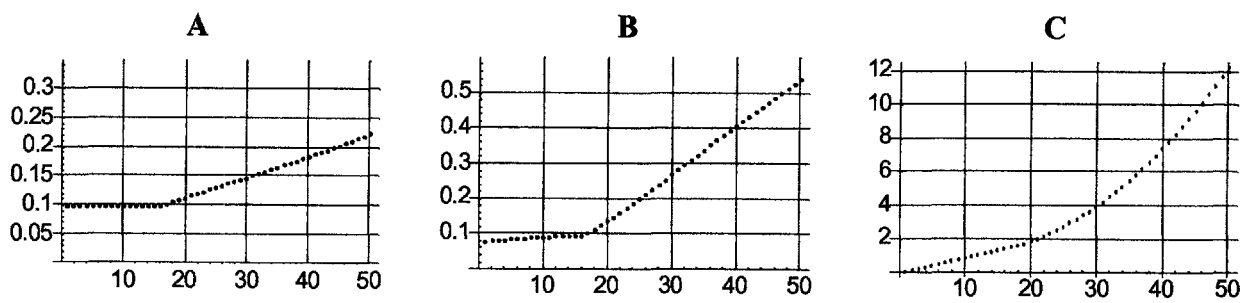

Figure 9.5: The first order spring design results of its 50 segments. (A) Thickness of segment N. (B) Length of segment N. (C) Starting point of segment N.

This data was next used to create a thickness function for the spring relative to its neutral axis, starting at the spring's drive end:

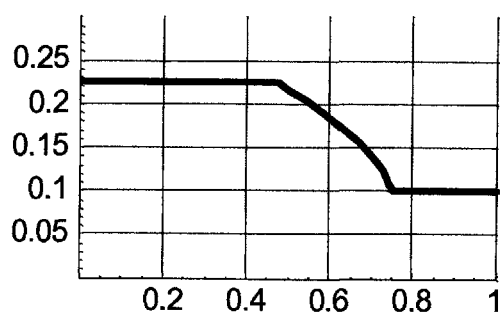

Figure 9.6: First order spring thickness (inches) along its neutral axis (normalized to unit length 1).

Using this data, an averaged geometric profile was created. Due to the minimum spring thickness to prevent buckling, this initial calculation weighed 1.28% more than the maximum energy density case. This difference occurs since the thickness not decrease to zero and the

length of the lower numbered spring segments significantly increases to create the appropriate stiffness, thereby giving rise to a quadratic cost for the minimum spring thickness requirement.

Spring Synthesis

Analyzing the deformational behavior of the first order spring revealed that additional parameters are required to constrain the drive end of the spring. Without additional constraints, the drive end of the spring does not stay on the correct rotational path, inhibiting the correct torques to be applied. In addition, the second round synthesis algorithm used differential curvature equations instead of simple beam bending equations to calculate the deflections. The elegant quality of working in the curvature domain is that it holds true for N-Dimensional space. This eases the calculations since any desired geometry coordinate system can be chosen to conduct the necessary calculations. Having determined a first order approximation for the length and thickness of the torsional spring's geometry, these values are used as guesses for initial conditions in the new synthesis algorithm.

Wikipedia defines that the curvature of a function has a given point *P* with a magnitude equal to the reciprocal of the radius of an osculating circle (a circle that "kisses" or closely touches the curve at the given point), and is a vector pointing in the direction of that circle's center (Figure 9.7) [59]. The change in curvature along the spring is governed by the applied bending moment, the moment of inertia of the segment, and the interface between the spring and the housing drum wall. This change in curvature determines the spring's deformation and segment deflection.

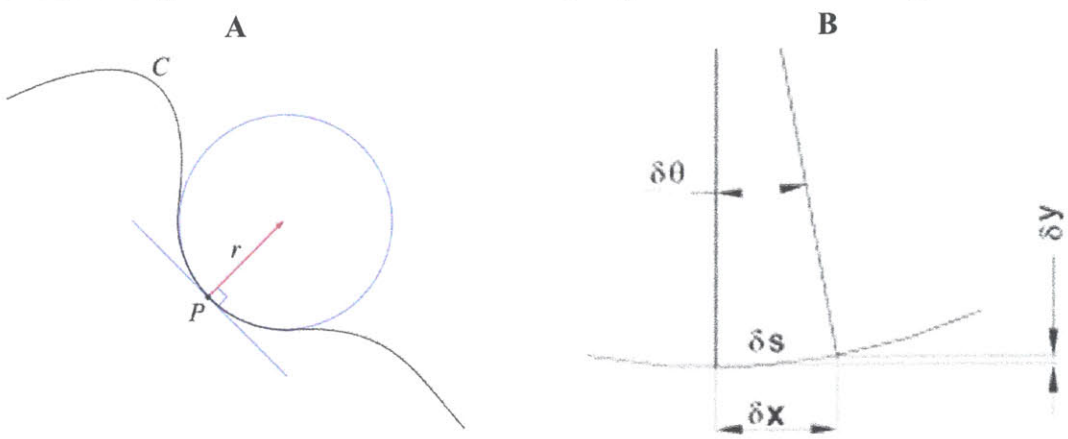

Figure 9.7: (A) Curvature of a function at a defined point. (B) Change in curvature as a result of an applied moment over the segment. [59]

When dealing with curvature calculations, the independent variable used in the calculations is 's'; the distance along the neutral axis of the spring. To determine the curvature of a profile, we define the function in terms of the radius of the neutral axis along the spring. Figure 9.8 assist us in determining this.

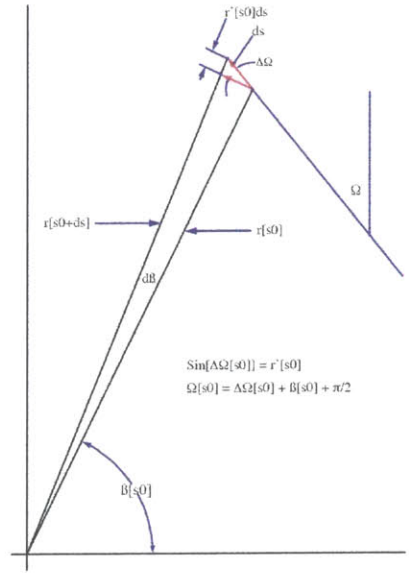

Figure 9.8: Curvature is derived from the change in the tangent angle of function along 's'.

Curvature can be thought of as the derivative of the tangent angle with respect to the distance 's' along the profile. Taking a profile function, the tangent angle is:

$$TangentFunction[s] = \beta[s] + \frac{\pi}{2} - ArcSin[r'[s]] \qquad \textbf{Equation 9.18}$$

Differentiating both sides yields the curvature function of the profile:

$$Curvature[s] = \beta'[s] + \frac{r''[s]}{\sqrt{1 - r'[s]^2}} \qquad \textbf{Equation 9.19}$$

This can be simplified to show the simplified curvature to be:

$$Curvature[s] = \frac{1 - r'[s]^2 - r[s] \cdot r''[s]}{r[s] \cdot \sqrt{1 - r'[s]^2}} \qquad \textbf{Equation 9.20}$$

For our spring system, 's' varies from 'sEnd' to zero and has an intermediate value 'sBendStart' which is the distance along the spring were the spring makes contact from the drum wall. s=sEnd is the end of the spring driven by the shank strut frame. s=0 is the termination length where the spring is attached to the inner edge of the spring drum housing. The spring only bends in the section from the start s=sEnd, to the drum housing contact point at s=sBendStart. sBendStart varies with flexion.

Since the spring's non-linear torsional profile results from being constrained by the inner edge of the spring drum housing, we synthesis the spring in reverse; starting with the maximum torsional requirements at maximum flexion and work backwards to zero degrees of flexion. Using this defined geometry, as the spring unbends from max torque to zero torque, there is the Primary Segment, a spring length section between the end of the Primary Segment away from the drive end and sBendStart which is not in contact with the wall (zero at max torque), and a spring

length section from sBendStart to zero in contact with the wall. As torsional rotation decreases, less and less of the spring contacts the wall. It is assumed no bending or deformation will occur along the spring length in contact with the drum wall.

The first order calculations revealed that the shank drive end of the spring did not remain along the desired drive trajectory. In order to compensate for this, two additional forces were instilled at the drive end, resulting in three applied bending moments which change the curvature of the spring. Along the spring segment sBendStart < s < sEnd, all three bending moments are in general non-zero and need to be considered while calculated the spring's bending.

The three bending moments are:

bendingMoment	Independent of 's'. Torsional bending moment.
forceR*bendingMomentRfunction[s]	'forceR' is the radial force applied to the spring (i.e. directed from the drum center to r[sEnd]. 'bendingMomentRfunction[s]' is the bending moment function of 's' due to a one Newton 'forceR'.
forceA*bendingMomentAfunction[s]	'forceA' is the axial force (i.e. perpendicular to the radial force). 'bendingMomentAfunction[s]' is the bending moment function of 's' due to a one Newton 'forceA'.

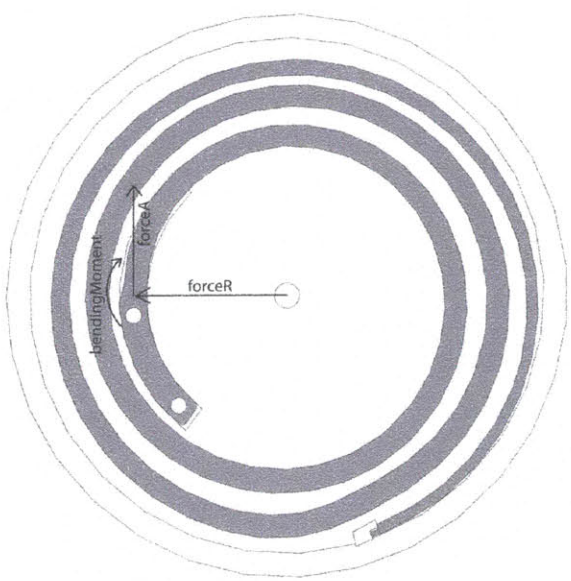

Figure 9.9: The three resulting moments on the torsional energy spring.

At each iteration in the synthesis for a given applied torque, the net bending moment (consisting of the bendingMoment and the axial force times the radius) and the radial force 'forceR' are computed to maintain constant r[0] and r'[0] in order to keep the drive end of the spring at a fixed rotational distance from the pivot. In general, 'bendingMoment' is independent of 's' and 'forceA' and 'forceR' will be non-zero. These non-zero forces are generated by the drive pins connecting the shank strut frame to the drive end of the spring, and are allowed to vary within

the limits of the pins' shear strength. Since 'bendingMomentAfunction' and 'bendingMomentRfunction' are functions of 's', we expect the change in curvature to be non-uniform over the range sBendStart < s < sEnd. Since the compliance of a rectangular bar is inversely proportional to the cube of the thicknessF[s], it also determines how the spring's curvature will be affected by the moments acting on it. By selecting the correct variation thickness we can ensure that the overall maximum stress limit is not exceeded during the synthesis process.

Clarifying the forces and moments acting on the drive end of the torsion spring, we can better calculate how the spring will react during deformation. For the synthesis algorithm, three functions act in a larger function called **Eqs** which defines the set of equations which interrelates the change in curvature due to the applied bending moments; this is the heart of the entire synthesis procedure. The three main functions used are:

comp[x]	The compliance of a rectangular bar of thickness x
stress[x, y]	The maximum stress for a rectangular bar of thickness x under bending moment y
curv[r, r', r'']	The curvature in terms of radius 'r'

The general compliance of a rectangular bar:

$$compliance[thick] = \frac{12}{E \cdot widthSpring \cdot thick^3}$$ **Equation 9.21**

The stress of a rectangular bar as a function of the thickness and applied bending moment:

$$stress[bm, thick] = \frac{6 \cdot bm}{widthSpring \cdot thick^2}$$ **Equation 9.22**

The curvature function in terms of r, r', and r'':

$$curv = \frac{1 - r'^2 - r \cdot r''}{r \cdot \sqrt{1 - r'^2}}$$ **Equation 9.23**

The basic premise for the curvature calculations to be conducted is that the new curvature of the function is equal to the present curvature plus the curvature change created by the bending moment times the compliance of the segment which the torque is applied.

$$curv[s_{i+1}] = curv[s_i] + compliance[s_i] \cdot \sum BendingMoment[s_i]$$ **Equation 9.24**

Using these equations, we now create two differential equations which govern the relationship between r[s], r'[s] and the applied bending moment on the spring. To simplify the calculations using dSolve, we create a mapping of r[s] = u[s], and r'[s] = v[s].

Equation 9.25

$$eqs = \frac{1 - v[s]^2 - u[s]v'[s]}{u[s] \cdot \sqrt{1 - v[s]^2}} ==$$

$$eqs == baseCurvature + comp[thicknessF[s]] *$$
$$(bendingMoment - ForceA * bendingMomentAfunction[s] - forceR * bendingMomentRfunction[s])'$$
$$u'[s] == v[s]$$

Initial Spring Geometry

Since we are determining the spring geometry in reverse, the first step in the synthesis process is to create the desired spring shape when the maximum torque is applied. Creating the desired spring shape for the outermost coil is fairly straight forward since at maximum torque, the outer surface of the outermost coil between 0 < s < sBendStart is tangent everywhere to the inner surface of the drum's outer ring. We define the spring in terms of its thickness 'thick[s]' and the distance of its neutral axis from the spring center r[s]. Both functions use the independent variable of s=distance along the outer surface of the spring. s=sEnd corresponds to that point touching the shank frame drive end. At zero applied torque, there exists a s=sZeroTrq where the outer surface touches the inside surface of the drum's outer ring; there is a region of the spring from 0 <s < sZeroTrq where the spring is always in contact with the inner wall of the drum housing.

Creating the desired spring shape for the inner coils spring is more challenging because we do not know how r[s] changes as a function applied torque, we do not accurately know the length of the spring, and we do not accurately know the thick[s].

Let rMaxTrq[s] be the outer surface at maximum torque and rZeroTrq[s] be the outer surface at zero applied torque , and Δr[s] = rMaxTrq[s] - rZeroTrq[s]. Then we know Δr[0] = 0, Δr[sZeroTrq] = 0 and Δr[S] >= 0 for all 0 < s < sZeroTrq for all applied torques. The main concern in the synthesis process is providing sufficient clearance between spring coils as the spring bends.

From the chosen geometry, the spring housing drum has an inner diameter of 5.11" and the drive end of the spring rotates around an inner drum with an external diameter of 2.8". From the first order spring calculations, coiling the spring within this geometry requires approximately 940° of rotation for the calculated length. Assuming that it is desired to maximize the length of 0 < s < sBendStart[MaxTrq] to almost the full circumference for the inside of the drum housing wall, we can create an initial external profile of the outer coil edge for the spring.

From these constraints, we can create the initials rMaxTrq[s] and rZeroTrq[s] profile functions for the outer coil of the spring. Using these start and end contour states in junction with the curvature equations, the spring geometry can be interpolated. The total length of the spring during the synthesis is a critical factor since all the deformation must occur within the defined spring length; if more spring length is needed to complete flexural relaxation to its zero torque state, and there is none, the program will not be able to complete the synthesis and it will have to restart with a longer initial length. The iteration process is conducted in three nested loops. The outermost loop iterates to find the thickness profile for each spring segment. The middle loop iterates to find each spring segment length. The innermost loop checks to ensure that the net bending moment, axial and radial forces result in the correct bending deformation for each segment length. A Newton-Raphson search function adjusts each segment length so the bend magnitude is correct.

Upon determining correct thickness and length for each segment of the spring, an interpolation profile for the outer and inner coil of the spring can be created from the data points in order to achieve the geometry of the spring in its natural zero-torque state.

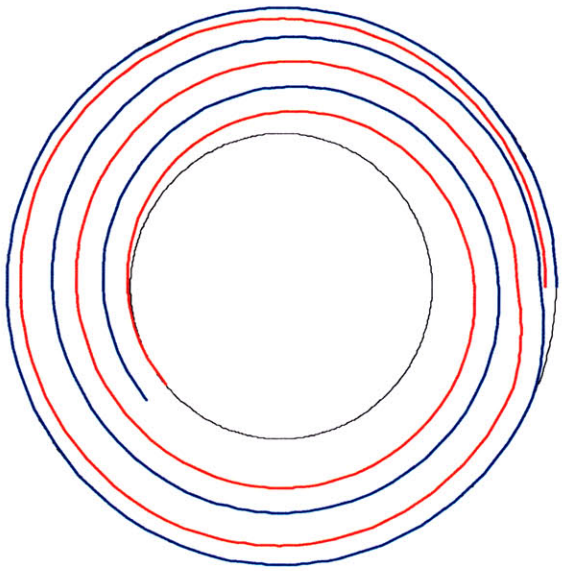

Figure 9.10: The outer (blue) and inner (red) edge of the torsion spring at maximum torque.

The data points used to create the outer and inner coil curvature were exported to a text file. This text file was then imported to a spreadsheet program and the data was manipulated so it could be imported into SolidWorks as a design table. This table allowed a 3D solid model to generated; which was eventually used for CNC fabrication of the spring for physical testing. The results of the physical testing of the spring are shown in the body of the thesis.

References

[1] A. M. Wilson, "Horses damp the spring in their step," *Nature,* vol. 414, pp. 895 - 899, 2001.

[2] http://en.wikipedia.org/wiki/Locomotion, "Define: Locomotion," 2006.

[3] J. Rose and J. Gamble, "Human Walking," Second ed Baltimore, Maryland: Williams & Wilkins, 1994.

[4] "Tuberosity of the ischium," G. s. Anatomy, Wikipedia, August 14, 2006, <http://en.wikipedia.org/wiki/Image:Gray343.png>.

[5] "Cane - Rattan," Wikipedia, Wikipedia, January 17, 2006, <http://en.wikipedia.org/wiki/Crutch#Types>.

[6] "Crutches", May 5, 2006, <http://acdk.tripod.com/images1/CRUTCHES%20ALU&WOOD.jpg>.

[7] "Wheeled Walker", C. Channel, April 26, 2006, <http://comfortchannel.com/prod.itml/icOid/6667,>.

[8] "Crutches", performanceptri.com, 4-26-2006, <http://www.performanceptri.com/_images/Crutches.jpg>.

[9] www.phc-online.com, "wheel chair," 2006.

[10] Www.phc-online.com, "wheel chair - powered," 2006.

[11] Dicks.Sporting.Goods, "Cramer T1 Active Ankle Support," 2006.

[12] "CTi2VAPOR", Ossur, April 26, 2006, http://ossur.com/shared/FileGallery/SharedFiles/Ossurcom/BracesAndSupports/IS_ProductCatalogPages/KNEE.CUSTOM.CTi2VAPOR.pdf

[13] www.teufel-international.com, "Hip Orthosis Stuttgart type," 2006.

[14] "Leg Brace," Wikipedia, Wikipedia, April 26, 2006, <http://en.wikipedia.org/wiki/Leg_brace>.

[15] KanGooJumps.com, "KJ4-XR (X-Rebound)," 2006.

[16] "PowerSkip Pro", PowerSkip, 4-17-2006, <http://www.powerskip.de/mainpage3.html>.

[17] Discover, "Springwalker," in *Discover*, December 1992.

[18] "Russian Rocket Boots", Wood, 6-23-2006, <http://www.imperialyt.com/boots.htm>.

[19] A. Carvey, Interview with Becky Kusko, Boston, July 7, 2006.

[20] "Premium Sized Knee Immobilizer", Ossur, March 21, 2006, <http://ossur.com/template110.asp?pageid=2467>. http://ossur.com/shared/FileGallery/SharedFiles/Ossurcom/BracesAndSupports/RoyceProdCat/9LowExtremBracesAndSupports.pdf

[21] "Knee PostOp Option", Ossur, April 11, 2006, <http://ossur.com/template110.asp?pageid=2202>. http://ossur.com/shared/FileGallery/SharedFiles/Ossurcom/BracesAndSupports/IS_ProductCatalogPages/KNEE.POSTOP.OPTION.pdf

[22] A. Carvey, Interview with Matthew Carvey, Bedford MA, March 3, 2006.

[23] "Total Knee", Ossur, July 16, 2006, <http://www.ossur.com/template110.asp?pageid=160>.

http://www.ossur.com/shared/FileGallery/SharedFiles/Ossurcom/Product%20files/2005ProductCatalog/TK2000Pages.pdf
[24] "Stance-Control Orthosis", StanceControl.com, 7-23-2006, <http://www.stancecontrol.com>.
[25] "Rheo Knee", Ossur, August 16, 2006, <http://www.ossur.com/template110.asp?PageID=1780>. http://www.ossur.com/shared/FileGallery/SharedFiles/Ossurcom/Bionics/Brohures/RheoKneeBrochLR.pdf
[26] "Flex Foot", Ossur, July 16, 2006, <http://www.ossur.com/template110.asp?PageID=1782>. http://www.ossur.com/shared/FileGallery/SharedFiles/Ossurcom/Product%20files/Brochures/Flex-FootAxiaBrochure.pdf
[27] "Earle Connor gains second nomination for Laureus Awards", Ossur, August 16, 2006, <http://www.ossur.com/template110.asp?PageID=1581&newsid=626&Tpl=0>.
[28] S. Designs, "ADA Flex Knee Orthosis," 2006.
[29] S. Agrawal, S. Banala, and A. Fattah, "A Gravity Balancing Passive Exoskeleton for the Human Leg," in *Robotics: Science and Systems II*, University of Pennsylvania, 2006.
[30] "6 Million Dollar Man," Wikipedia, Wikipedia, August 8, 2006, <http://en.wikipedia.org/wiki/6_Million_Dollar_Man>.
[31] J. E. Pratt, B. T. Krup, C. J. Morse, and S. H. Collins, "The RoboKnee: An Exoskeleton for Enchancing Strength and Endurance During Walking," in *International Conference on Robotics & Automation*, New Orleans, LA, 2004.
[32] B. Lemley, "Future Tech: Really Special Forces," in *Discover*. vol. 23, 2002.
[33] "Humanoid Robot," Wikipedia, Wikipedia, February 27, 2006, <http://en.wikipedia.org/wiki/Humanoid_robot>.
[34] "Exoskeleton," Wikipedia, Wikipedia, February 27, 2006, <http://en.wikipedia.org/wiki/Exoskeleton>.
[35] A. Carvey, Interview with Paul Carvey, Chicago, IL, July 3, 2005.
[36] J. Blaya and H. Herr, "Adaptive Control of a variable-Impedance Ankle-Foot orthosis to Assist Drop-Foot Gait," *IEEE TRANSACTIONS ON NEURAL SYSTEMS AND REHABILITATION ENGINEERING,* vol. 12, March 2004.
[37] C. Walsh and H. Herr, "Development of a lightweight, underactuated exoskeleton for load-carrying augmentation," in *ICRA Exo*, 2006.
[38] "Yobotics Home. Legged Robots, Simulation, Actuators", Yobotics, <http://www.yobotics.com/index.html>.
[39] A. Chu, H. Kazerooni, and A. Zoss, "On the Biomimetc Design of the Berkeley Lower Extremity Exoskeleton (BLEEX)," in *International Conference on Robotics and Automation*, Barcelona, Spain, 2005, pp. 4345 - 4352.
[40] Ossur, "Ossur - Power Knee," 2006.
[41] R. Kram, "Energetics of running: a new perspective," *Nature,* vol. 346, pp. 265 - 267, 1990.
[42] W. DA, "Energy generation and absorption at the ankle and knee during fast, natural, and slow cadences," *PubMed,* pp. 147 - 154, 1983.
[43] J. Jansen, B. Richardson, F. Pin, R. Lind, and J. Birdwell, "Exoskeleton for Soldier Enhancement Systems Feasibility Study," Oak Ridge, Tennessee September 2000.

[44] "Bone_Muscle_Tendon", Anonymous, July 12, 2006, <http://www.cs.cmu.edu/People/tissue/bone_muscle_tendon.jpg>.

[45] B. AA, "Muscle-tendon stresses and elastic energy storage during locomotion in the horse," *PubMed,* vol. 120, pp. 73 - 87, May 1998.

[46] J. Anat, "The unique action of bi-articular muscles in complex movements," *PubMed,* vol. 155, pp. 1 - 5, December 1987.

[47] A. J. v. d. Bogert, "Exotendons for Assistance of Human Locomotion," *Biomed Eng Online,* vol. 2, October 14, 2003.

[48] JumpsWest.com, "clinic.jpg," 2006.

[49] S. Collins, A. Ruina, R. Tedrake, and M. Wisse, "Efficient Bipedal Robots Based on Passive-Dynamic Walkers," *Science,* vol. 307, pp. 1082 - 1085, 18 February 2005.

[50] M. Garcia, A. Ruina, M. Coleman, and A. Chatterjee, "Passive-Dynamic Models of Human Gait," in *Engineering Foundation Conference on Biomechanics and Neural Control of Human Movement*, Mt. Sterling, Ohio, 1996.

[51] M. Garcia, A. Ruina, and M. Coleman, "Some Results in Passive-Dynamic Walking," in *Euromech*, 1997.

[52] J. E. Wilson, "Walking Toy." vol. 2,140,275, USPO, Ed., 1936, p. 3.

[53] R. Tedrake, T. W. Zhang, M.-f. Fong, and H. S. Seung, "Actuating a Simple 3D Passive Dynamic Walker," in *International Conference on Robotics and Automation (ICRA)*, New Orleans, LA, 2004, pp. 4656 - 4661.

[54] "Walking Robots", S. Collins, 7-13-2006, <http://www-personal.engin.umich.edu/~shc/robots.html>.

[55] "List of muscles of the human body," Wikipedia, Wikipedia, March 13, 2006, <http://en.wikipedia.org/wiki/List_of_muscles_of_the_human_body>.

[56] "List of bones of the human skeleton," Wikipedia, Wikipedia, March 16, 2006, <http://en.wikipedia.org/wiki/List_of_bones_of_the_human_skeleton>.

[57] J. K. Jaromír Sedláček, Tomáš Kampmiller, Iveta Dremmelová, "THE USE OF SUPRA-MAXIMAL RUNNING SPEED MEANS IN SPRINTER TRAINING," *ACTA UNIVERSITATIS PALACKIANAE OLOMUCENSIS GYMNICA,* vol. 34, pp. 15 - 22, June 2003 2004.

[58] M. Kevin R. Stone, and Abhi Freyer, BAS, "Natural Anti-Inflammatories: Dealing with Arthritic Pain Drugs versus Diet," *Orthopedic Technology Review,* vol. 7, July / August 2005 2005.

[59] "Curvature," Wikipedia, 2-3-2007, <http://en.wikipedia.org/wiki/Curvature>.